NASA TECHNICAL
MEMORANDUM

NASA TM X-58043
April 1970

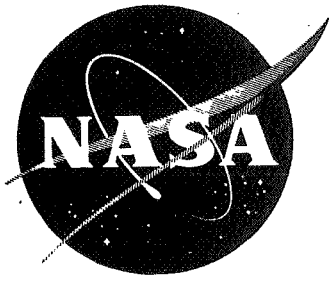

EFFECT OF CHAMBER-TO-NOZZLE HEAT EXCHANGE ON FROZEN AND EQUILIBRIUM FLOWS IN DE LAVAL NOZZLES

A Thesis Presented to the
Faculty of the Graduate School of the
University of Texas at Austin
in Partial Fulfillment of the
Requirements for the Degree of
Master of Science in Aerospace Engineering

NATIONAL AERONAUTICS AND SPACE ADMINISTRATION
MANNED SPACECRAFT CENTER
HOUSTON, TEXAS

NASA TM X-58043

EFFECT OF CHAMBER-TO-NOZZLE HEAT EXCHANGE ON FROZEN AND EQUILIBRIUM FLOWS IN DE LAVAL NOZZLES

Raymond LeRoy Nieder
Manned Spacecraft Center
Houston, Texas

DEDICATION

This thesis is dedicated to my parents, Leonard and Ellen Nieder, who have always been a source of encouragement and assistance in all of my endeavors.

ACKNOWLEDGEMENTS

I wish to extend my grateful appreciation to my supervising professor, Dr. John W. Porter, for his invaluable assistance in the preparation of this thesis. Also deserving of recognition for their many suggestions and kind assistance are Mr. George E. Griffith and Mr. Donald C. Wade of the National Aeronautics and Space Administration, Manned Spacecraft Center, Structural Dynamics Branch.

April 3, 1969

ABSTRACT

A rocket thrust chamber assembly was analyzed to determine the exit conditions that result when heat is withdrawn from the combustion chamber and simultaneously added to the gas flow in the nozzle. The analysis was performed for three cases. The first case considers the flow of an inert gas in the nozzle, the second considers the equilibrium flow of a dissociating diatomic gas, and the third case considers the addition of heat to the dissociating diatomic gas flow in the nozzle without the removal of heat from the combustion chamber.

Results of the inert gas analysis show that transferring heat from the combustion chamber to the nozzle causes a decrease in both exit velocity and specific impulse but results in an increase in exit pressure and exit temperature. The dissociating diatomic gas behaves in a manner similar to the inert gas, but the magnitude of the decrease is not as great. This damping effect is caused by dissociation of the diatomic gas.

When heat is applied to the nozzle, but not removed from the chamber, the dissociating diatomic gas shows an increase in exit velocity, exit pressure, exit temperature, and specific impulse.

CONTENTS

FIGURES

Figure Page

NOTATION

A	cross sectional area
a	speed of sound
C_p	specific heat at constant pressure
F	force
g	acceleration due to gravity
H	enthalpy per mole
ΔH°_f	standard heat of formation
h	enthalpy per unit mass
I_{sp}	specific impulse
K_p	pressure equilibrium constant
M	Mach number
P	pressure
Q	thermal energy per mole
q	heat exchange parameter
$\hat{q}$	thermal energy per unit mass
R	molar gas constant
S	entropy per mole
s	entropy per unit mass
T	temperature
V	velocity
W	weight per mole
X	mole fraction

Z	compressibility factor
β	degree of dissociation
γ	ratio of specific heats
ρ	density

Superscripts:

*	throat condition
**	plane where flow becomes sonic (M = 1.0) due to addition of heat
—	average value for gas mixture

Subscripts:

am	ambient condition
C	specified chamber condition
ex	exit condition
f	reservoir condition after heat removal
FE	first estimate
H	atomic hydrogen
H2	molecular hydrogen
i	initial reservoir condition
j	general subscript for gas specie
T	total (stagnation) condition
th	throat condition
y	specified point in the nozzle
o	reference condition (q = 0)
1	condition immediately in front of heat addition plane
2	condition immediately behind heat addition plane

Flow Chart Conventions Used

Symbol shape	Meaning	Information inside symbol
	Input statement	List of items inputted
	Output statement	List of items outputted or Hollerith statement
	Assignment statement	One or more statements of the form y = f(x)
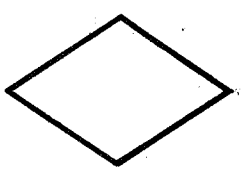	Conditional or IF statement	Condition which is true or false or algebraic value which is less than, equal to, or greater than zero
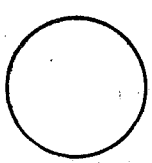	Unconditional transfer or GO TO statement	Next statement label

INTRODUCTION

Many authors have investigated various aspects of gas flows in nozzles, ranging from determining the effects on performance of employing different nozzle designs to using various combinations of fuels and oxidizers. Recent analytical investigations conducted by Michael Smith (ref. 1) have been concerned with external heat addition to the nozzle exhaust gases and sudden freezing of chemical and vibrational rate processes during flow in de Laval nozzles.

The author of this paper has extended Smith's work to the case where the quantity of heat added to the nozzle is simultaneously withdrawn from the combustion chamber. The analysis is extended to cover two cases: the first case considers the flow of an inert gas in the nozzle, and the second case considers the equilibrium flow of a dissociating diatomic gas. In both cases it is assumed that the gas flows isentropically from the combustion chamber to a position immediately ahead of the heat addition plane and also from immediately behind the plane to the nozzle exit. If the zone of heat addition is infinitesimally thin, then constant-area heat addition equations can be used to represent the flow at the heat addition plane. The combustion chamber is treated as a large reservoir of stationary gases with heat being removed. The appropriate equations for each flow regime are derived and a check calculation of the computer solution is made. In addition, the case of external heat addition to a dissociating diatomic gas without heat removal from the combustion chamber is investigated.

One possible application of this analysis can be found in nuclear rocket engines where a large amount of thermal energy is available. However, since the combustion chamber and nozzle material have certain temperature and pressure limitations, only a limited amount of energy can be added to the combustion chamber. Excess energy can be added to the flow at a plane in the nozzle at which the temperature and pressure are lower. The uniform addition of heat at a particular cross section of the nozzle presents a major difficulty if the flow is not to be disturbed mechanically. One means of accomplishing this energy transfer is by thermal radiation; however, this thesis does not investigate methods of heat transfer. Uniform heat addition in an infinitesimally thin plane is simply assumed and an analysis is made based on this assumption.

CHAPTER I

GENERAL DISCUSSION

The rocket engine thrust assembly used in this paper consists of a combustion chamber and a nozzle. The combustion chamber is considered as that portion of the overall assembly where the majority of the conversion from chemical to thermal energy occurs and where the gas speed is much less than its speed in the nozzle. The nozzle is, in turn, considered as that portion of the assembly where the majority of the conversion from thermal to kinetic energy occurs. A profile view of this configuration for a liquid rocket engine thrust assembly is shown in figure 1.

Penner (ref. 2) derived the relations for the thrust and specific impulse of a rocket motor in the following manner: from the equation for conservation of momentum, the thrust on a rocket motor is given by

$$F = (1 + \cos \alpha) \frac{\dot{W} V_{ex}}{2g} + \left(P_{ex} - P_{am} \right) A_{ex} \quad , \tag{1}$$

where

α = half of the divergence angle of the nozzle

$\dot{W}$ = the rate of total weight flow

V_{ex} = linear flow velocity at the nozzle exit position

g = acceleration due to gravity

P_{ex} = absolute pressure at the nozzle exit

P_{am} = ambient atmospheric pressure

A_{ex} = cross-sectional area at the nozzle exit position

If α is sufficiently small, equation (1) can be approximated by

$$F = \frac{\dot{W} V_{ex}}{g} + \left(P_{ex} - P_{am}\right) A_{ex} \quad . \tag{2}$$

The most generally accepted measure of the performance of a rocket motor is its specific impulse I_{sp}, which is defined as the ratio of thrust to propellant weight flow rate. Thus, when equation (2) is divided by $\dot{W}$ and α is small, the specific impulse equation for a rocket motor is found to be

$$I_{sp} = \frac{F}{\dot{W}} = \frac{V_{ex}}{g} + \left(P_{ex} - P_{am}\right) \frac{A_{ex}}{\dot{W}} \quad . \tag{3}$$

Maximum thrust, and thus maximum specific impulse for a constant $\dot{W}$, is obtained for ideal conditions in which the exit pressure P_{ex} equals the external pressure P_{am}. If $P_{ex} = P_{am}$, then

equation (3) reduces to

$$I_{sp} = \frac{V_{ex}}{g} \tag{4}$$

A nozzle expansion for which $P_{ex} = P_{am}$ is sometimes referred to as being ideally expanded.

In order to utilize equations (3) and (4) for practical evaluation of motor performance, an ideal motor can be hypotesized; such a motor satisfies the following assumptions:

1. Thermodynamic equilibrium is reached in the combustion chamber after the original adiabatic reaction.
2. Expansion of the combustion products through the de Laval nozzle is adiabatic.
3. The products of combustion behave as ideal gases.
4. The expansion process is considered to involve one-dimensional flow (parallel to the nozzle axis) of non-viscous ideal gases.
5. The velocity of the gases at the nozzle entrance position is negligibly small compared to the velocity at the exit position.

This idealized rocket motor is used as a standard of comparison for two specialized thrust chambers investigated in this thesis. For a more detailed development of the subject matter presented above, the reader should consult Penner (ref. 2), Barrere (ref. 3), Hesse (ref. 4), or other authors of texts concerning rocket propulsion systems.

The purpose of this thesis is to examine, for two specific cases, the theoretical effects on exit velocity and specific impulse

due to a transfer of thermal energy. For this first case (chapter II), the effects on exit velocity and specific impulse will be determined when heat is taken out of the combustion chamber and the same amount of heat is added simultaneously to the flowing gas behind the nozzle throat for a steady state inert gas system. Previous work in this area by Michael L. Smith (ref. 1) involved heat addition to the gas in the nozzle. Results from this work indicated that the addition of heat to the flow of an inert gas in a de Laval nozzle always results in larger values for specific impulse and exit pressure. On the other hand, the kinetic energy of the exhaust gases may or may not be increased, depending on where heat is added to the flow. Heat addition ahead of a particular area ratio, which Smith found to be approximately half the exit area ratio, resulted in an increase in exit velocity. Smith also found that heat added downstream of the "critical" area ratio decreased the exit velocity. Thus, there exists a critical area ratio at which heat addition yields an exit velocity identical to the exit velocity with no heat addition. As the location of the heat addition plane moves downstream from near the throat to the exit area, Smith's results showed that the specific impulse ratio and exit velocity ratio both decreased, whereas the exit pressure ratio increased. Chapter II is thus an extension of Smith's work to the case where the external heat added to the gas flow comes from the reservoir (or combustion chamber) of the rocket motor.

In the second case (chapter III), the gas employed is hydrogen in equilibrium flow instead of an inert gas. The gas is assumed to be in chemical, vibrational, and rotational equilibrium throughout the nozzle. Other assumptions are the following:

1. Ionization is considered to be negligible.
2. The flow is choked (i.e., the Mach number is unity at the nozzle throat).
3. No flow separation occurs in the system.

The calculated exit velocity and specific impulse values of the inert gas case and the calculated exit velocity of the real gas case are compared with their counterparts for similar initial conditions for an idealized thrust chamber. The idealized system is one in which the assumptions listed for a hypothesized ideal motor are valid and the flow is ideally expanded (i.e., exit pressure equals ambient pressure). The ambient pressure for both cases is constant for all calculations.

CHAPTER II

INERT GAS CASE

A. General Considerations

This chapter considers the equilibrium flow of an inert, ideal gas in a thrust chamber. If the chamber pressure is greater than the critical chamber pressure needed to achieve sonic conditions at the throat, the flow upstream of the throat is subsonic and downstream of the throat is supersonic. The specific impulse of this system is given by equation (4) for an ideal expansion process (i.e., $P_{ex} = P_{am}$).

A predetermined amount of thermal energy $\hat{q}$ per unit mass flowing through the nozzle is removed from the reservoir and simultaneously added to the flow in the nozzle at a specified location. Removing heat from the reservoir results in a decrease in the temperature of the gas. The chamber pressure, meanwhile, is assumed to remain constant. The next assumption is that the gas flows isentropically from the reservoir through the throat and up to the plane where the heat is being added. At the heat addition plane, the heat is assumed to be added to the flow in an infinitesimally thin region and, as a result, the thermodynamic state variables and the gas velocity are discontinuous across the plane. Immediately behind and downstream of the heat-addition plane, complete equilibrium is assumed and the gas expands isentropically to the nozzle exit.

The objective is to determine the conditions at the nozzle exit (i.e., V_{ex}, T_{ex}, P_{ex}, M_{ex}, I_{sp}) when the initial reservoir conditions (P_i, T_i), the heat exchange parameter q, the ratio of the nozzle exit area to the throat area (A_{ex}/A^*), and the area ratio of the heat addition plane (A_1/A^{**}) are known. The results will be compared with those for an identical system but with zero heat exchange (i.e., one with an isentropic, adiabatic, and ideal expansion process). Note that for a fixed nozzle configuration, the exit pressure P_{ex} will not necessarily be equal to the ambient pressure P_{am} for the case of heat addition. Thus, when q is non-zero, the effect of the pressure difference term in equation (3) must be included when calculating the specific impulse.

B. Mathematical Development

As seen in figure 2, the flow in the nozzle can be divided into three discrete regions: isentropic flow from the entrance of the nozzle to the area ratio where heat is being added to the flow, flow with heat addition across the discontinuity in the nozzle, and isentropic flow from immediately downstream of the discontinuity to the nozzle exit. The necessary equations for each of these regions will be derived, as well as the appropriate equations for heat removed from a large reservoir of stationary gas at constant pressure.

1. Basic Equations for the Reservoir

The equation for conservation of energy equation for the gas in the reservoir may be written as

$$h_i - h_f = \hat{q} \quad , \tag{5}$$

or, using the caloric equation of state for perfect gas, as

$$C_p \left(T_i - T_f \right) = \hat{q} \quad , \tag{6}$$

where T_f is the temperature of the gas in the reservoir after the thermal energy $\hat{q}$ has been removed and T_i is the initial reservoir temperature. Since the heat exchange parameter q is defined as

$$q = \frac{\hat{q}}{C_p \, T_i} \quad , \tag{7}$$

equation (6) may be rearranged to yield

$$T_f = T_i \, (1 - q) \tag{8}$$

For the type of reservoir specified, T_i and T_f represent stagnation temperatures. As mentioned earlier, the reservoir pressure will be assumed to remain constant (i.e., $P_i = P_f$).

2. Basic equations for Isentropic Flow Regimes of the Nozzle

The assumption of isentropic flow and the requirement that mass, momentum, and energy be conserved can be used to derive the following relations for the isentropic flow regimes in the nozzle, see Hesse (ref. 4):

$$\frac{P}{P^*} = \left\{ \frac{\frac{\gamma + 1}{2}}{1 + \frac{\gamma - 1}{2} M^2} \right\}^{\frac{\gamma}{\gamma - 1}} , \tag{9}$$

$$\frac{T}{T^*} = \frac{\frac{\gamma + 1}{2}}{1 + \frac{\gamma - 1}{2} M^2} , \tag{10}$$

$$\frac{A}{A^*} = \frac{1}{M} \left\{ \frac{1 + \frac{\gamma - 1}{2} M^2}{\frac{\gamma + 1}{2}} \right\}^{\frac{\gamma + 1}{2(\gamma - 1)}} , \tag{11}$$

and

$$\frac{P_T}{P_T^*} = \frac{T_T}{T_T^*} = 1 , \tag{12}$$

where M, the Mach number, is defined by

$$M = V/a , \tag{13}$$

and the speed of sound a for a perfect gas is

$$a = (g \gamma RT)^{1/2} \tag{14}$$

In this nozzle configuration, there exist two isentropic flow regimes. For the flow between the chamber and the heat addition plane located downstream of the throat, A^* is the throat area. For the flow behind the heat addition plane, A^* is an imaginary throat area at which the Mach number would be unity for the new flow.

3. Basic Equations for Rayleigh Flow in Constant Area Ducts

The assumption that the flow properties are discontinuous across the heat addition plane is equivalent to assuming that this region is infinitesimally thin. This observation leads to the conclusion that the equations developed for the flow of an inviscid, inert gas in a constant area duct with heat addition, can be used for this region. This type of flow is often referred to as a Rayleigh process. The Rayleigh equations used to relate flow parameters across the plane of heat addition are, see Hesse (ref. 4):

$$\frac{P}{P^{**}} = \frac{\gamma + 1}{1 + \gamma M^2} \quad , \tag{15}$$

$$\frac{T}{T^{**}} = M^2 \left\{ \frac{\gamma + 1}{1 + \gamma M^2} \right\}^2 \quad , \tag{16}$$

and

$$\frac{T_T}{T_T^{**}} = \frac{2 M^2 \left(\gamma + 1\right)\left(1 + \frac{\gamma - 1}{2} M^2\right)}{\left(1 + \gamma M^2\right)^2} \quad , \tag{17}$$

where $\frac{T_T}{T_T^{**}}$ is the ratio of total temperatures. The above relations were derived from the continuity equation

$$\rho V A = \text{Constant} \quad , \tag{18}$$

the equation of state for a perfect gas

$$P = \rho R T \quad , \tag{19}$$

the conservation of momentum equation

$$P_1 + \rho_1 V_1^2 = P_2 + \rho_2 V_2^2 \quad , \tag{20}$$

and the conservation of energy equation

$$C_p T_1 + \frac{V_1^2}{2} = C_p T_2 + \frac{V_2^2}{2} \tag{21}$$

Equation (21) may be rewritten as

$$T_{T_2} = T_{T_1} + q T_i \quad , \tag{22}$$

where the total temperature is defined by

$$T_T = T + \frac{V^2}{2\,C_p} \tag{23}$$

Equations (5) through (23) can be used to solve for values of all the flow parameters at the nozzle exit.

C. Example Check Calculations and Comparison With Computer Results

Several check calculations were performed for the computer program with the result that the answers calculated by hand compared very favorably with those calculated by the computer. One of these check calculations was performed for the following set of conditions:

$$\frac{A_{ex}}{A^*} = 20.0 \quad ,$$

$$\frac{A_1}{A^*} = 10.0$$

$$T_i = 4000^\circ \text{ R}$$

$$P_i = 30 \text{ atm} \quad ,$$

$$\gamma = 1.40$$

and

$$q = 0.25$$

The following is the method used to perform the check calculation for the above conditions.

A series of calculations is first performed that yields values for the reference conditions (i.e., for the case of $q = 0$).

$$\frac{A_{ex}}{A^*} = \frac{1}{M_{ex_o}} \left\{ \frac{1 + \frac{\gamma-1}{2} M_{ex_o}^2}{\frac{\gamma+1}{2}} \right\}^{\frac{\gamma+1}{2(\gamma-1)}} = 20$$

The preceding equation is satisfied when $M_{ex_o} = 4.7245$. The values of T_{ex_o} and P_{ex_o} are calculated by

$$T_{ex_o} = T_i \left\{ \frac{1}{1 + \frac{\gamma-1}{2} M_{ex_o}^2} \right\} = 4000\ (0.18303) = 732.131^\circ\ R,$$

and

$$P_{ex_o} = P_i \left\{ \frac{1}{1 + \frac{\gamma-1}{2} M_{ex_o}^2} \right\}^{\frac{\gamma}{\gamma-1}} = \frac{30}{381.1966} = 0.0787\ atm\ .$$

Equation (22) is now used in the following manner for the case of heat addition,

$$T_f = T_i (1 - q) = 4000 (0.75) = 3000^\circ \text{ R}$$

$$P_f = P_i = 30 \text{ atm.}$$

For an area ratio of heat addition equal to 10, the following equation is solved for the value of M_1

$$\frac{A_1}{A^*} = \frac{1}{M_1} \left\{ \frac{1 + \frac{\gamma - 1}{2} M_1^2}{\frac{\gamma + 1}{2}} \right\}^{\frac{\gamma + 1}{2(\gamma - 1)}} = 10$$

This equation gives a value for M_1 of 3.92313. The values of T_1 and P_1 are calculated by

$$T_1 = T_f \left\{ \frac{1}{1 + \frac{\gamma - 1}{2} M_1^2} \right\} = 3000 (0.2452) = 735.621^\circ \text{ R} \quad ,$$

and

$$P_1 = P_f \left\{ \frac{1}{1 + \frac{\gamma - 1}{2} M_1^2} \right\}^{\frac{\gamma}{\gamma - 1}} = \frac{30}{136.9735} = 0.21902 \text{ atm}$$

Equation (18) gives the following two relations

$$\frac{T_{T_1}}{T_T^*} = \frac{2 M_1^2 \left(\gamma + 1\right)\left(1 + \frac{\gamma - 1}{2} M_1^2\right)}{\left(1 + \gamma M_1^2\right)^2} \quad ,$$

and

$$\frac{T_{T_2}}{T_T^{**}} = \frac{2 M_2^2 \left(\gamma + 1\right)\left(1 + \frac{\gamma - 1}{2} M_2^2\right)}{\left(1 + \gamma M_2^2\right)^2} \quad .$$

Since $T_{T_2} = T_i$ and $T_{T_1} = T_f$, equation (22) also implies that

$$T_{T_1} = T_{T_2} (1 - q) \quad ,$$

or

$$T_{T_2} = T_{T_1} + q T_i = T_{T_1} \left(1 + q \frac{T_i}{T_{T_1}}\right) \quad .$$

Thus

$$\frac{T_{T_2}}{T_T^{**}} = \frac{T_{T_1}}{T_T^*} \left(1 + \frac{q T_i}{T_{T_1}}\right) \quad .$$

M_2 is then found by solving the following equation

$$\frac{M_2^2\left(1 + \frac{\gamma - 1}{2} M_2^2\right)}{\left(1 + \gamma M_2^2\right)^2} = \frac{M_1^2\left(1 + \frac{\gamma - 1}{2} M_1^2\right)}{\left(1 + \gamma M_1^2\right)^2}\left(1 + q \frac{T_i}{T_{T_1}}\right) .$$

For the values of M_1, q, T_i, and T_{T_1} previously determined, this equation yields $M_2 = 2.0163$. The values of T_2 and P_2 are calculated by

$$T_2 = T_{T_2}\left(\frac{1}{1 + \frac{\gamma - 1}{2} M_2^2}\right) = 2206.166\ ^{\circ}R ,$$

and

$$P_2 = P_1\left(\frac{1 + \gamma M_1^2}{1 + \gamma M_2^2}\right) = 0.737976 \text{ atm}$$

The pressure relation was found by dividing $\frac{P_2}{P^{**}}$ by $\frac{P_1}{P^{*}}$ as given by equation (15).

$$\frac{A_2}{A_{ex}} = \frac{A_1}{A^*}\frac{A^*}{A_{ex}} = \frac{10}{20} = \frac{M_{ex}}{M_2}\left\{\frac{1 + \frac{\gamma - 1}{2} M_2^2}{1 + \frac{\gamma - 1}{2} M_{ex}^2}\right\}^{\frac{\gamma + 1}{2(\gamma - 1)}} .$$

Solving for M_{ex} yields $M_{ex} = 2.77573$. The values of T_{ex} and P_{ex} are found by

$$T_{ex} = T_2 \left\{ \frac{1 + \frac{\gamma - 1}{2} M_2^2}{1 + \frac{\gamma - 1}{2} M_{ex}^2} \right\} = 1574.22^\circ \text{ R} \quad ,$$

and

$$P_{ex} = P_2 \left\{ \frac{1 + \frac{\gamma - 1}{2} M_2^2}{1 + \frac{\gamma - 1}{2} M_{ex}^2} \right\}^{\frac{\gamma}{\gamma - 1}} = 0.22648 \text{ atm} \quad .$$

Forming the ratios of interest gives the following:

$$\frac{T_{ex}}{T_{ex_o}} = \frac{1574.22}{732.131} = 2.150189$$

$$\frac{M_{ex}}{M_{ex_o}} = \frac{2.77573}{4.72415} = 0.587562$$

$$\frac{P_{ex}}{P_{ex_o}} = \frac{.22648}{.078699} = 2.87777$$

$$\frac{V_{ex}}{V_{ex_o}} = \frac{M_{ex}}{M_{ex_o}} \left\{ \frac{\gamma\, g\, RT_{ex}}{\gamma\, g\, RT_{ex_o}} \right\}^{1/2} = 0.86157 \quad ,$$

and

$$\frac{I_{sp}}{I_{sp_o}} = \frac{V_{ex}}{V_{ex_o}} + \left(\frac{P_{ex}}{P_{ex_o}} - 1 \right) \frac{1}{\gamma\, M_{ex_o}^2} = 0.92167 \; .$$

For the above initial conditions, the computer solution gave the following values for the ratios of interest:

$$\frac{T_{ex}}{T_{ex_o}} = 2.1512$$

$$\frac{M_{ex}}{M_{ex_o}} = 0.58740$$

$$\frac{P_{ex}}{P_{ex_o}} = 2.88323$$

$$\frac{V_{ex}}{V_{ex_o}} = 0.86153$$

and

$$\frac{I_{sp}}{I_{sp_o}} = 0.92177$$

D. Results and Conclusions

The results of applying the mathematical relations developed in section B and used in the formulation of the computer solution are presented in figures 4 through 13.

Figure 4 shows the effect of the location of the heat addition plane on the exit velocity ratio for several different values of the heat exchange parameter q. Figure 5 is a plot of heat addition location versus exit velocity ratio for three values of the exit area ratio A_{ex}/A^*. Figure 6 shows the effect of the heat addition plane location on the exit pressure ratio for several values of q while figure 7 shows the effect of different exit area ratios. Figures 8 and 9 are similar to figures 4 and 5 except that the specific impulse ratio is plotted instead of the exit velocity ratio. Similarly, figures 10 and 11 show the exit temperature ratio and figures 12 and 13 show the exit Mach number ratio.

Figures 4, 8, and 12 show that the exit velocity ratio, specific impulse ratio, and exit Mach number ratio decrease as the heat exchange parameter q increases and also as the heat addition plane area ratio increases. The three ratios approach unity for low values of q and when the area ratio of heat addition is near unity. Figures 5,

9, and 13 show that this trend is found for all three exit area ratios considered. As for the exit pressure ratio and exit temperature ratio, figures 6 and 10 show that these ratios increase as either q or the area ratio of heat addition increases. The ratios are again closest to unity for the heat addition plane located near the throat of the nozzle. Figures 7 and 11 show that for the three exit area ratios considered, the curves are homothetic. That is, the size of the nozzle has very little effect on the exit parameters. Changing the value of the heat exchange parameter causes the greatest variation in the exit parameters of interest.

Note that there is no "crossover point" as was found by Smith in his work (ref. 1) on heat addition to the nozzle (i.e., there is no location at which heat addition yields an exit velocity identical to the exit velocity for the case of no heat addition). To transfer heat from the combustion chamber or reservoir and add the thermal energy somewhere downstream of the throat, it is best to transfer as little thermal energy as possible and then introduce the heat back into the gas flow as close to the throat as practical, providing the desired exit parameter to be maximized is the exit velocity or the specific impulse. If, instead, the exit pressure or exit temperature is to be maximized, then the amount of heat transferred should be large and should be added to the gas at the nozzle exit.

CHAPTER III

REACTING GAS CASE

A. General Considerations

This chapter considers the equilibrium flow of hydrogen gas in a rocket engine thrust chamber assembly. If the gas is introduced into the combustion chamber at a sufficiently high temperature T_i, dissociation of the molecular species H_2 will occur in accordance with the following endothermic reaction:

$$L + H_2 \longrightarrow 2H + L \quad , \tag{24}$$

where L is a third body (either H or H_2). The dissociation reaction will be in chemical equilibrium with the reverse exothermic recombination reaction

$$L + 2H \longrightarrow H_2 + L \quad , \tag{25}$$

if sufficiently low flow velocities are maintained in the combustion chamber. For equilibrium, the relative concentrations of the atomic and diatomic species are dependent on the pressure P_i and temperature T_i existing in the chamber. Ionization of the hydrogen atom, which becomes appreciable for temperature greater than 10 000° K, is assumed to be negligible for the pressure-temperature combinations considered in this thesis.

The velocity of the dissociated gas will increase as the gas enters the convergent nozzle section and begins its expansion to the nozzle exit. The gas will be considered to be in equilibrium flow from the combustion chamber to immediately in front of the heat addition plane (where a known amount of thermal energy is added) and also from immediately behind the plane of heat addition to the nozzle exit. The terminology "equilibrium flow" refers to the condition that the chemical reactions as represented by equations (24) and (25), in addition to other relaxation rate processes (e.g., vibrational, rotational) proceed at a sufficiently rapid rate to adjust to the equilibrium conditions corresponding to the local pressure P and temperature T in the nozzle.

The flow system of the thrust chamber assembly consists of hydrogen gas entering the combustion chamber at pressure P_i and temperature T_i. A predetermined amount of thermal energy is then withdrawn from the combustion chamber and simultaneously added to the flowing gas at a known plane downstream of the throat. It is assumed that the gas in the chamber immediately attains a new equilibrium temperature T_f and pressure P_f after the heat removal. The pressure P_f is further assumed to be equal to the initial pressure P_i. The dissociated gas then flows from the combustion chamber through the nozzle throat to the plane of heat addition. Throughout this portion of the flow, the molecular weight $\overline{W}$, the specific heat at constant pressure $\overline{C}_p$, and the ratio of specific heats γ of the equilibrium

gas mixture vary during the expansion due to the shift in equilibrium concentrations of the species H and H_2 as well as to the shift in internal energy distribution of the gas. At the heat addition plane, the thermal energy extracted from the gas mixture in the reservoir is added to the gas flowing in the nozzle. It is again assumed that the gas flow reaches a new equilibrium temperature T_2 and pressure P_2 immediately after heat addition. The resulting gas mixture then expands isentropically to the nozzle exit.

The major difference between the reacting-gas case and the inert-gas case is that, in the former, there is an added internal "heat addition" effect caused by recombination of the hydrogen atoms.

B. Mathematical Development

As seen in figure 14, the flow in the nozzle can be divided into three different flow regimes. These consist of isentropic flow from the nozzle entrance to a position immediately in front of the heat addition plane, flow with heat addition across the discontinuity in the nozzle, and isentropic flow from immediately downstream of the plane to the exit. The problem of heat removal from a large reservoir of gases at constant pressure and zero velocity (i.e., the combustion chamber) is also considered.

1. Calculations of Thermodynamic Properties at a Given Point in the Flow

If the temperature and pressure at a point in the equilibrium gas flow are specified, it is possible to find K_p, C_{P_H}, $C_{P_{H2}}$, H_H, H_{H2},

S_H, and S_{H2} by using tables such as the JANAF Thermochemical Tables (ref. 5) or those furnished by the National Bureau of Standards. Once the values of the thermodynamic properties are known for molecular and atomic hydrogen at the specified conditions, the mole fraction (i.e., X_H and X_{H2}) and the thermodynamic properties of the gas mixture can be calculated by using the following sequence of operations as described by Penner (ref. 2). The degree of dissociation β may be calculated using the equation

$$\beta = \left\{ \frac{K_p}{4P + K_p} \right\}^{1/2} \quad . \qquad (26)$$

Once β has been calculated, the mole fractions are given by

$$X_H = \frac{2\beta}{1 + \beta} \quad , \qquad (27)$$

$$X_{H2} = \frac{1 - \beta}{1 + \beta} \quad , \qquad (28)$$

or

$$X_{H2} = 1 - X_H \qquad (29)$$

Now that the mole fractions have been calculated, it is possible to calculate the entropy, enthalpy, and coefficient of specific heat at

constant pressure for the gas mixture using relations derived by Penner (ref. 2) for a mixture of ideal gases:

$$\overline{W} = \sum_{j=1}^{N} X_j W_j \quad , \tag{30}$$

$$\overline{S} = \sum_{j=1}^{N} X_j S_j - R \left(\ln P + \sum_{j=1}^{N} X_j \ln X_j \right) \quad , \tag{31}$$

$$\overline{H} = \sum_{j=1}^{N} X_j \left(\Delta H_f^\circ + H_j - H_{j,\ 298.16^\circ K} \right) , \tag{32}$$

and

$$\overline{C}_p = \sum_{j=1}^{N} X_j C_{p_j} \tag{33}$$

The ratio of specific heats for the specific conditions can then be calculated by the following equation

$$\gamma = \frac{\overline{C}_p}{\overline{C}_p - R} \tag{34}$$

2. Equations for Heat Removal From the Reservoir

Assuming that the reservoir is initially at equilibrium with a temperature T_i and P_i, the enthalpy of the gas mixture and any of the other desired thermodynamic properties can be calculated by using the above procedure (Section B, part 1). Next is the problem of

determining the new equilibrium reservoir conditions after a given amount of thermal energy Q has been removed from the reservoir. Starting with the conservation of energy equation and making two assumptions that the pressure of the reservoir remains constant and that the velocity of the gas mixture in the reservoir is zero, the equilibrium temperature in the reservoir after heat removal, T_f, is found by a trail and error solution. The conservation of energy equation with the above assumptions can be written as

$$dh = d\,\hat{q} \quad , \tag{35}$$

which, when expanded mathematically, becomes

$$h_i - h_f = \hat{q} \tag{36}$$

Making the substitution that $h = \overline{H}/\overline{W}$ and rearranging yields the following relation

$$\frac{\overline{H}_f}{\overline{W}_f} = \frac{\overline{H}_i - Q}{\overline{W}_i} \quad . \tag{37}$$

Since the heat exchange parameter q is defined as

$$q = \frac{Q}{\overline{H}_i} \quad , \tag{38}$$

equation (37) can be rearranged to yield

$$\frac{\overline{H}_f}{\overline{W}_f} = (1 - q) \frac{\overline{H}_i}{\overline{W}_i} \tag{39}$$

Since the values of $\overline{W}_i$, $\overline{H}_i$, and q are known, equation (39) can be solved by trial and error to obtain T_f. The method is to assume a value for T_f, find $\overline{W}_f$ and $\overline{H}_f$ by the procedure outlined in part 1, and compare the two sides of equation (39). This method is repeated until covergence or satisfactory agreement is reached.

3. Equations for Isentropic Flow From a Specified Chamber Condition to a Specified Pressure in the Nozzle

With the temperature and pressure of the chamber known, the entropy, enthalpy, and other thermodynamic properties of the dissociated hydrogen gas in the chamber can be calculated by the procedure outlined in part 1. For isentropic flow between the chamber after heat removal and a specified point in the nozzle, y, the change in the entropy per unit mass is zero; that is,

$$s_f = s_y \quad , \tag{40}$$

or

$$\frac{\overline{S}_f}{\overline{W}_f} = \frac{\overline{S}_y}{\overline{W}_y} \tag{41}$$

Assuming that the pressure is known at position y, the temperature T_y, can be found by a trial and error method. This involves making an estimate for T_y, performing the calculations in part 1, and then substituting the results into equation (41). This process is repeated until the entropies converge or until satisfactory agreement is reached. Once the temperature at y has been determined, the composition and other thermodynamic properties of the gas mixture are found by using the method outlined in part 1 involving equations (26) through (34).

The velocity V_y may now be calculated using

$$\Delta h = -\Delta \frac{V^2}{2} \tag{42}$$

where use has been made of assumptions (1) through (5) listed in chapter I. Since $h = \overline{H}/\overline{W}$ and $V_f = 0$, equation (42) may be written

$$\frac{\overline{H}_f}{\overline{W}_f} - \frac{\overline{H}_y}{\overline{W}_y} = \frac{V_y^2}{2} \quad , \tag{43}$$

or

$$V_y^2 = \frac{2}{\overline{W}_f} \left\{ \overline{H}_f - \frac{\overline{W}_f}{\overline{W}_y} \overline{H}_y \right\} \tag{44}$$

Since the thermodynamic properties of the gas at f and y have been determined as outlined above, equation (44) may be used to calculate V_y.

Thus, by using the procedure outlined in this part, it is possible to find all of the desired conditions at point y providing the temperature and pressure in the reservoir (i.e., T_f and P_f) and the pressure at point y are known.

Instead of designating the area ratio as the parameter defining the point of interest in the nozzle (chapter II), the pressure P_y was chosen as the designating factor. The calculation of the area ratio at position y in terms of the pressure P_y will be shown in part 5.

4. Equations for Heat Addition in the Nozzle

The problem in this segment of the nozzle is to find the thermodynamic properties of the gas mixture behind the heat addition plane. The conditions existing immediately in front of the heat addition plane are known from the procedure described earlier in this chapter (part 3), and the amount of thermal energy being added to the gas flow is the same as that subtracted from the chamber (part 2). Across the heat addition plane, the mass, momentum, and energy conservation equations must hold. Penner (ref. 2) combines these conservation equations and derives a relation between the initial pressure and final pressure and a relation between the initial and final enthalpies. These relations are

$$\frac{P_2}{P_1} = \frac{\left(\gamma_2 + 1\right) + \left\{\left(\gamma_2 + 1\right)^2 - 4\gamma_2 \frac{T_1}{T_2}\right\}^{1/2}}{2\gamma_2 \frac{T_1}{T_2}} , \qquad (45)$$

and

$$\frac{2\rho_1}{P_1}\left(h_2 - h_1 - \hat{q}\right) = \left(\frac{P_2}{P_1} - 1\right)\left\{\frac{1 + 2\gamma_2 - \frac{P_1}{P_2}}{1 + \gamma_2 - \frac{P_1}{P_2}}\right\} . \qquad (46)$$

Equations (45) and (46), along with equation (34), are used in the iteration scheme to provide better values for γ_2 as the iteration progresses.

In order to start the iteration, it is necessary to estimate a value for T_2. This first estimate can be obtained by solving the Rayleigh relations as was done in chapter II, equation 17.

$$\frac{T_{T_1}}{T_T^*} = \frac{2\,M_1^2\left(\gamma_1 + 1\right)}{\left(1 + \gamma_1 M_1^2\right)^2}\left(1 + \frac{\gamma_1 - 1}{2} M_1^2\right) , \qquad (47)$$

and

$$\frac{T_{T_2}}{T_T^*} = \frac{2\,M_{FE}^2\left(\gamma_{FE} + 1\right)}{\left(1 + \gamma_{FE} M_{FE}^2\right)^2}\left(1 + \frac{\gamma_{FE} - 1}{2} M_{FE}^2\right) . \qquad (48)$$

Dividing equation (47) by equation (48) results in

$$\frac{T_{T_2}}{T_{T_1}} = \frac{M_{FE}^2}{M_1^2}\left\{\frac{1 + \gamma\, M_{FE}^2}{1 + \gamma\, M_1^2}\right\}^2\left\{\frac{1 + \frac{\gamma - 1}{2} M_1^2}{1 + \frac{\gamma - 1}{2} M_{FE}^2}\right\} , \qquad (49)$$

assuming that $\gamma_1 = \gamma_{FE} = \gamma$ as was assumed in chapter II. Since M_1, T_{T_1}, and T_{T_2} are known, equation (49) can be solved for the first estimate of the Mach number behind the heat addition plane (M_{FE}). Once M_{FE} had been calculated, the first estimate of the temperature behind the heat addition plane (T_{FE}) can be found by using

$$T_{FE} = \frac{T_{T_2}}{1 + \frac{\gamma - 1}{2} M_{FE}^2} \quad , \qquad (50)$$

where the stagnation temperature T_{T_2} is, in reality, the initial reservoir temperature T_i.

The procedure to be followed is to calculate the first estimated value of the temperature T_{FE} by using equations (47) through (50). Then assuming that the first estimate for γ_2 equals γ_1, equation (45) can be solved with T_{FE} substituted in place of T_2 for the ratio P_2/P_1. Next, using the first estimates for P_2 and T_2, an improved value of γ_2 can be found from equation (34). With the improved estimates for P_2 and γ_2, equation (46) can be solved for h_2 and, thus, T_2. With new values for T_2 and γ_2, equation (45) again yields an improved value for P_2. The iteration is continued until the temperature, pressure, and ratio of specific heats have converged to definite values. After convergence the thermodynamic properties of the gas mixture immediately behind the heat addition plane can be found by the procedure developed in part 1.

5. Calculations of the Area Ratio

Given the pressure, temperature, gas velocity, and all other flow properties at a point in the nozzle, the only remaining desired parameter of interest is the area ratio. This ratio can be calculated by using the continuity equation and table II of NASA SP-3002 (ref. 6). From this table for a specified temperature and pressure, the compressibility factor Z and the ratio of the equilibrium speed of sound to the equilibrium speed of sound at 0° C can be found. The equation of state yields the density

$$\rho = \frac{P}{ZRT} \quad , \tag{51}$$

and the ratio a/a_o yields the equilibrium speed of sound

$$a = a_o\left(\frac{a}{a_o}\right) \tag{52}$$

Assuming that the Mach number is equal to unity at the throat, the gas velocity is given by the equilibrium speed of sound. NASA TN-D 1454 (ref. 7) reaches the conclusion that an excellent estimate for the throat pressure P^* for equilibrium flow is

$$\frac{P_c}{P^*} = \left(\frac{\gamma_c + 1}{2}\right)^{\frac{\gamma_c}{\gamma_c - 1}} \quad , \tag{53}$$

where γ_c is the isentropic exponent in the combustion chamber and P_c is the pressure in the combustion chamber. The throat temperature T^* can be calculated from

$$\frac{T_c}{T^*} = \frac{\gamma_c + 1}{2} \quad , \tag{54}$$

where T_c is the chamber pressure.

Using the continuity equation, the area ratio may be written as

$$\frac{A}{A^*} = \frac{\rho^* V^*}{\rho V} \quad . \tag{55}$$

The density at the throat ρ^* is calculated by using equations (51), (53), and (54). The density ρ and the velocity V are found by using equation (51) and the procedures described in part 3. V^* is the equilibrium speed of sound calculated by using equation (52) with the values of T^* and P^* determined from equations (53) and (54). These parameters, when substituted into equation (55), thus determine the area ratio at the point of interest.

C. Example Check Calculations

The method used to check the numbers calculated by the computer program was to compare the variables calculated during each step to values of the variables for the same initial conditions contained in

NASA TN D-275 (ref. 8). The conditions used for one set of comparisons were:

$$\frac{A_{ex}}{A^*} = 64.99$$

$$\frac{A_1}{A^*} = 27.77$$

$$T_i = 4000^\circ \text{ K}$$

$$P_i = 30 \text{ atm}$$

$$q = 0.25$$

The comparisons for the above conditions are presented in the following tables.

COMPARISON OF NASA TN D-275 AND CALCULATED VALUES

FOR SELECTED VARIABLES

[From ref. 8]

Variable	NASA TN D-275	Calculated	Difference, percent
Initial reservoir conditions			
T	4000.0	4000.0	N/A
P	30.0	30.0	N/A
h	23911.1	23979.6	0.29
m	1.763	1.7632	.00
X_{H2}	.74929	.74920	.01
s	24.2382	24.2399	.01
P*	17.0890	17.2058	.68
T*	3751.0	3750.9	.00
Reference exit conditions			
T	1347.0	1342.19	0.36
P	.0300	.0296	1.33
h	4725.1	4708.67	.35
m	2.016	2.016	.00
X_{H2}	.99999	.99998	.00
s	24.2382	24.2399	.01
M	4.617	4.61676	.01
I_{sp}	1292.1	1294.9	.22
Immediately in front of heat addition plane			
T	1821.0	1814.66	0.35
P	.1	0.099	1.00
h	6596.1	6574.3	.33
m	22.015	2.01456	.02
γ	1.3067	1.3208	1.08
X_{H2}	.99866	.998575	.01
s	24.2382	24.2399	.01
M	3.841	3.839	.05

COMPARISON OF NASA TN D-275 AND CALCULATED VALUES

FOR SELECTED VARIABLES - Concluded

[From ref. 8]

Variable	NASA TN D-275	Calculated	Difference, percent
Immediately behind heat addition plane			
T	2735.0	2746.04	0.40
P	.22334	.22161	.78
h	14448.1	14435.5	.09
m	1.875	1.878	.17
γ	1.145	1.148	.26
s	26.7426	26.7335	.03
Q	5977.78	5994.89	.29
Exit condition with heat addition			
T	2470.0	2472.18	0.09
P	0.0767	0.0761	.78
h	11559.	11508.	.44
m	1.93667	1.93577	.05
X_{H2}	0.9213	0.9204	.10
s	26.7425	26.7335	.03
M	3.855	3.7815	1.91
I_{sp}	1420.	1404.	1.13

COMPARISON OF NASA TN D-275 AND CALCULATED VALUES

FOR SELECTED RATIOS

[From ref. 8]

Ratio	NASA TN D-275	Calculated	Difference, percent
$\frac{M_{ex}}{M_{ex_o}}$	0.83516	0.81909	1.92
$\frac{P_{ex}}{P_{ex_o}}$	2.56667	2.56712	.02
$\frac{T_{ex}}{T_{ex_o}}$	1.8337	1.8419	.45
$\frac{X_{H2}}{X_{H2_o}}$	0.92131	0.92042	.10
$\frac{I_{sp}}{I_{sp_o}}$	1.09907	1.08426	1.35

D. Results and Conclusions

The results of applying the mathematical relations developed in section B and used in the formulation of the computer solution are presented in figures 19 through 42 for the two reacting gas cases investigated. For the first case heat was added to the nozzle gas flow with no heat being withdrawn from the combustion chamber (figs. 19 through 30) and, for the second case, heat was simultaneously withdrawn from the combustion chamber and transferred to the nozzle gas flow (figs. 31 through 42). The ratios of velocity, pressure, specific impulse, temperature, Mach number, and molecular hydrogen mole fraction were plotted against the area ratio. The area ratio of the heat addition plane was varied by moving the plane from the throat to the nozzle exit (fig. 14).

For the flow of a dissociating diatomic gas, with heat addition in the nozzle but no heat withdrawn from the combustion chamber, the exit velocity ratio decreased as the plane of heat addition was moved from near the throat to the nozzle exit (fig. 19). The decrease was small, however, with the velocity ratio remaining above 1.0 and with no "crossover" point, such as that found by Smith (ref. 1) for external heat addition to the nozzle gas flow for an inert gas. Increased exit area ratio resulted in an increase in the exit velocity ratio (fig. 20) and also in a smaller net decrease when the heat addition plane was moved from the throat to the nozzle exit. The exit pressure ratio increased as the plane of heat addition was moved from near the throat to the nozzle exit (fig. 21). Increased nozzle exit area ratio caused a

slight increase in the exit pressure ratio (fig. 22). The specific impulse ratio behaves similarly to the exit velocity ratio, thus the description of the exit velocity ratio is applicable to the specific impulse ratio (figs. 23 and 24). The exit temperature ratio behaved similarly to the exit pressure ratio (figs. 25 and 26). The ratio of the exit Mach number is always below 1.0 and decreases as the plane of heat addition is moved from near the throat to the nozzle exit (fig. 27). Increasing the exit area ratio causes a larger decrease in the exit Mach number ratio (fig. 28). The exit molecular hydrogen mole fraction ratio is below 1.0 and decreases as the plane of heat addition is moved from near the throat to the nozzle exit (fig. 29). Increasing the exit area ratio causes an increase in the exit molecular hydrogen mole fraction ratio (fig. 30). Thus when heat is added to the flow in the nozzle, but not removed from the chamber, the dissociating diatomic gas shows an increase in exit velocity, exit pressure, exit temperature, and specific impulse.

Comparison is made of the results of external heat addition to the nozzle gas flow for a dissociating diatomic gas (fig. 19 through 30) with the results of M. L. Smith's analysis (ref. 1) for external heat addition to the nozzle gas flow for an inert gas. The comparison shows similarities as well as differences. The tendency of the respective curves is the same. For example, if the analysis for the inert gas shows that a particular ratio decreases as the plane of heat addition is moved from near the throat to the nozzle exit, the same ratio will also decrease for the dissociating diatomic gas. The main difference is that the exit

velocity ratio for the dissociating diatomic gas case does not have the "crossover" that was shown by M. L. Smith in his analysis for an inert gas. The primary reason that the exit velocity ratio for the reacting gas remains above 1.0 is the fact that the chemical reaction of recombination causes larger amounts of heat to be added to the flowing gas upstream of Smith's "critical" point than are added downstream, thus causing a higher exit velocity.

Figures 31 through 42 present the results for the case of a dissociating diatomic gas in which heat was transferred from the combustion chamber, by some means unspecified in this analysis, to the flow in the nozzle. The exit velocity ratio, which is always less than 1.0, was found to decrease as the plane of heat addition was moved from near the throat to the nozzle exit (fig. 31). Increased exit area ratio caused an increase in the exit velocity ratio (fig. 32). The exit pressure ratio remained above 1.0 and increased as the plane of heat addition was moved from near the throat to the nozzle exit (fig. 33). Increased exit area ratio caused an increase in the pressure ratio (fig. 34). The specific impulse ratio behaved similarly to the exit velocity ratio (fig. 35). Increased area ratio caused an increase in specific impulse ratio (fig. 36). The exit temperature ratio remained above 1.0 and increased as the plane of heat addition was moved from near the throat to the nozzle exit (fig. 37). Increased exit area ratio caused an increase in the temperature ratio (fig. 38). The exit Mach number ratio decreased as the plane of heat addition was moved from near the throat to the nozzle exit and remained below 1.0 (fig. 39). Increased

exit area ratio caused a decrease in the exit Mach number ratio (fig. 40). The exit molecular hydrogen mole fraction ratio behaved similarly to the exit velocity ratio (figs. 41 and 42).

Comparison of the results of the analysis of heat transfer from the combustion chamber with the nozzle gas flow for both the inert gas case and dissociating diatomic gas shows several similarities as well as a few differences. Comparison of the two cases shows that the tendency of the curves is the same. For example, the exit velocity ratio in both cases decreased from a maximum close to 1.0 at the throat to the lowest value at the nozzle exit. The same similarity holds true for the respective curves of both cases. A direct comparison of the inert gas and dissociating diatomic gas (as far as the specific impulse ratio) shows that the specific impulse ratio for an inert gas varies from 0.94 to 0.84 while the reacting gas remains close to 1.0 (fig. 43). Results of the inert gas analysis show that transferring heat from the combustion chamber to the nozzle causes a decrease in both exit velocity and specific impulse but results in an increase in exit pressure and exit temperature. The dissociating diatomic gas behaves in a manner similar to the inert gas, but the magnitude of the decrease is not as great. The damping effect is caused by the recombination reactions and associated heat release in the diatomic gas.

BIBLIOGRAPHY

1. Smith, Michael Lynn: External Heat Addition and Sudden Freezing of Chemical and Vibrational Rate Processes During Flow in DeLaval Nozzles. Master's Thesis, Department of Aerospace Engineering, University of Texas, Austin, Texas, June 1967.

2. Penner, S. S.: Chemistry Problems in Jet Propulsion. New York: The MacMillan Company, 1957.

3. Barrere, Marcel, and others: Rocket Propulsion. New York: Elsevier Publishing Company, 1960.

4. Hesse, W. J.; and Mumford, N. V. S.: Jet Propulsion For Aerospace Applications. New York: Pitman Publishing Corporation, 1964.

5. JANAF Thermochemical Tables. The Dow Chemical Company, Midland, Michigan, 1961.

6. Kubin, R. F.; and Presley, L. L.: Thermodynamic Properties and Mollier Chart for Hydrogen from 300° K to 20 000° K. NASA SP-3002, 1964.

7. Zeleznik, F. J.; and Gordon, S.: A General IBM 704 or 7090 Computer Program for Computation of Chemical Equilibrium Composition, Rocket Performance, and Chapman - Joquet Detonations. NASA TN D-1454, 1962.

8. King, Charles R.: Compilation of Thermodynamic Properties, Transport Properties and Theoretical Rocket Performance of Gaseous Hydrogen. NASA TN D-275, 1960.

9. Krascella, N. L.: Tables of the Composition, Opacity and Thermodynamic Properties of Hydrogen at High Temperatures. NASA SP-3005, 1963.

10. McBride, et al: Thermodynamic Properties to 6000° K for 210 Substances Involving the First 18 Elements. NASA SP-3001, 1963.

11. Rosenbaum, B. M.; and Levitt, L.: Thermodynamic Properties of Hydrogen From Room Temperature to 100 000° K. NASA TN D-1107, 1962.

12. Geyer, E. W.; and Burges, E. A.: Tables of Properties of Gases with Dissociative Theory and Its Applications. New York: Longmans, Green and Co., 1948.

13. Hansen, C. F.: Approximation for the Thermodynamic and Transport Properties of High Temperature Air. NASA TR R-50, 1959.

14. Lee, John D.: The Molecular Flow of Diatomic Gases and Gas Mixture. Aeronautical Research CAB Rept. 62-346, 1962.

15. Liepman, H. W.; and Roshko, A.: Elements of Gasdynamics. New York: John Wiley and Sons, Inc., 1957.

16. Lewis, B.; Pease, R. N.; and Taylor, H. S.: Combustion Processes, Volume II of High Speed Aerodynamics and Jet Propulsion. Princeton, New Jersey: Princeton University Press, 1956.

17. Emmons, Howard W., editor: Fundamentals of Gas Dynamics, Volume III of High Speed Aerodynamics and Jet Propulsion. Princeton, New Jersey: Princeton University Press, 1958.

18. Yuan, S. W.: Foundations of Fluid Mechanics. Englewood Cliffs, New Jersey: Prentice - Hall, Inc., 1967.

19. Henneberry, Hugh M.; and others: A Thermodynamic Analysis of Thrust Augmentation for Nuclear Rockets. NASA TN D-581, 1961.

20. Sewell, K. G.: A Study of the Effect of Partition Function Cutoff For Hydrogen. L.T.V. Research Center, Report Number 0-71000/2R-19, 1962.

21. Organick, Elliott I.: A Fortran IV Primer. Reading, Massachusetts: Addison - Wesley Publishing Co., 1966.

22. Huff, V. N.; and Morrell, V. C.: General Methods for Computation of Equilibrium Composition and Temperature of Chemical Reactions. NASA TN D-2113, 1960.

23. Thompson, D.; and others: A Fortran Program to Calculate the Flow Field and Performance of an Axially Symmetric DeLaval Nozzle. NASA TN D-2579.

24. Harry, David P.: Formulation and Digital Coding of Approximate Hydrogen Properties for Application to Heat - Transfer and Fluid Flow Computations. NASA TN D-1664, 1961.

25. Vincenti, W. G.; and Kruger, C. H.: Introduction to Physical Gas Dynamics. New York: John Wiley and Sons, Inc., 1965.

26. Zucrow, Maurice J.: Aircraft and Missile Propulsion, Volume I. New York: John Wiley and Sons, Inc., 1958.

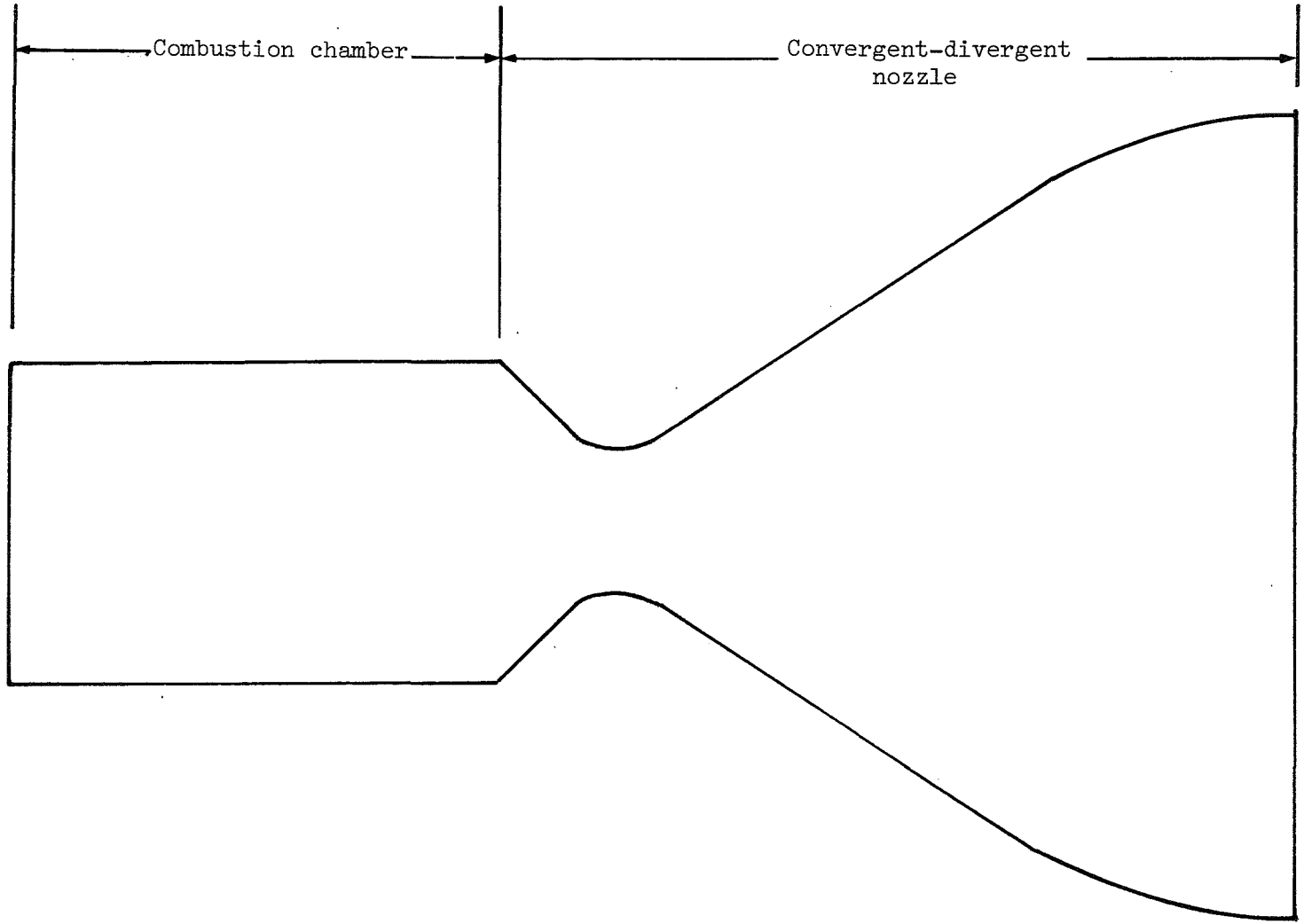

Figure 1.- Rocket engine thrust chamber assembly.

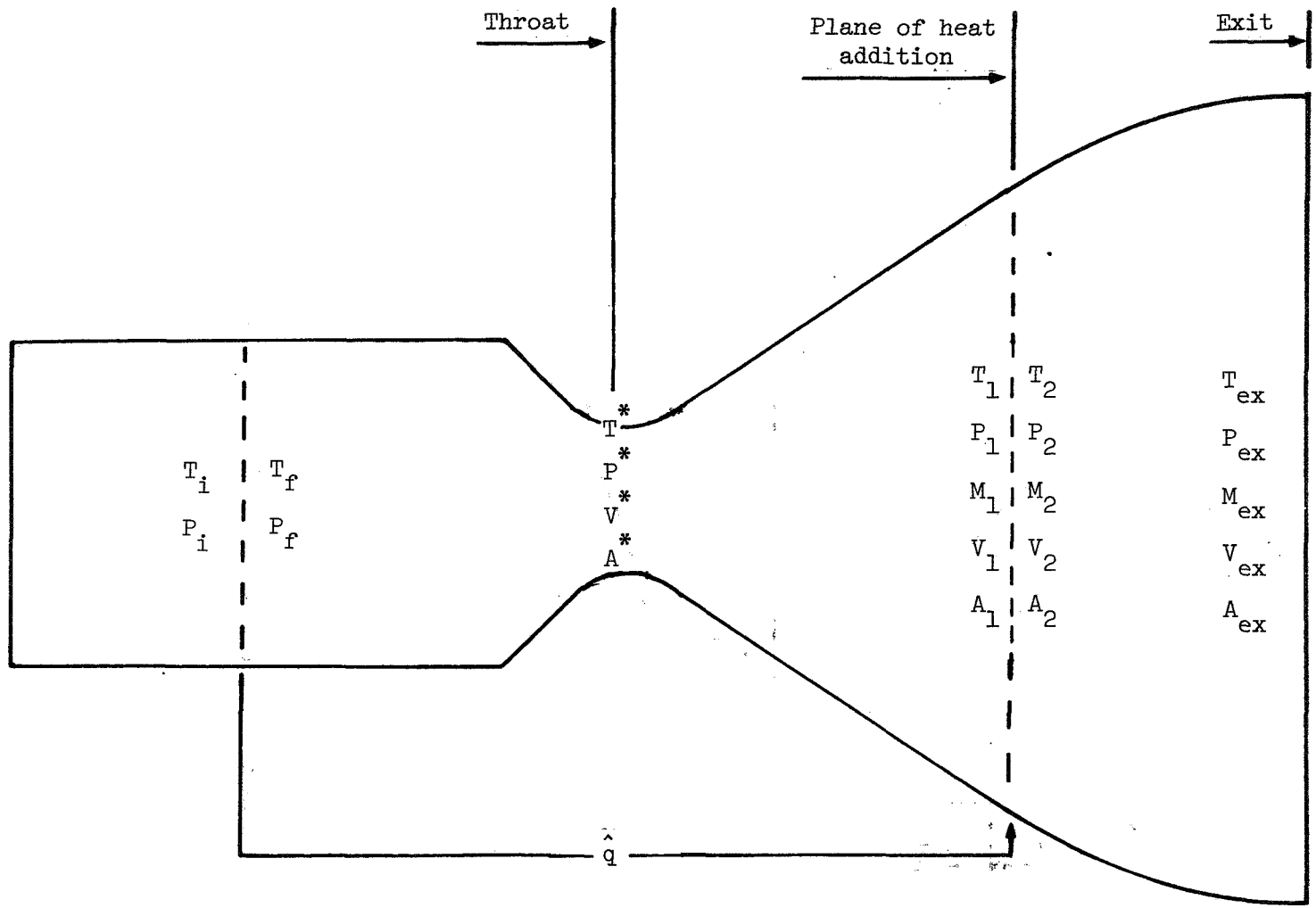

Figure 2.- Thrust chamber assembly for inert gas case.

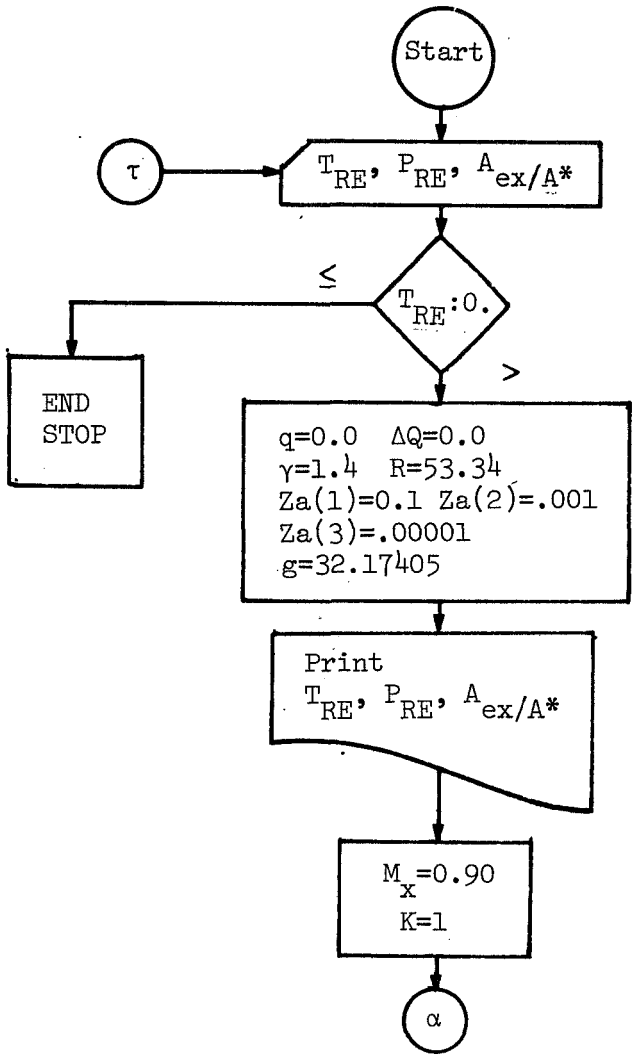

Figure 3.- Flow diagram for inert gas case.

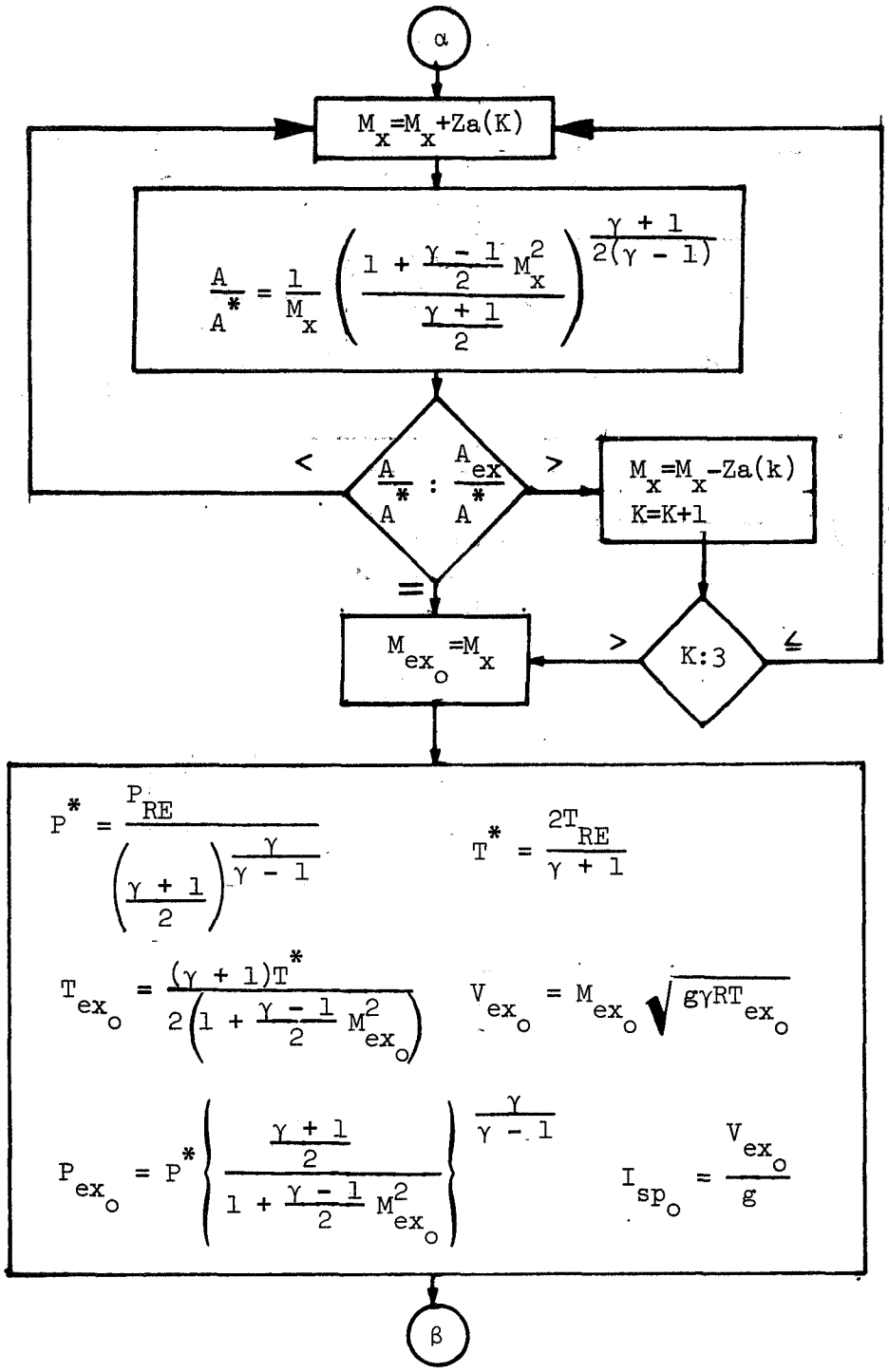

Figure 3.- Continued.

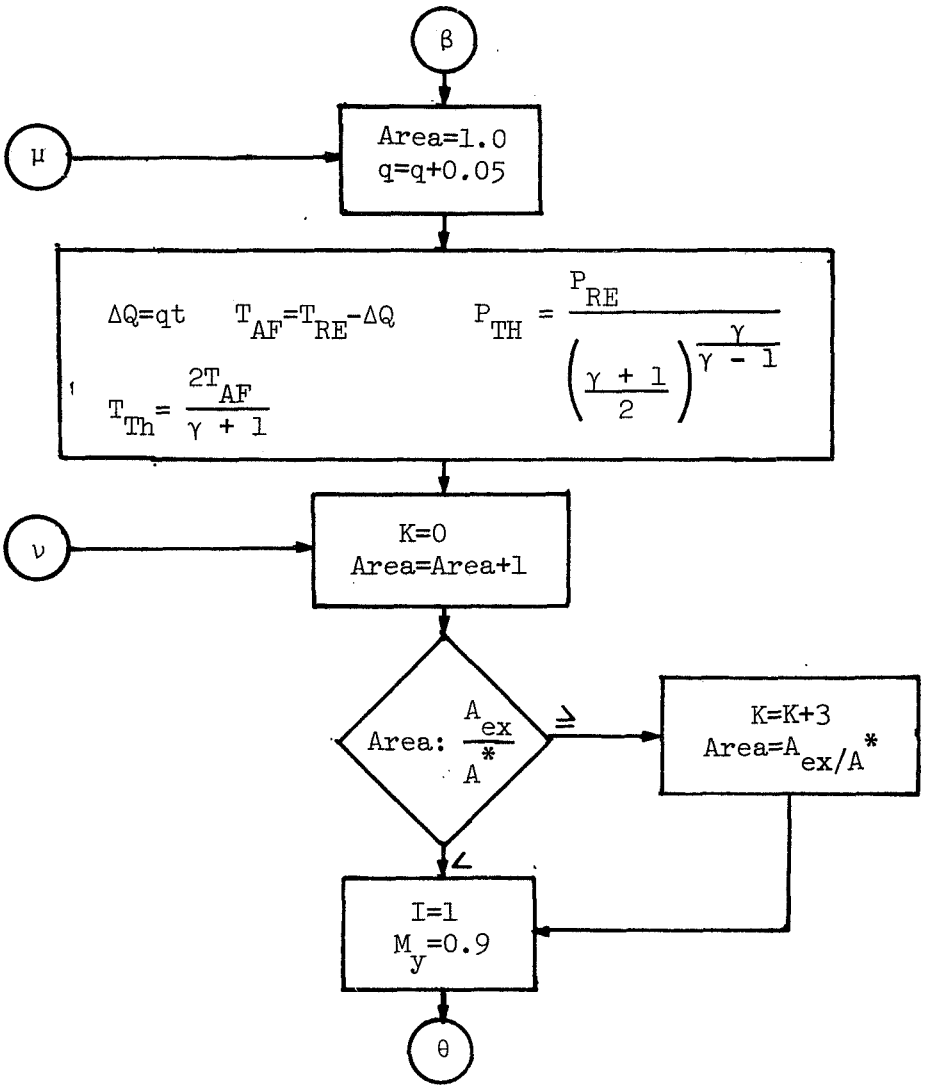

Figure 3.- Continued.

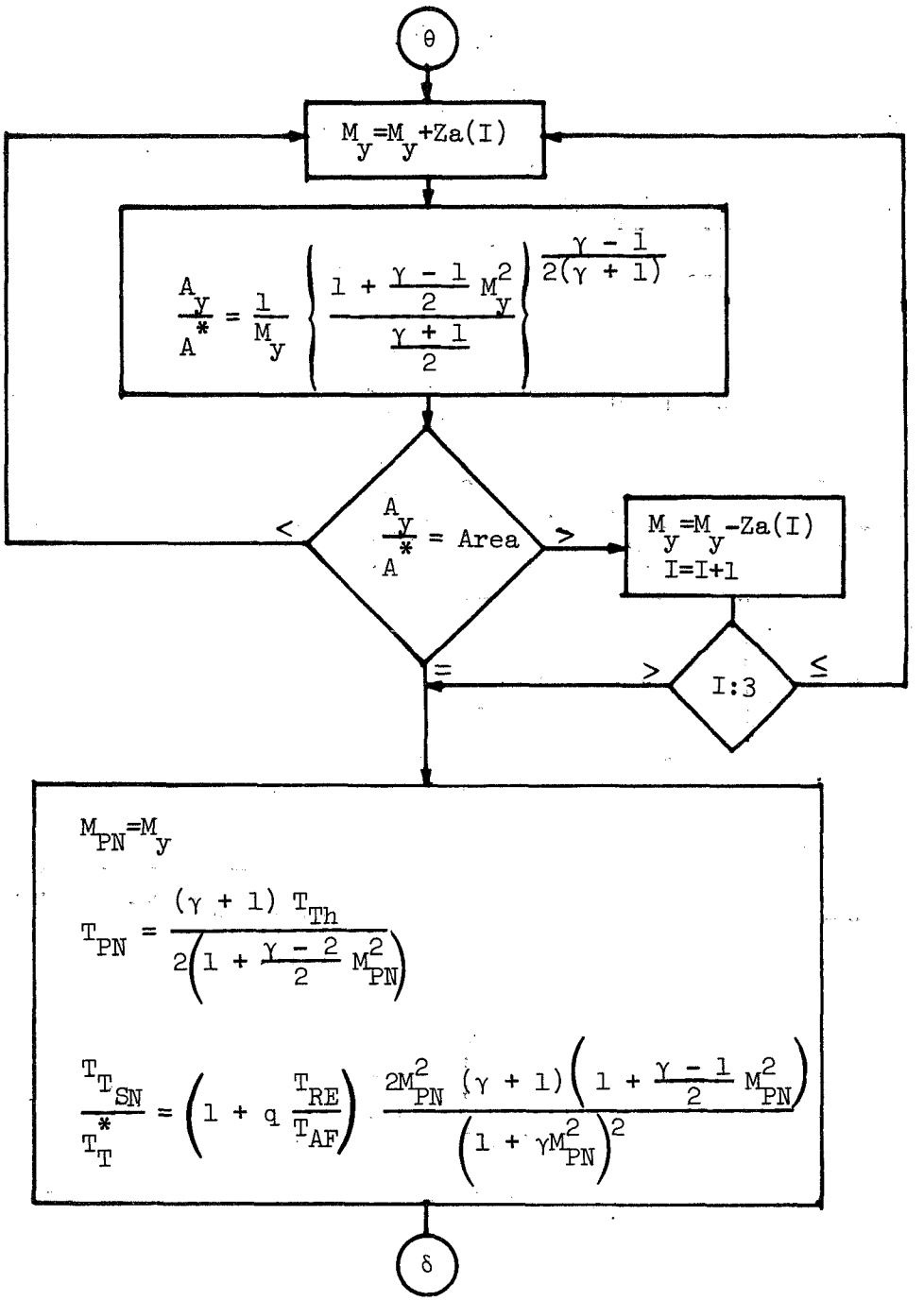

Figure 3.- Continued.

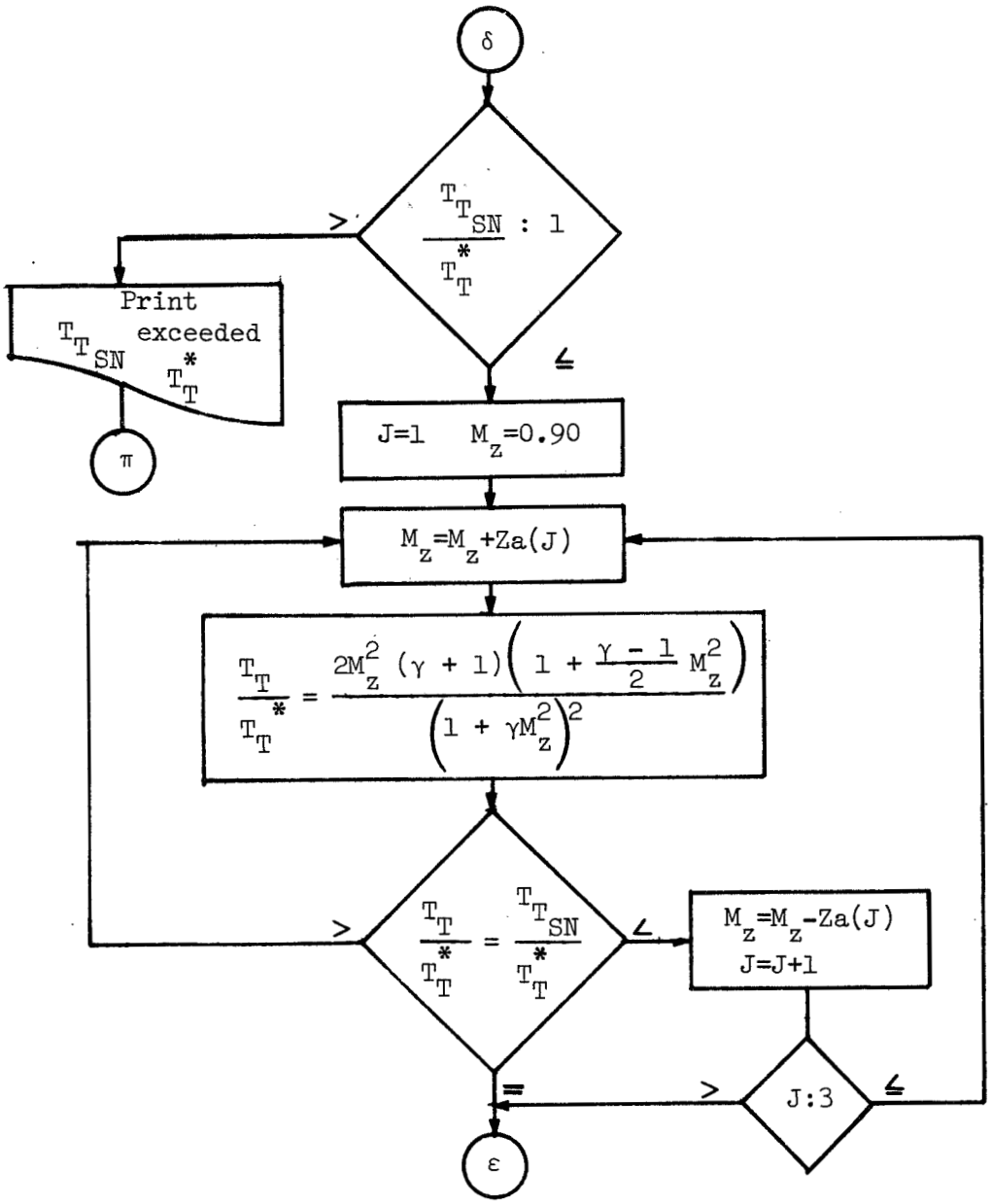

Figure 3.- Continued.

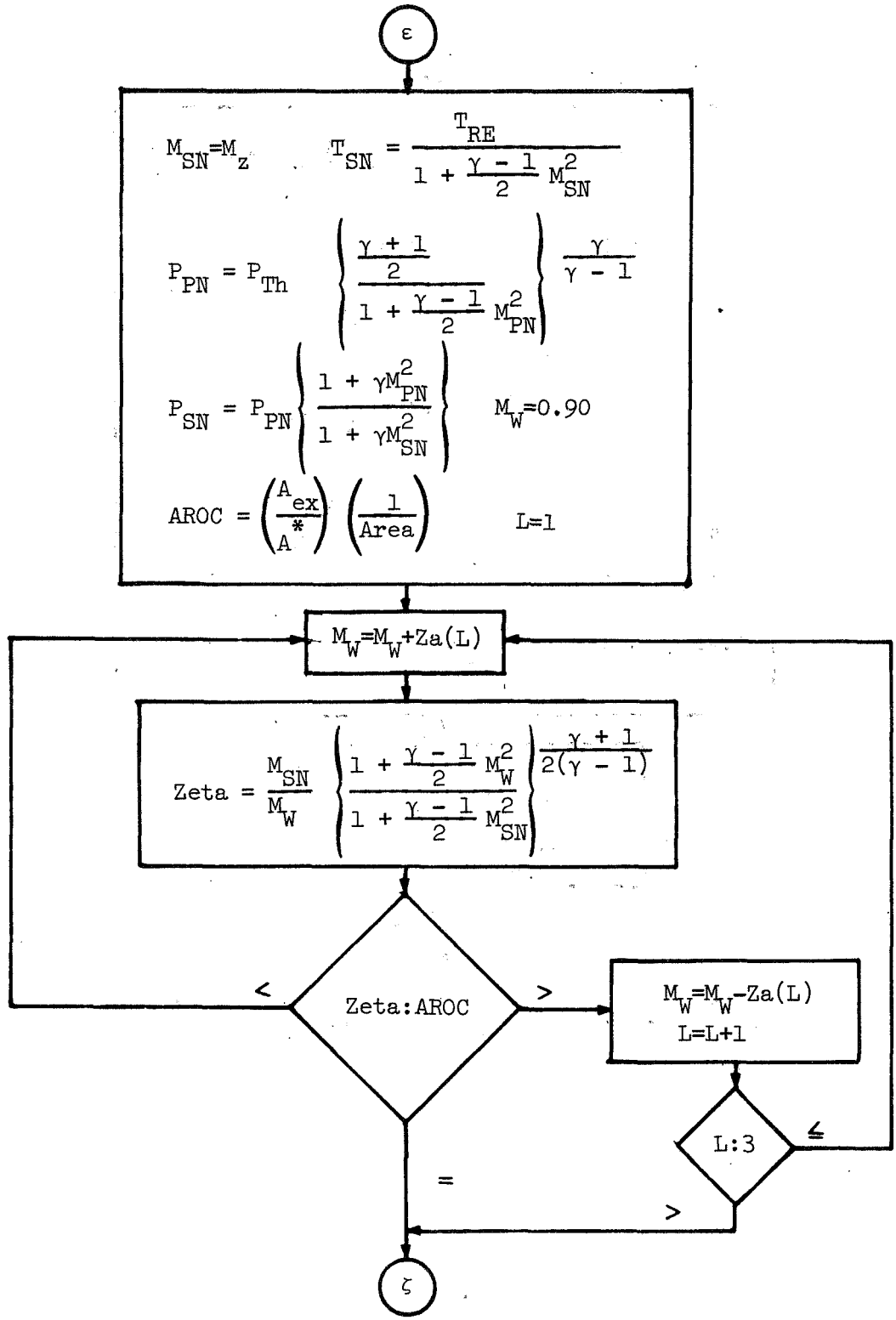

Figure 3.- Continued.

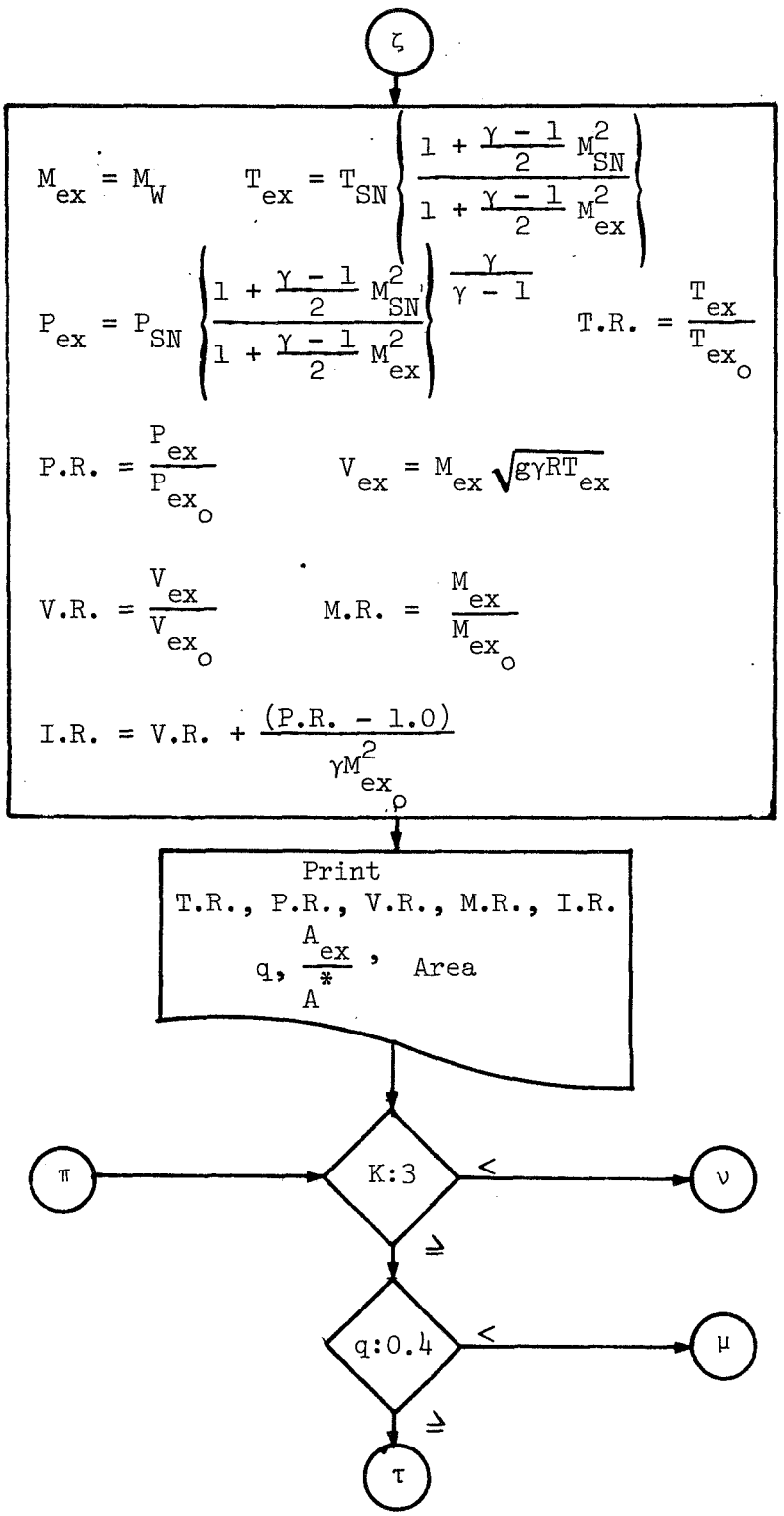

Figure 3.- Concluded.

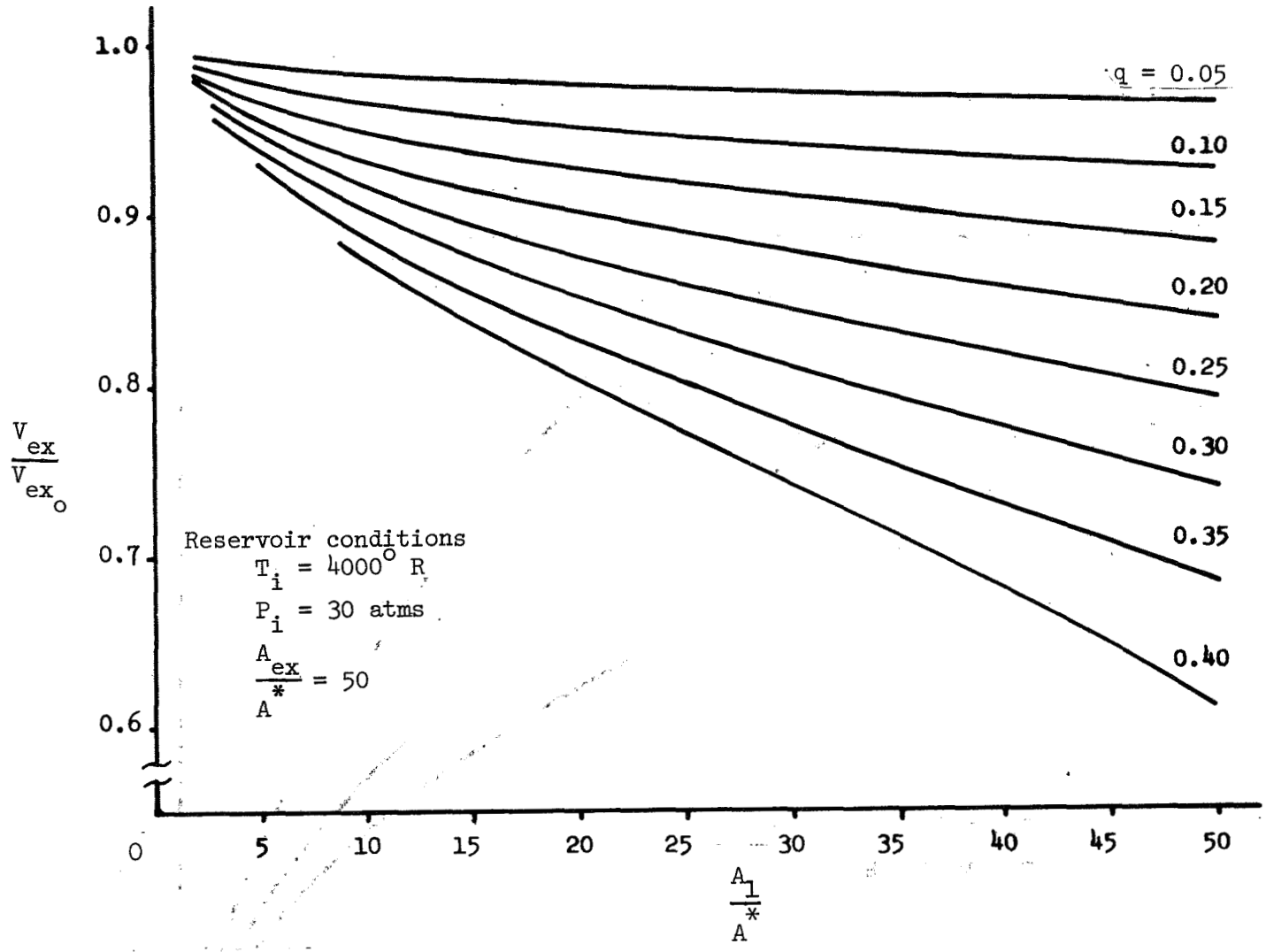

Figure 4.- Exit velocity ratio versus area ratio of heat addition for various values of heat exchange parameter (inert gas).

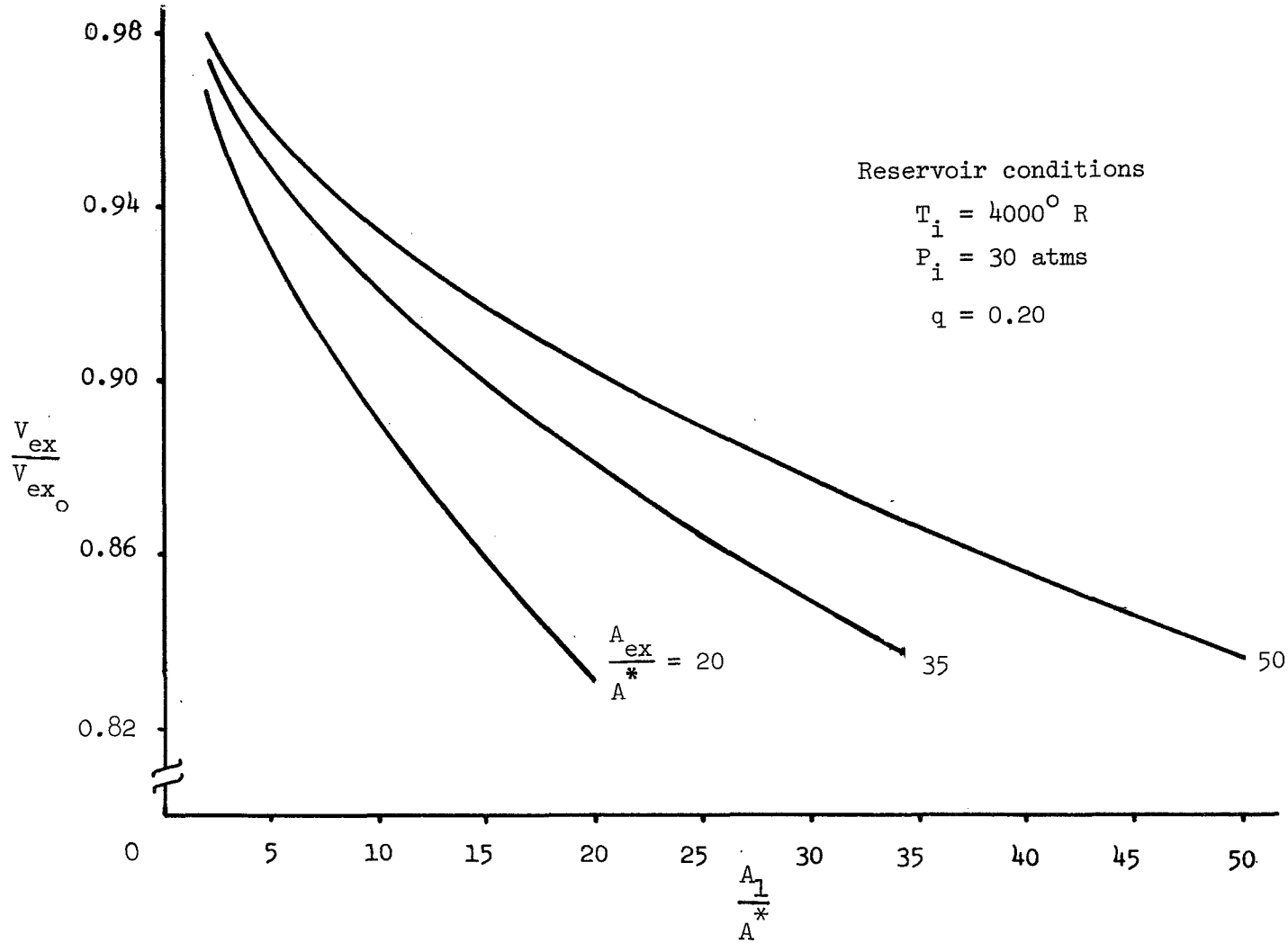

Figure 5.- Exit velocity ratio versus area ratio of heat addition for three values of exit area ratio (inert gas).

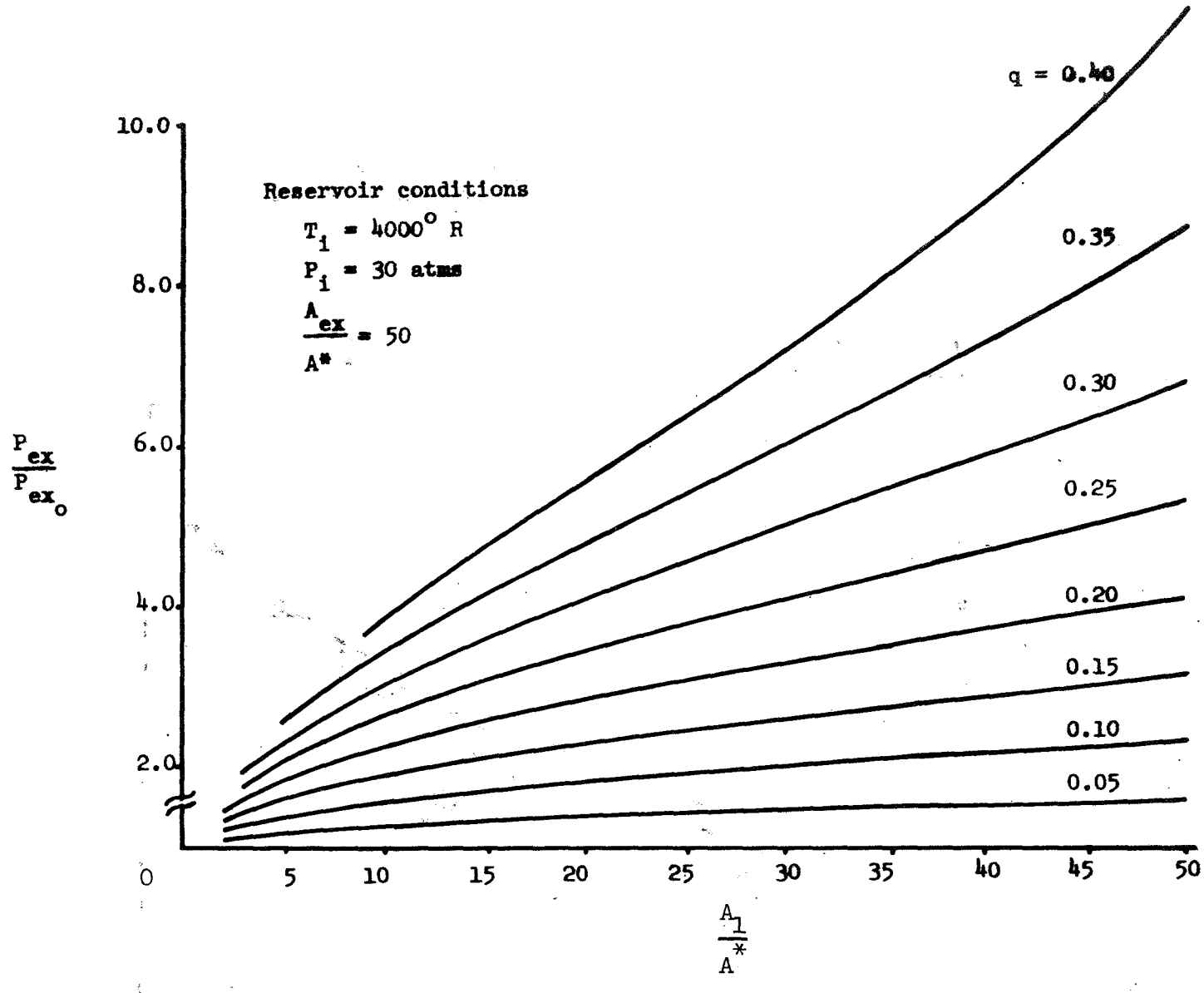

Figure 6.- Exit pressure ratio versus area ratio of heat addition for various values of heat exchange parameter (inert gas).

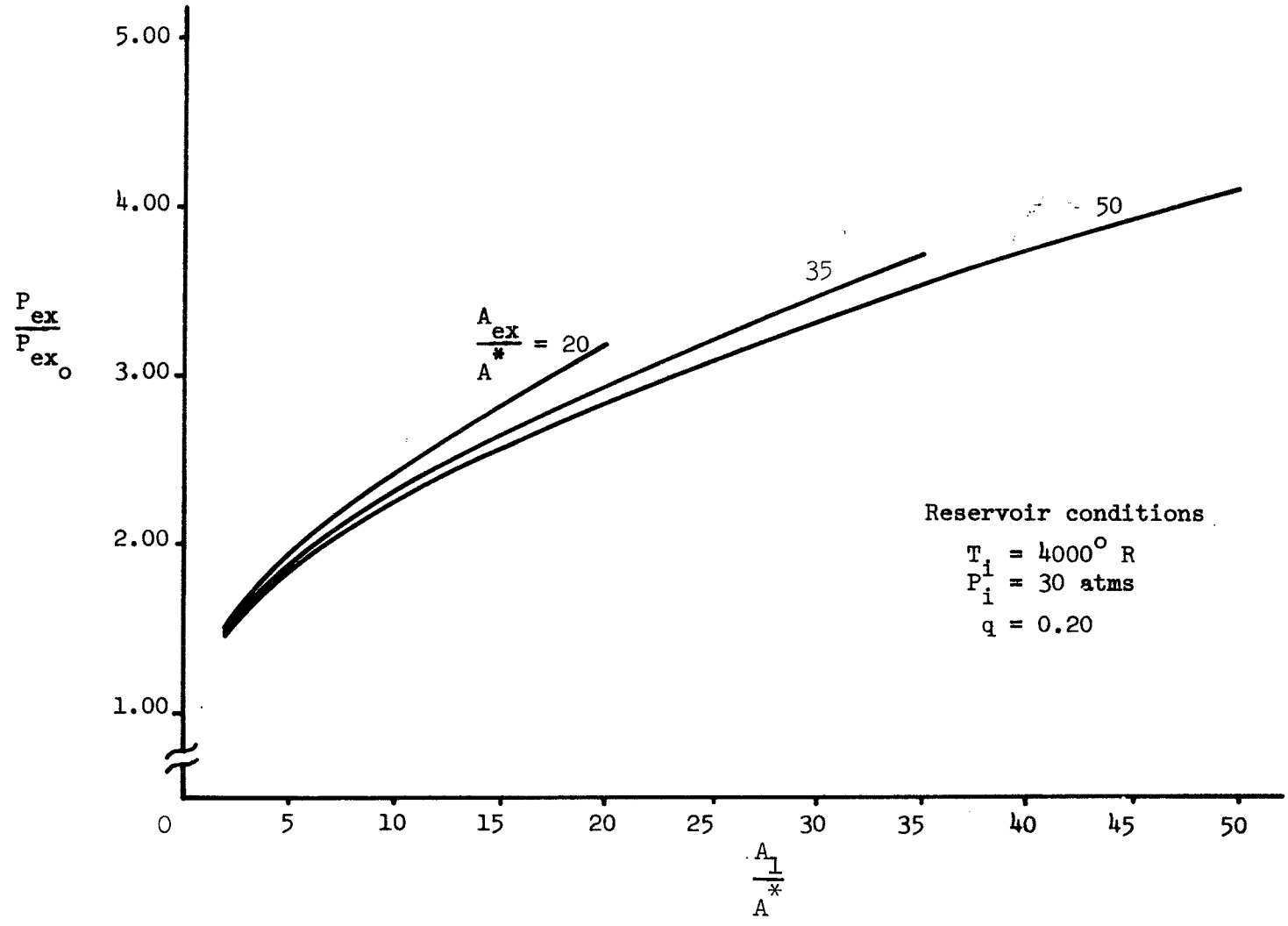

Figure 7.- Exit pressure ratio versus area ratio of heat addition for three values of exit area ratio (inert gas).

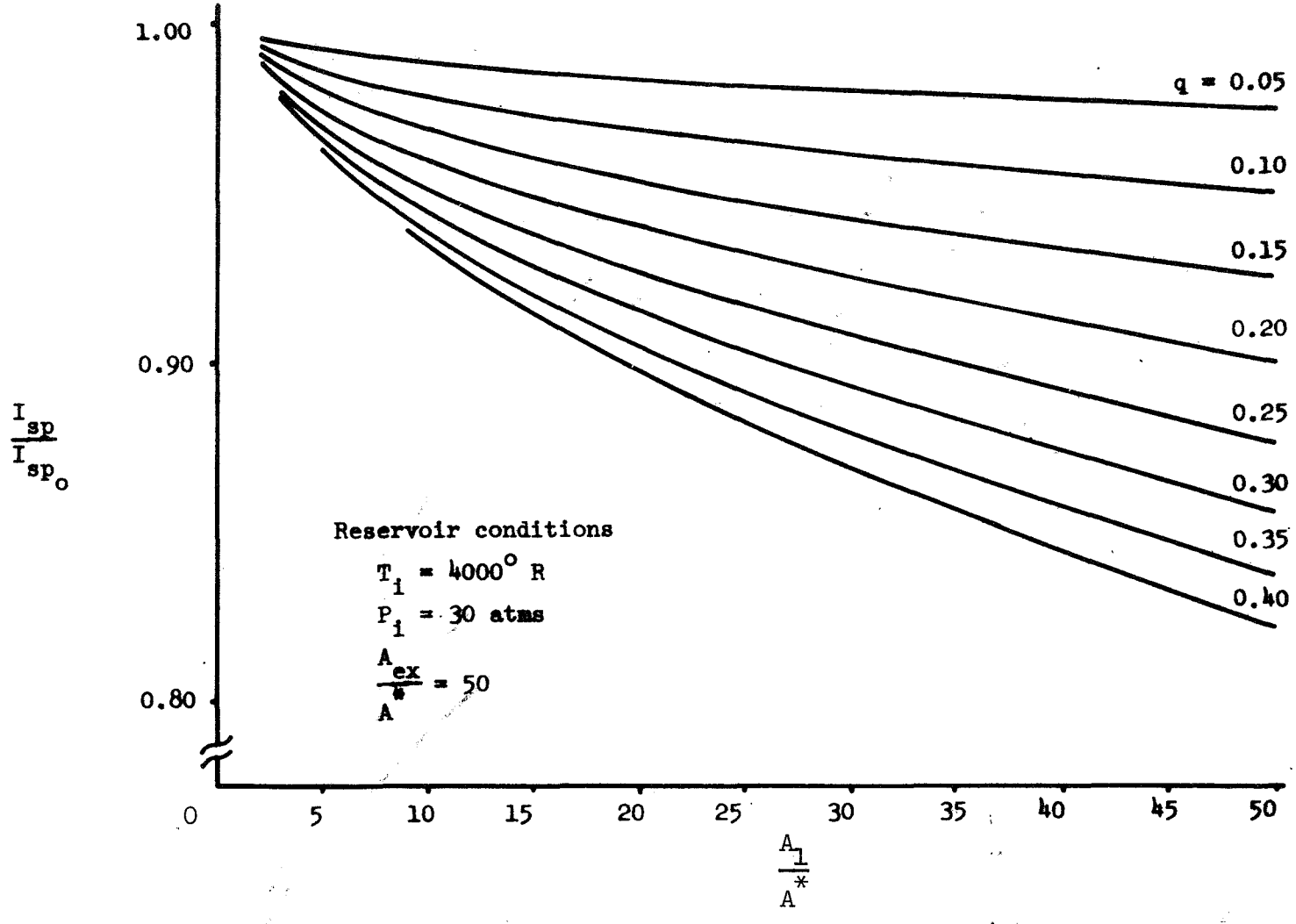

Figure 8.- Specific impulse ratio versus area ratio of heat addition for various values of heat exchange parameter (inert gas).

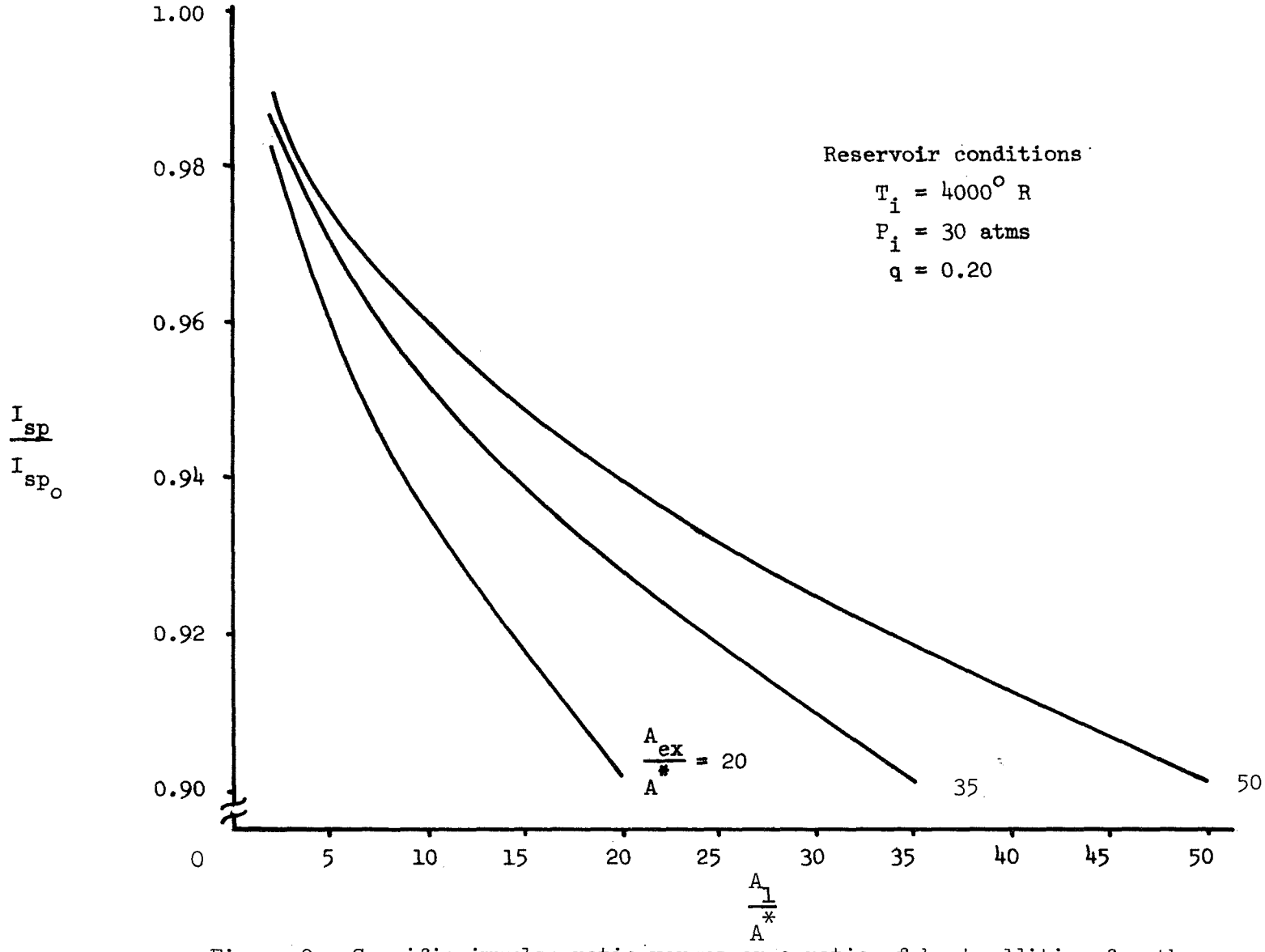

Figure 9.- Specific impulse ratio versus area ratio of heat addition for three values of exit area ratio (inert gas).

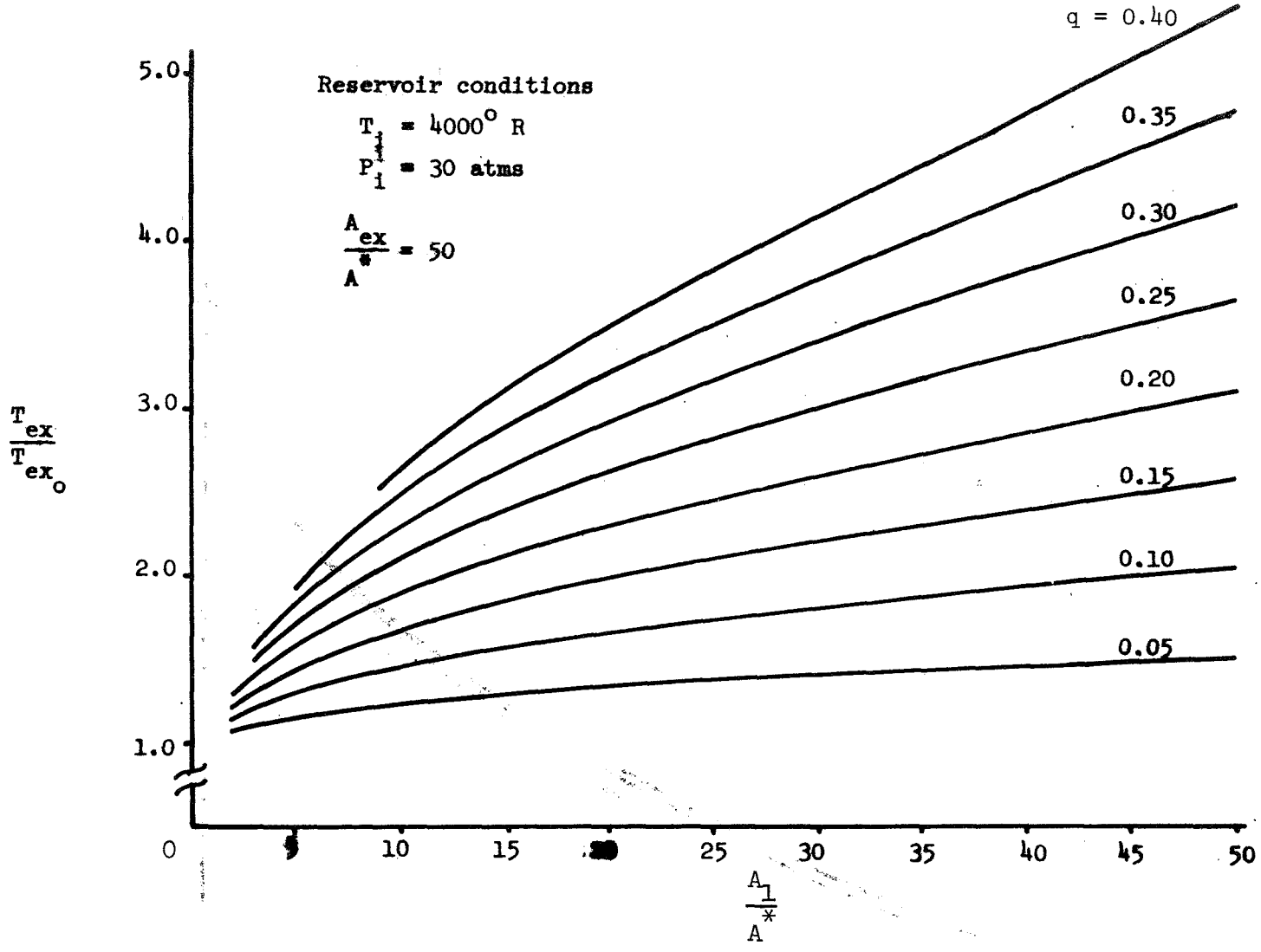

Figure 10.- Exit temperature ratio versus area ratio of heat addition for various values of heat exchange parameter (inert gas).

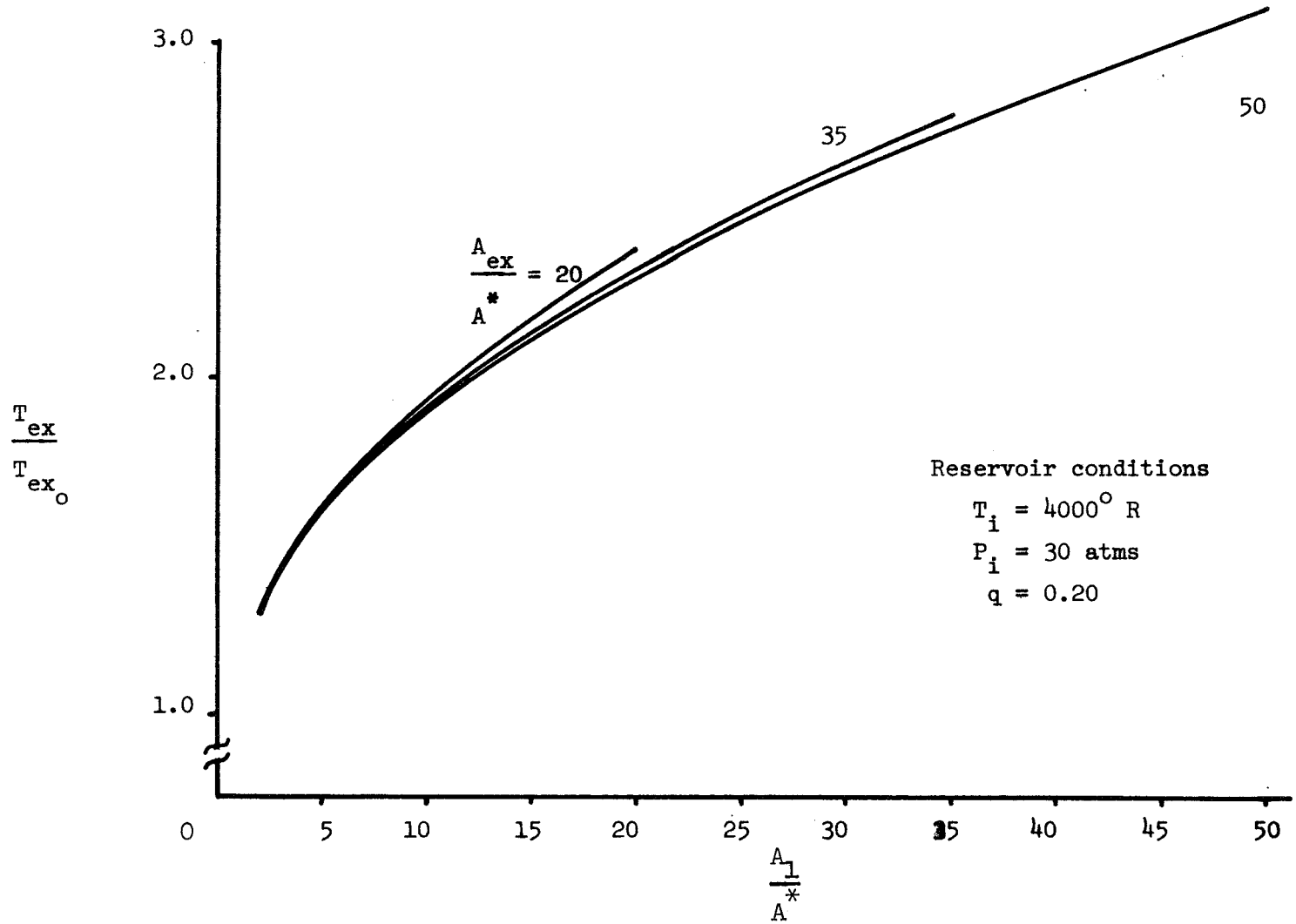

Figure 11.- Exit temperature ratio versus area ratio of heat addition for three values of exit area ratio (inert gas).

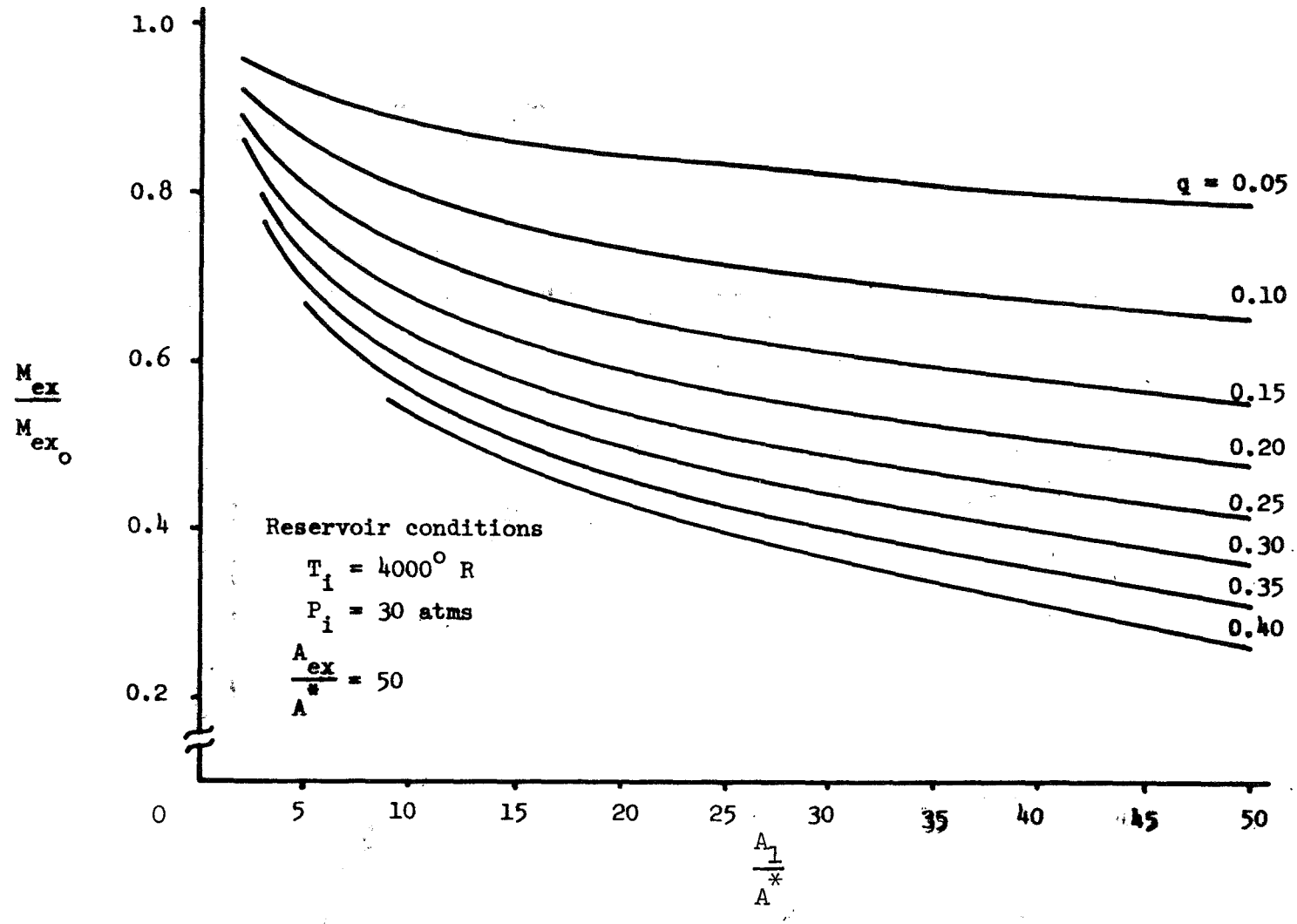

Figure 12.- Exit Mach number ratio versus area ratio of heat addition for various values of heat exchange parameter (inert gas).

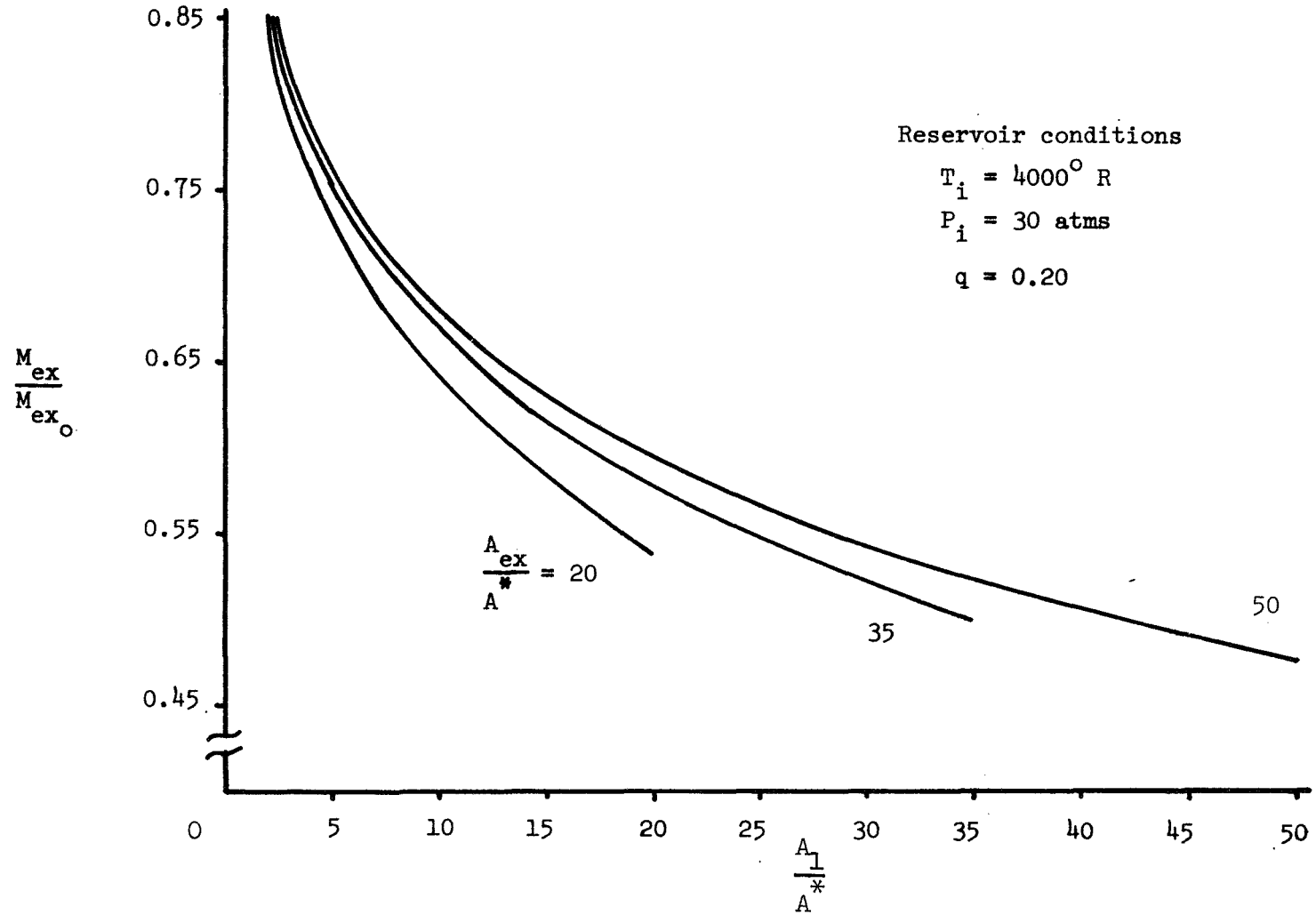

Figure 13.- Exit Mach number ratio versus area ratio of heat addition for three values of exit area ratio (inert gas).

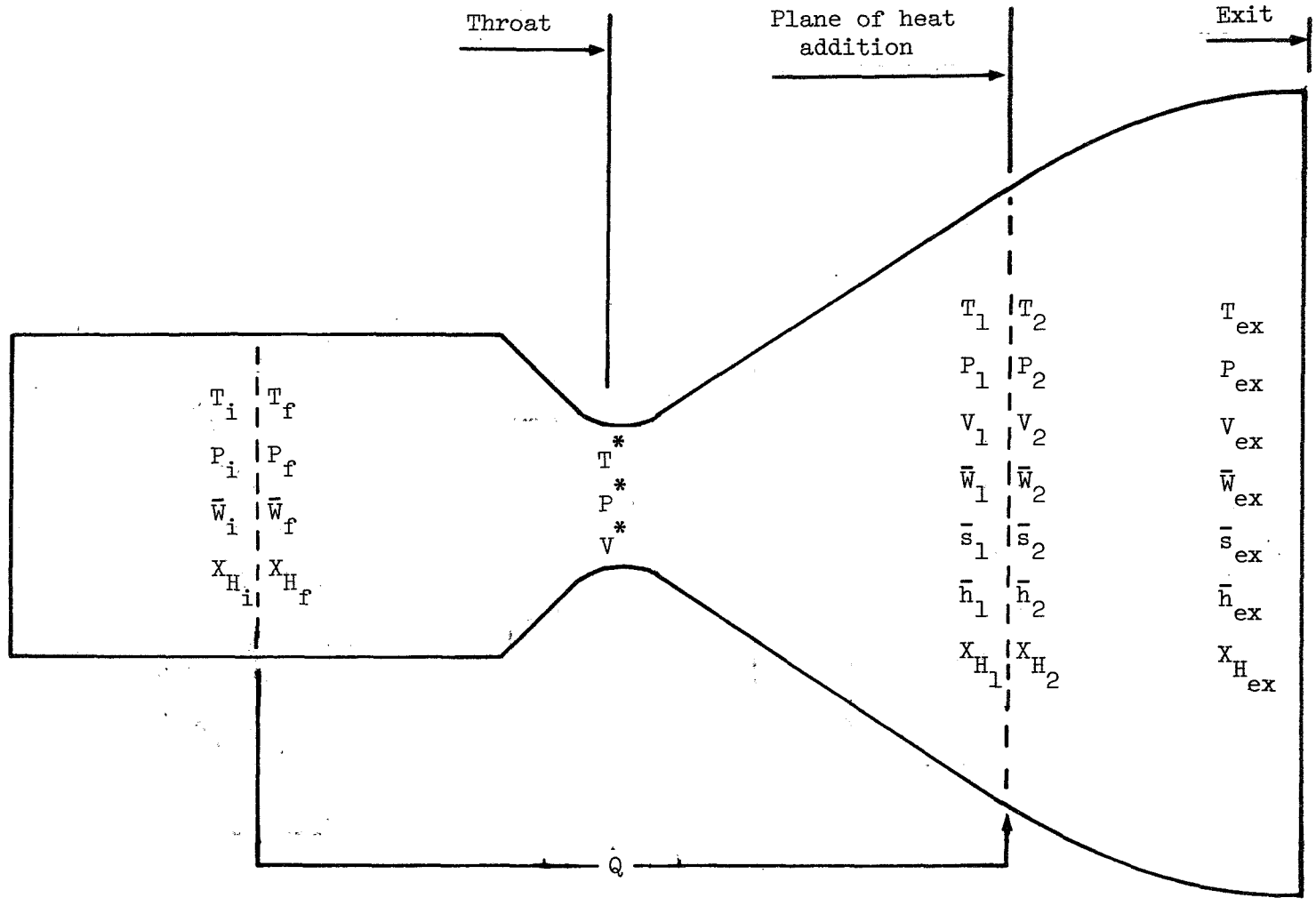

Figure 14.- Thrust chamber assembly for reacting gas case.

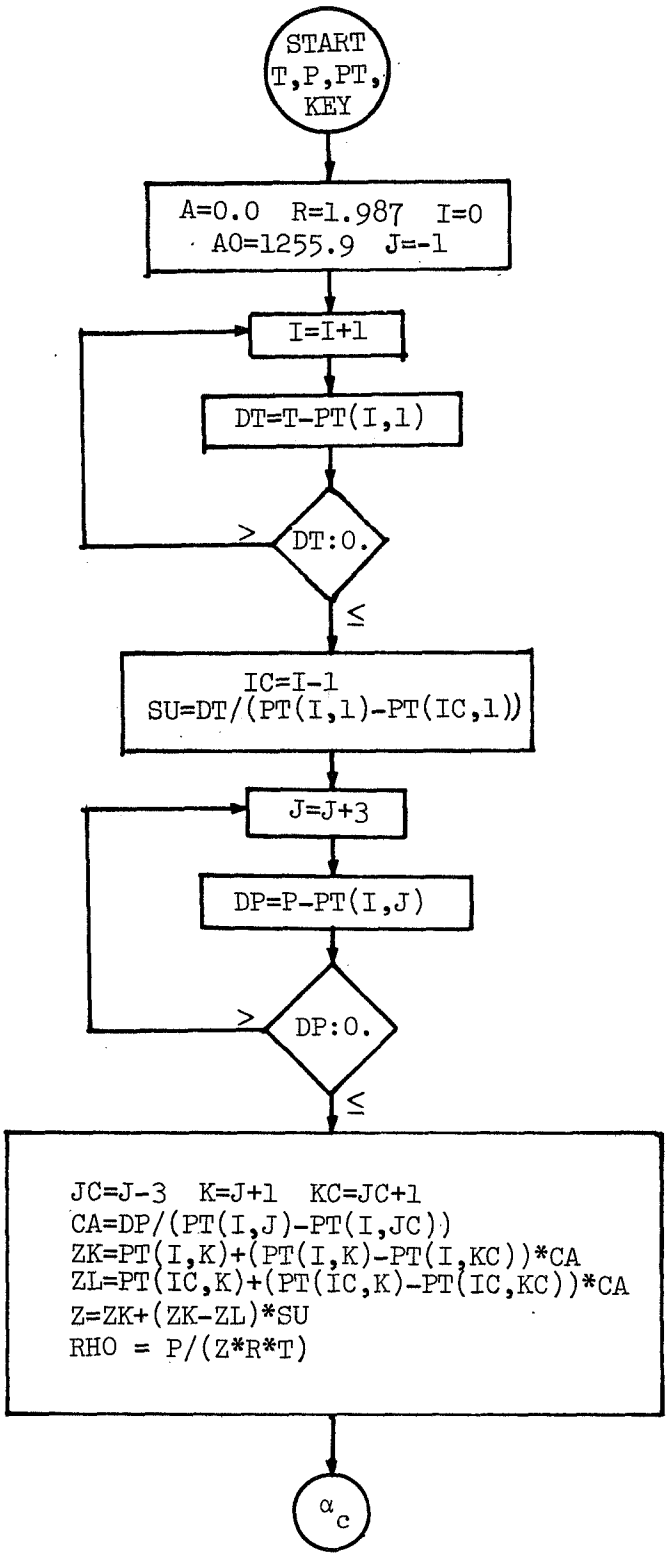

Figure 15.- Flow diagram for Subroutine Comput.

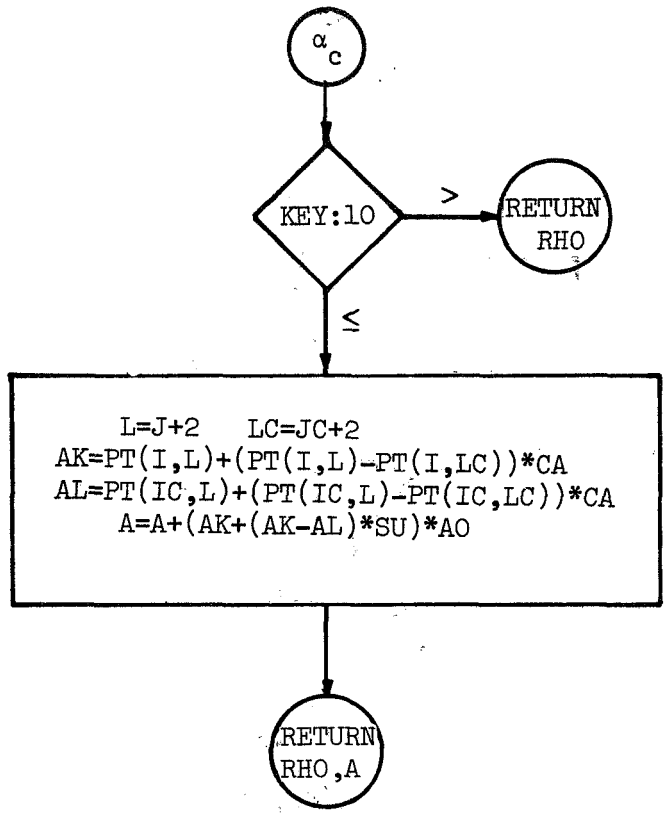

Figure 15.- Concluded.

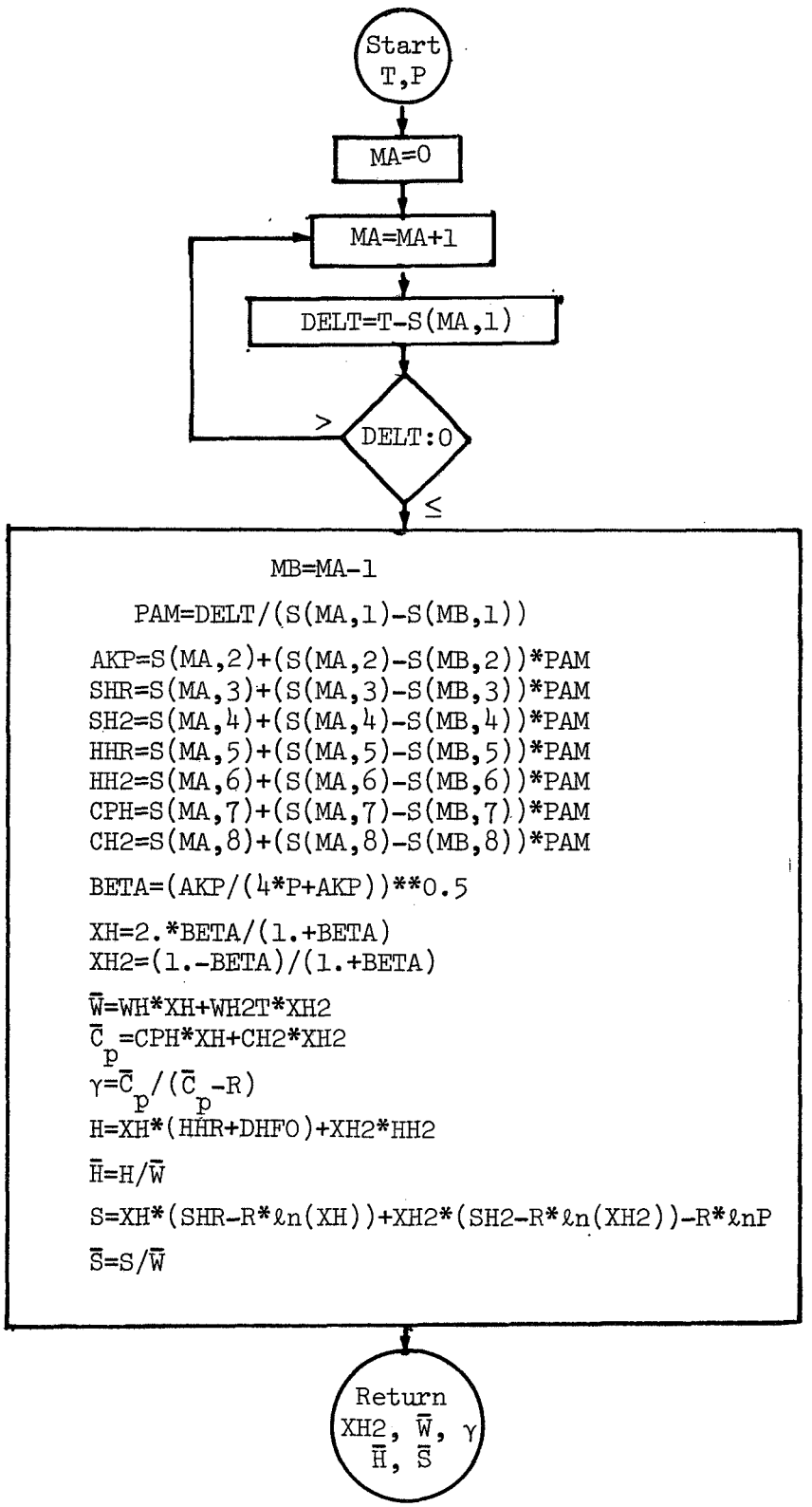

Figure 16.- Flow diagram for Subroutine Scan.

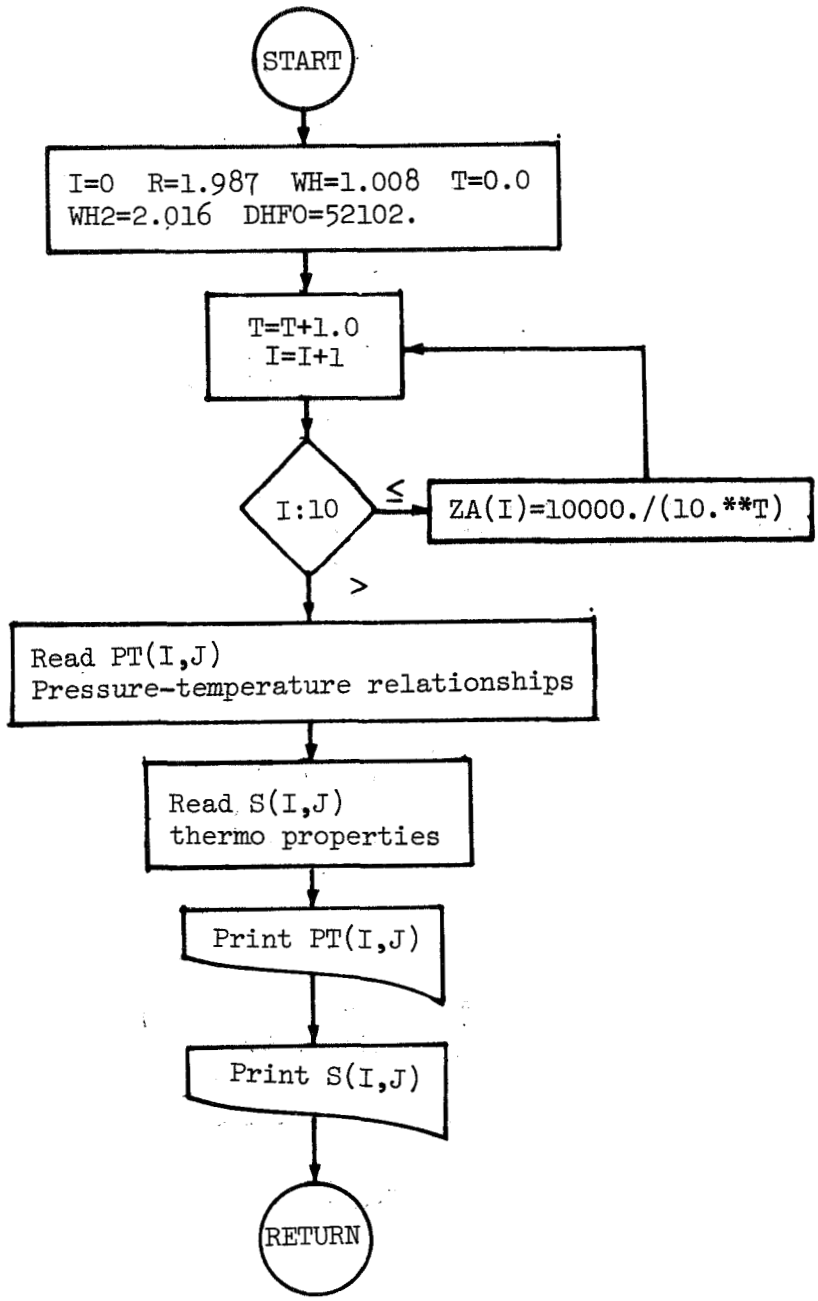

Figure 17.- Flow diagram for Subroutine Input.

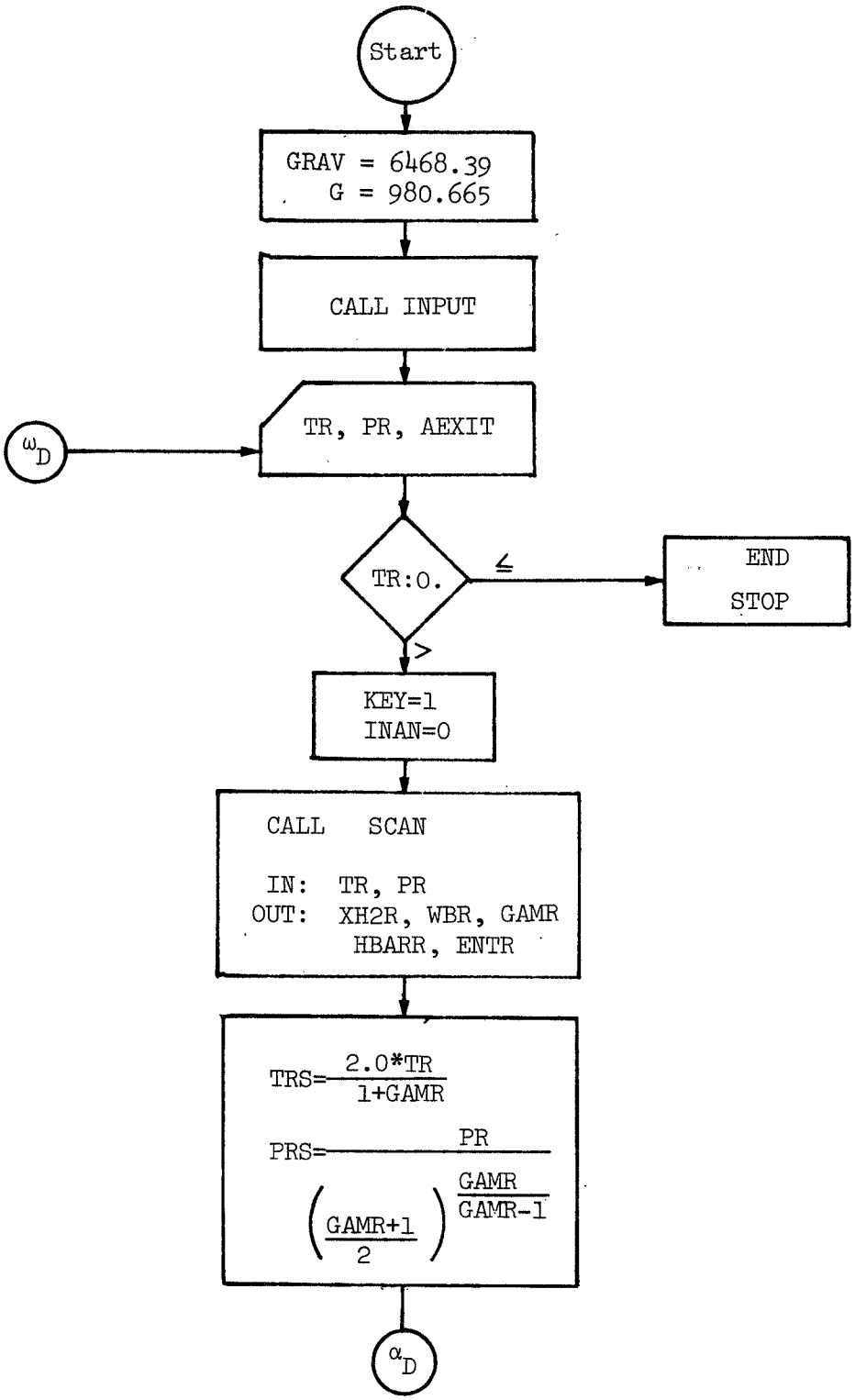

Figure 18.- Flow diagram for Program Dissoc.

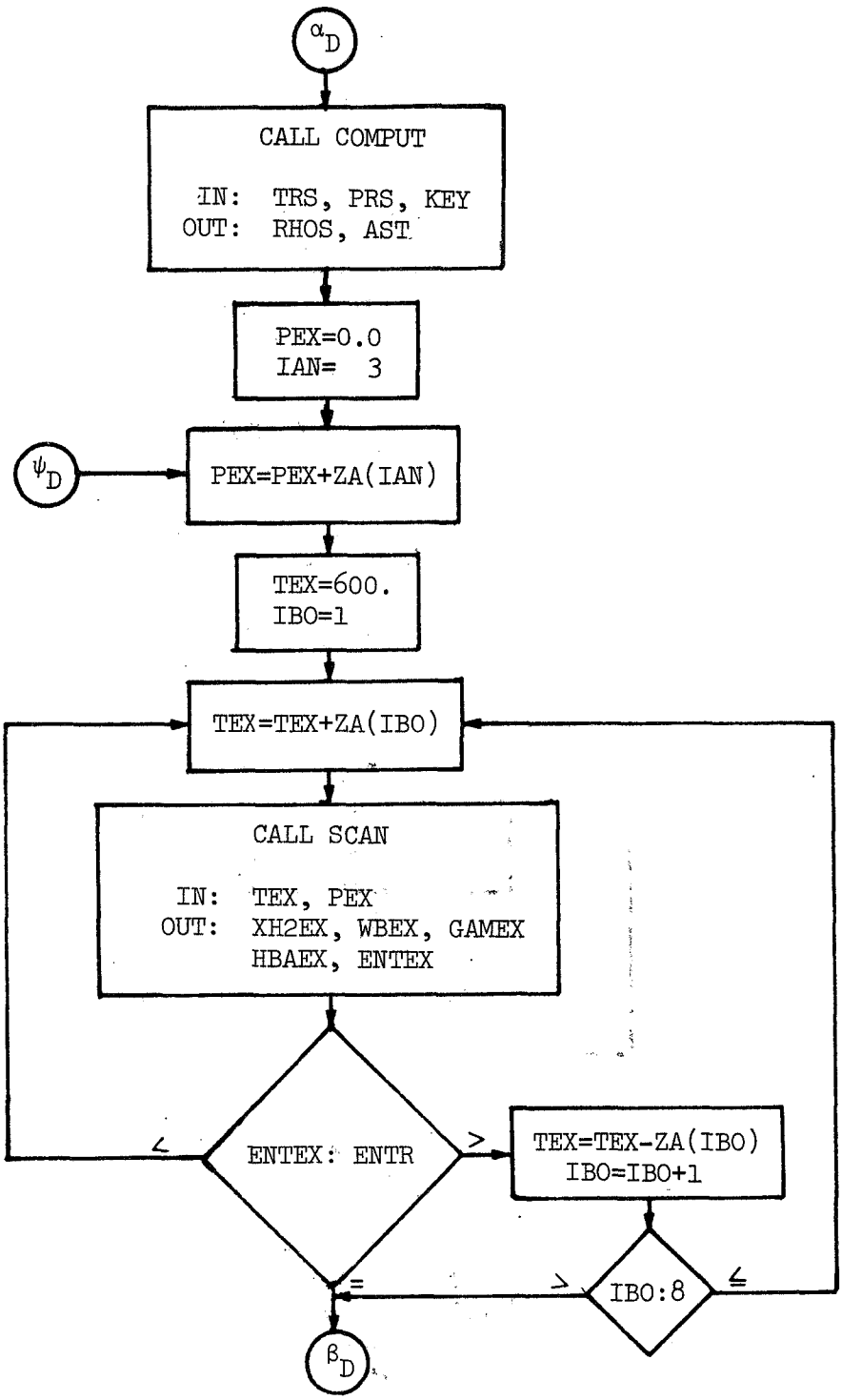

Figure 18.- Continued.

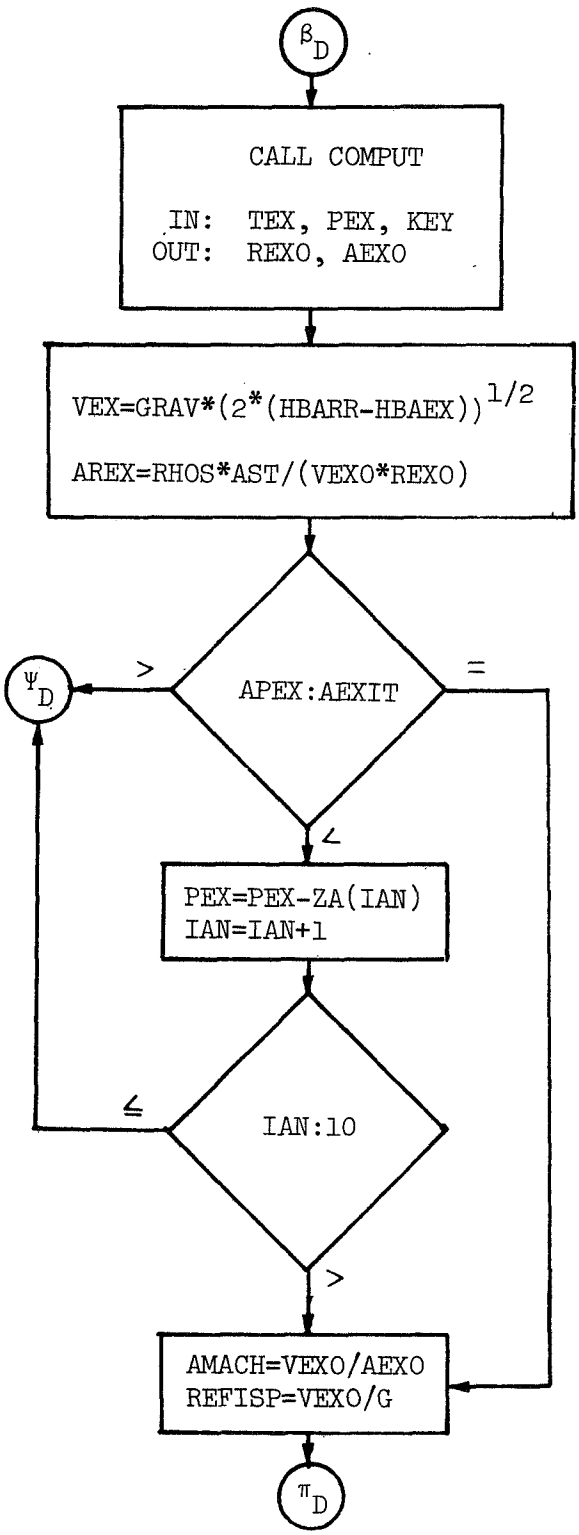

Figure 18.- Continued.

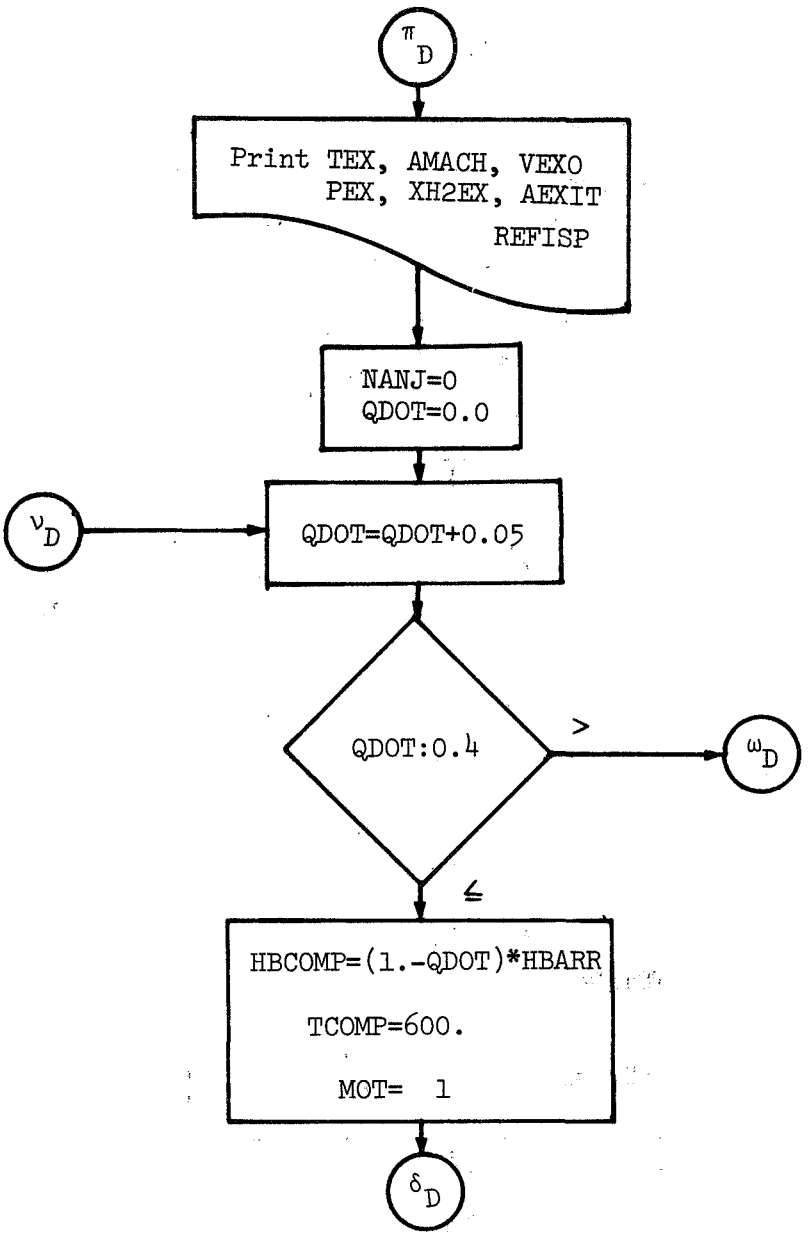

Figure 18.- Continued.

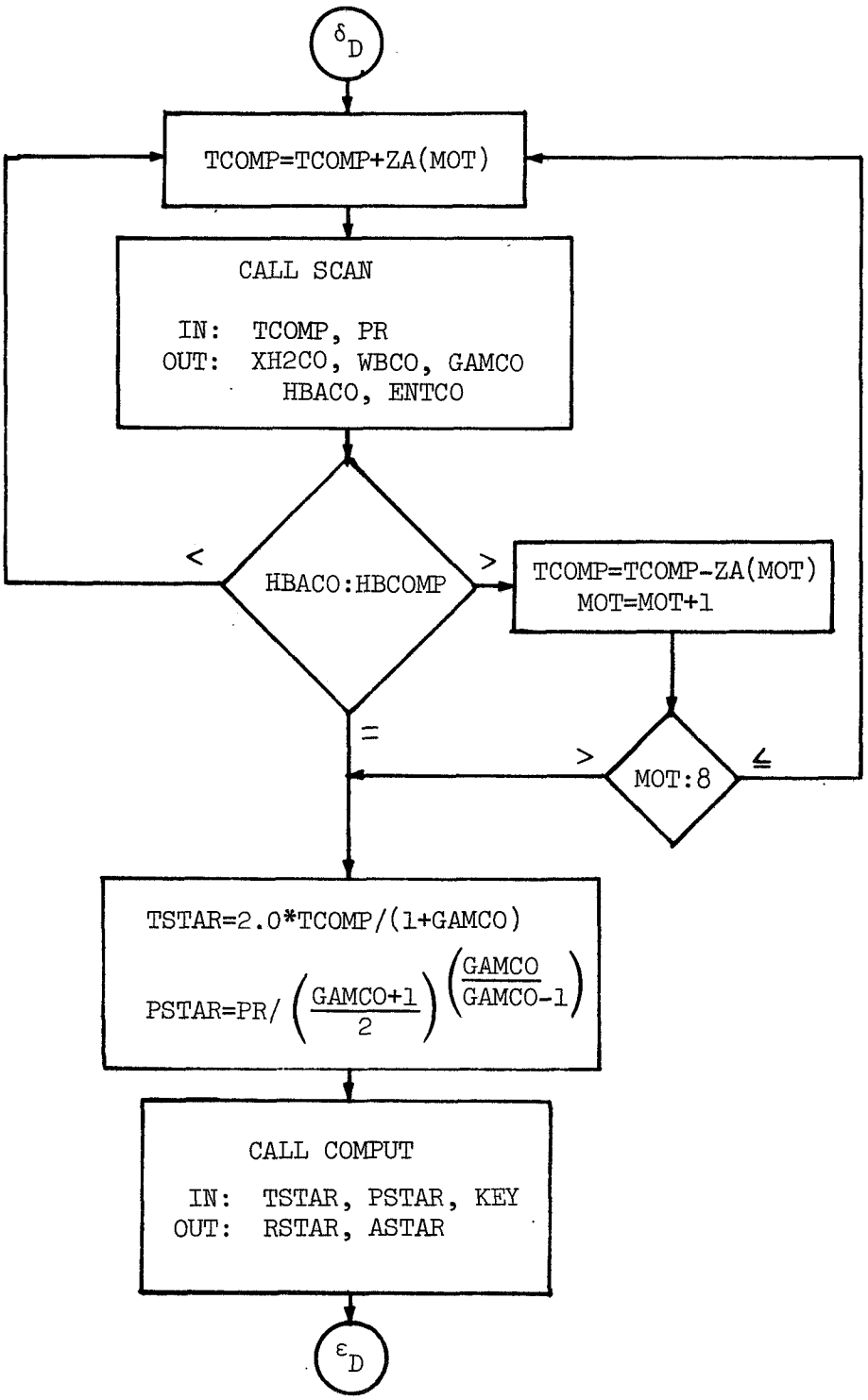

Figure 18.- Continued.

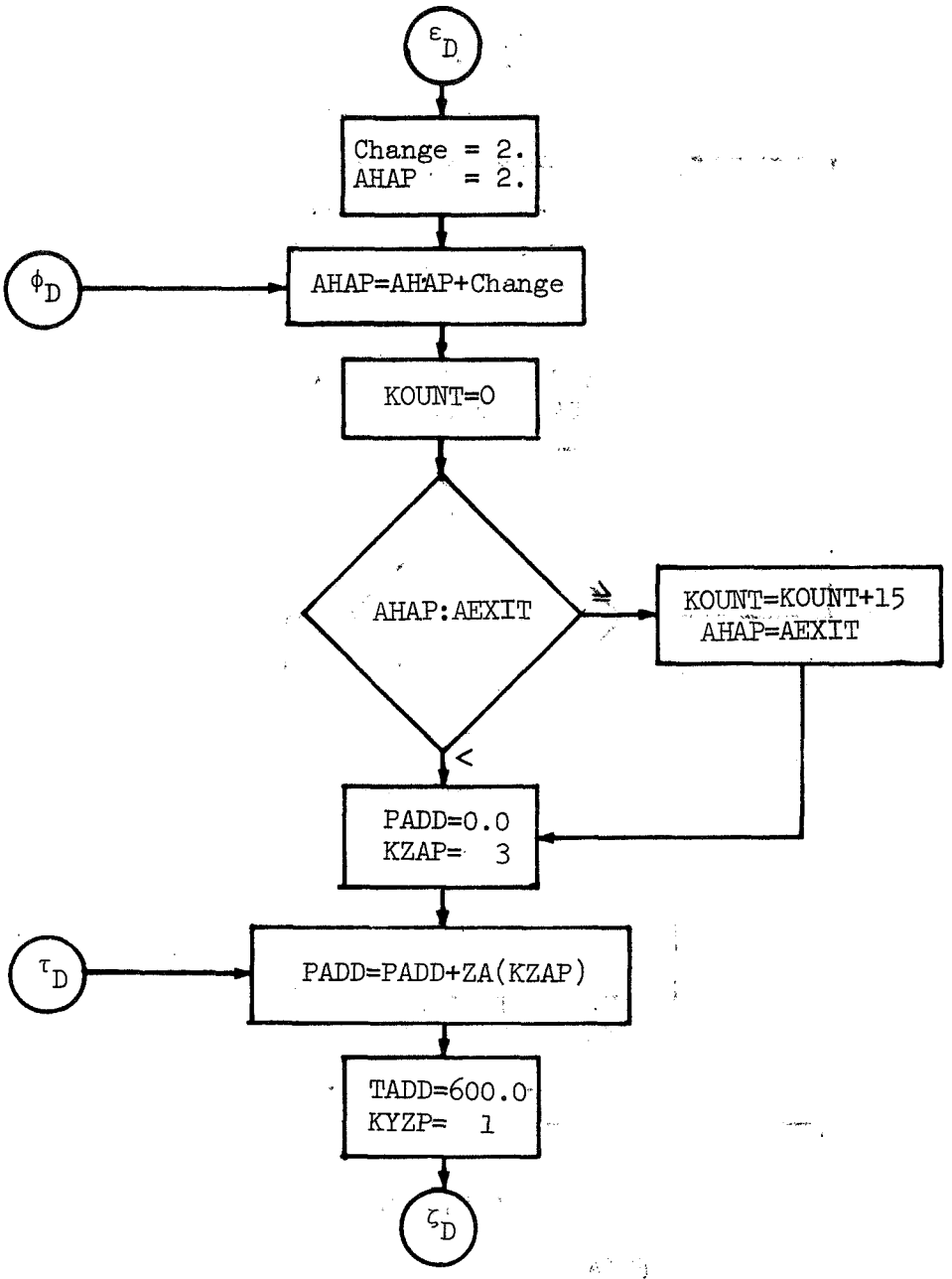

Figure 18.- Continued.

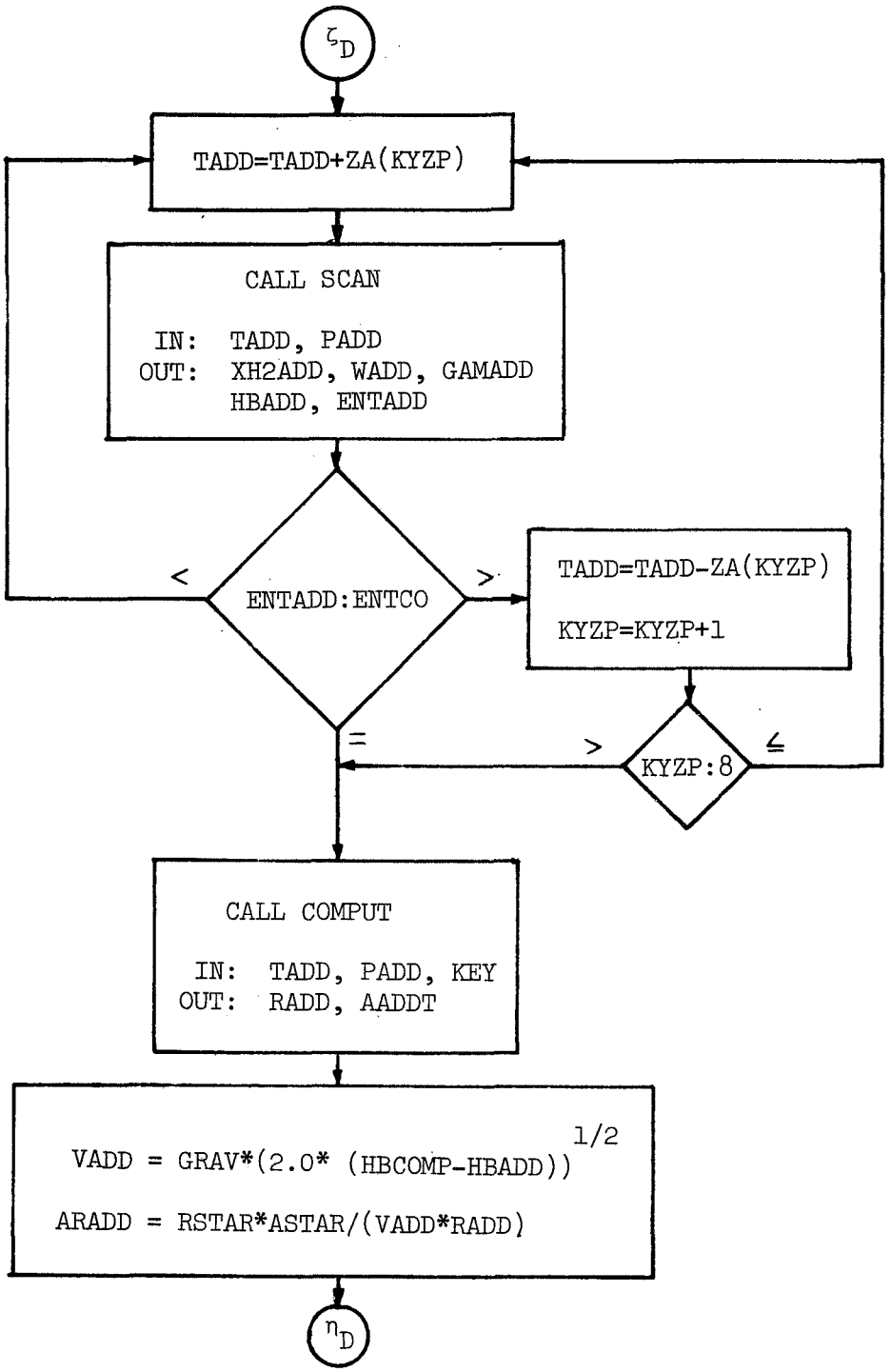

Figure 18.- Continued.

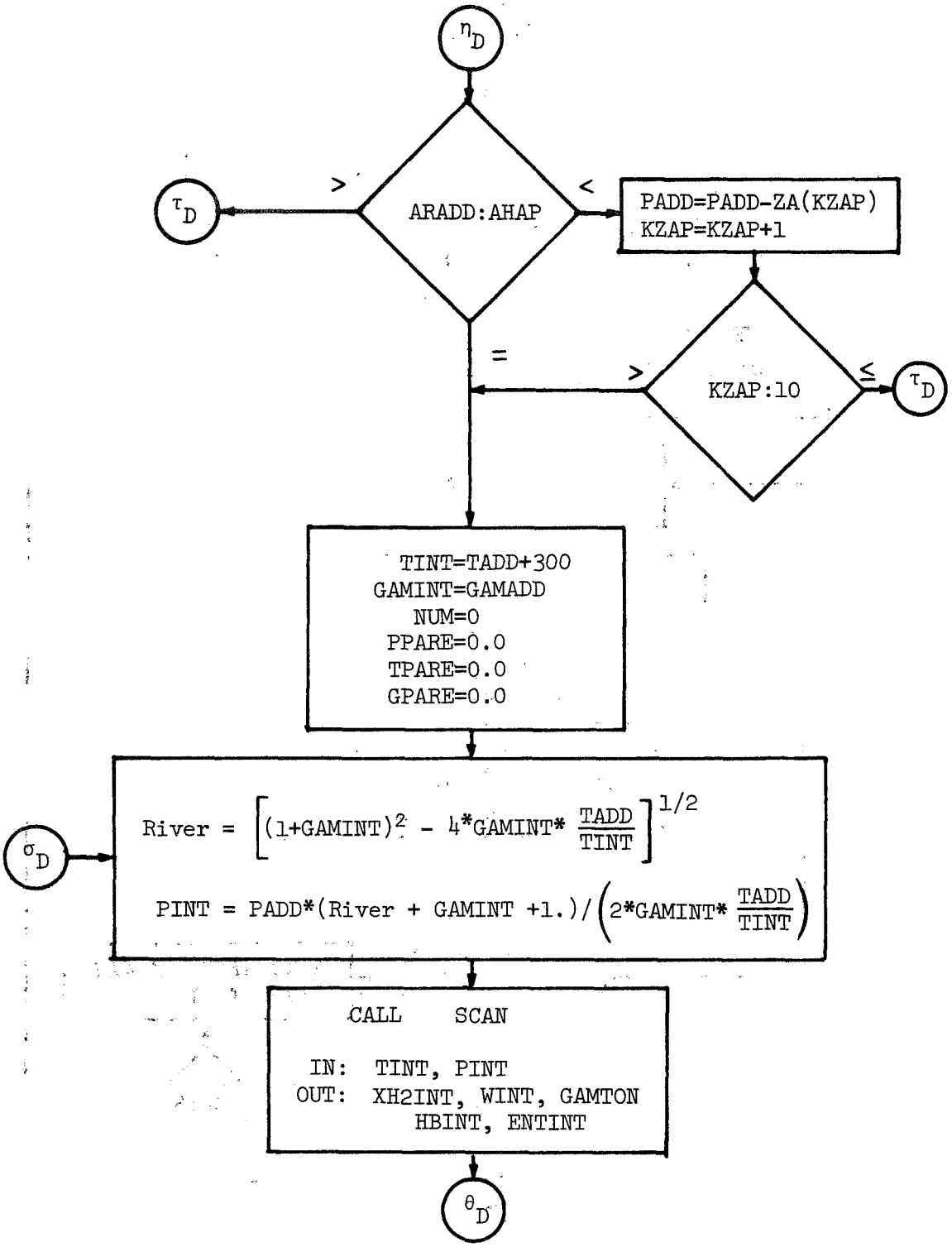

Figure 18.- Continued.

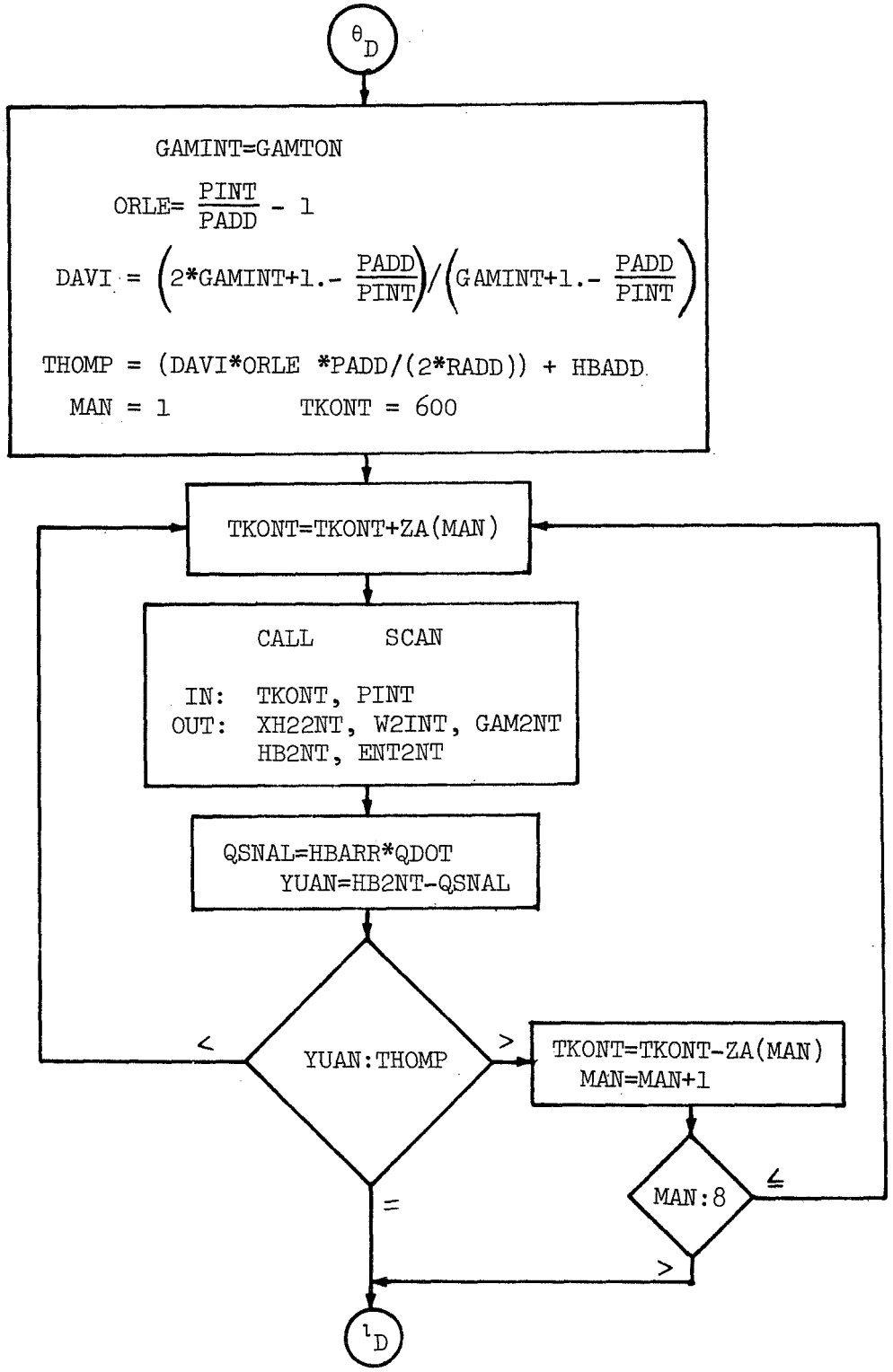

Figure 18.- Continued.

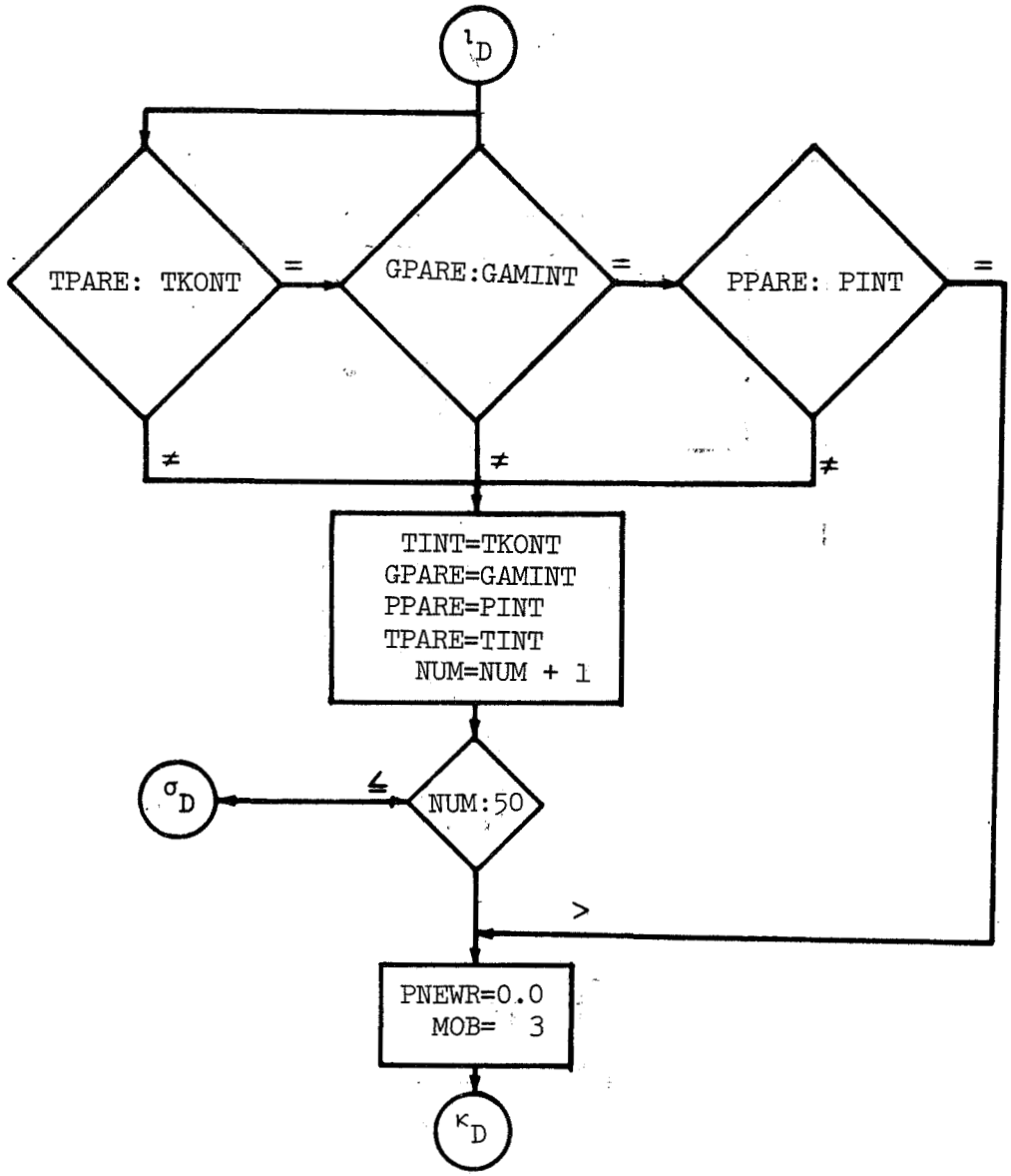

Figure 18.2 Continued.

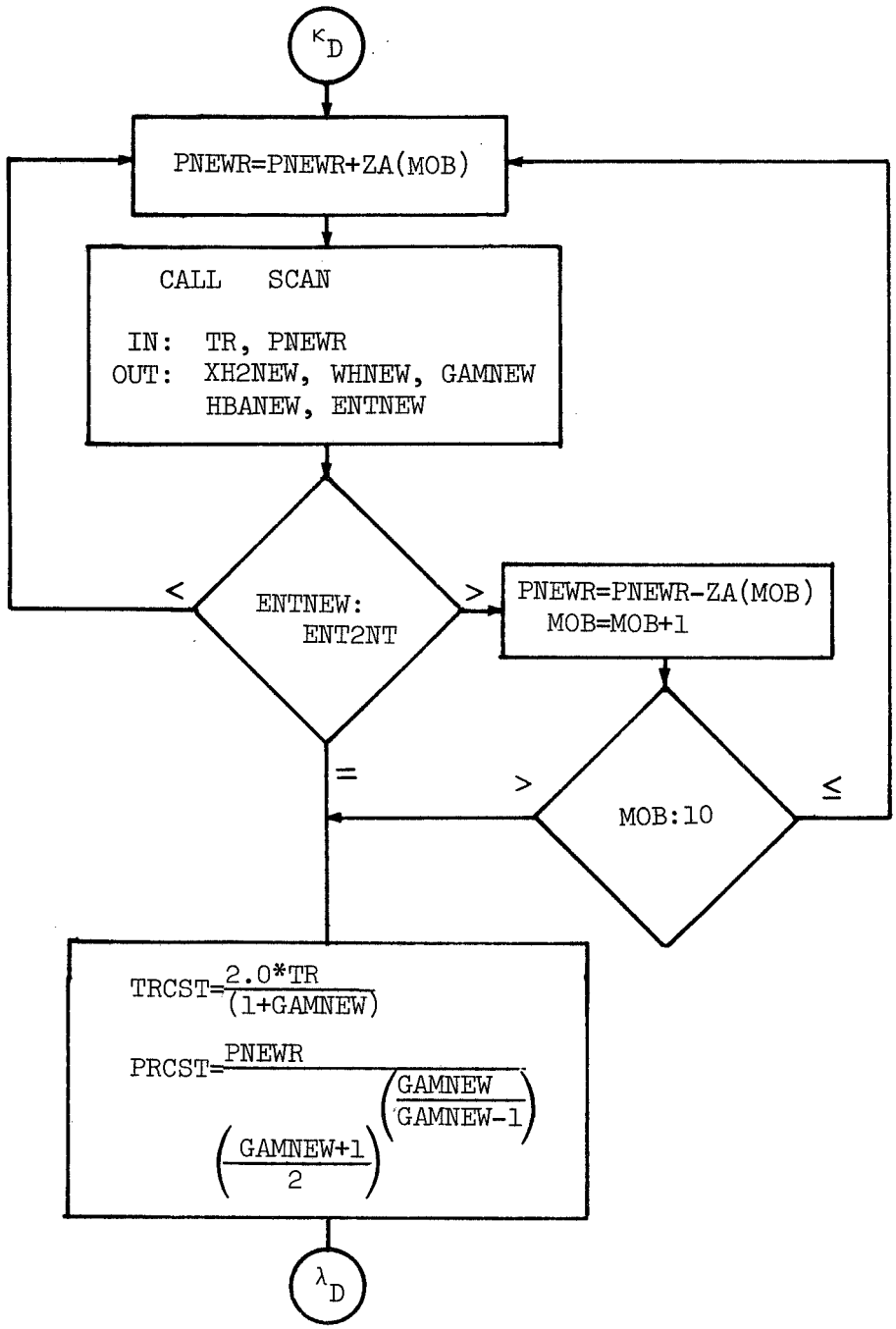

Figure 18.- Continued.

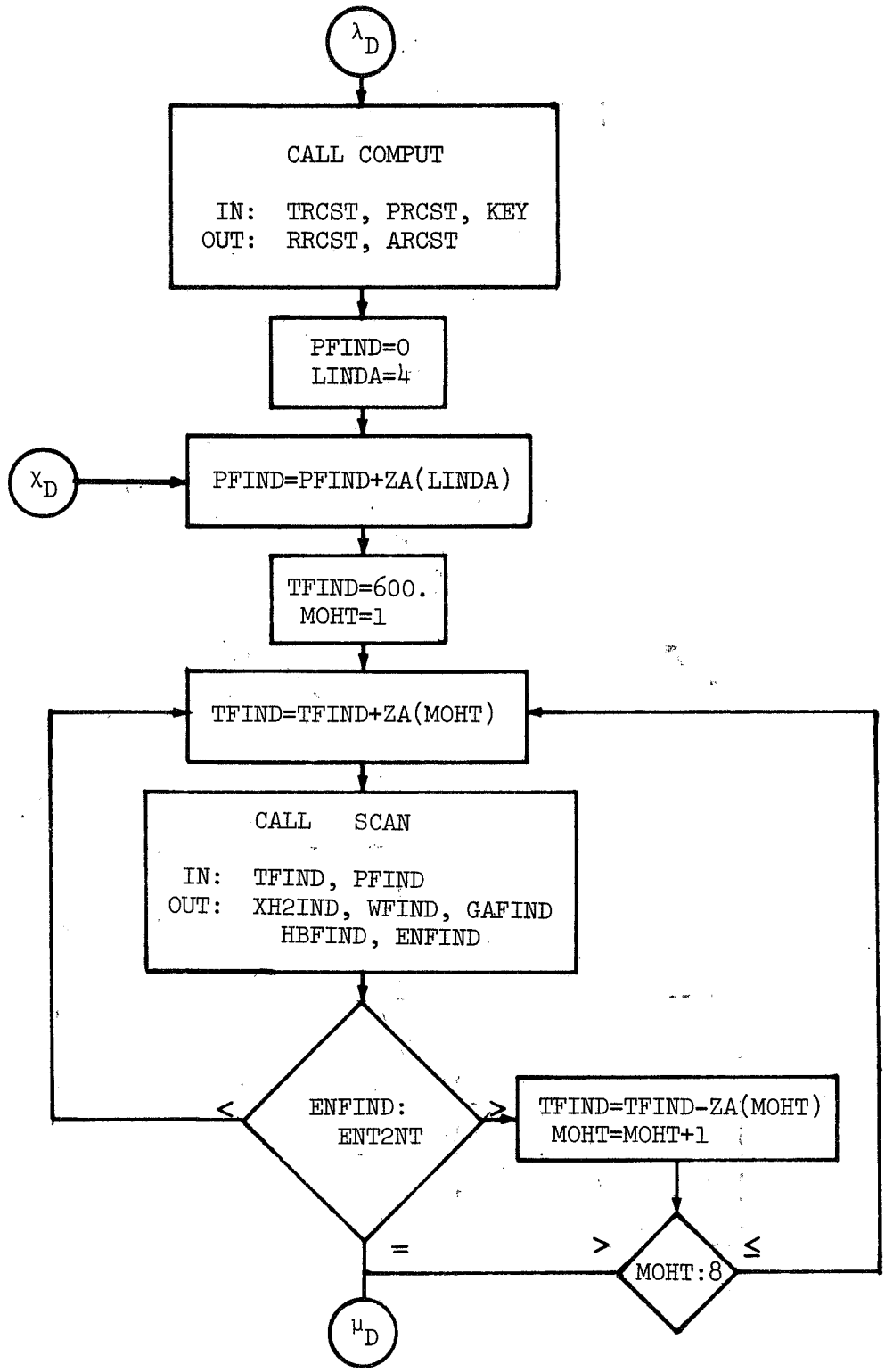

Figure 18.- Continued.

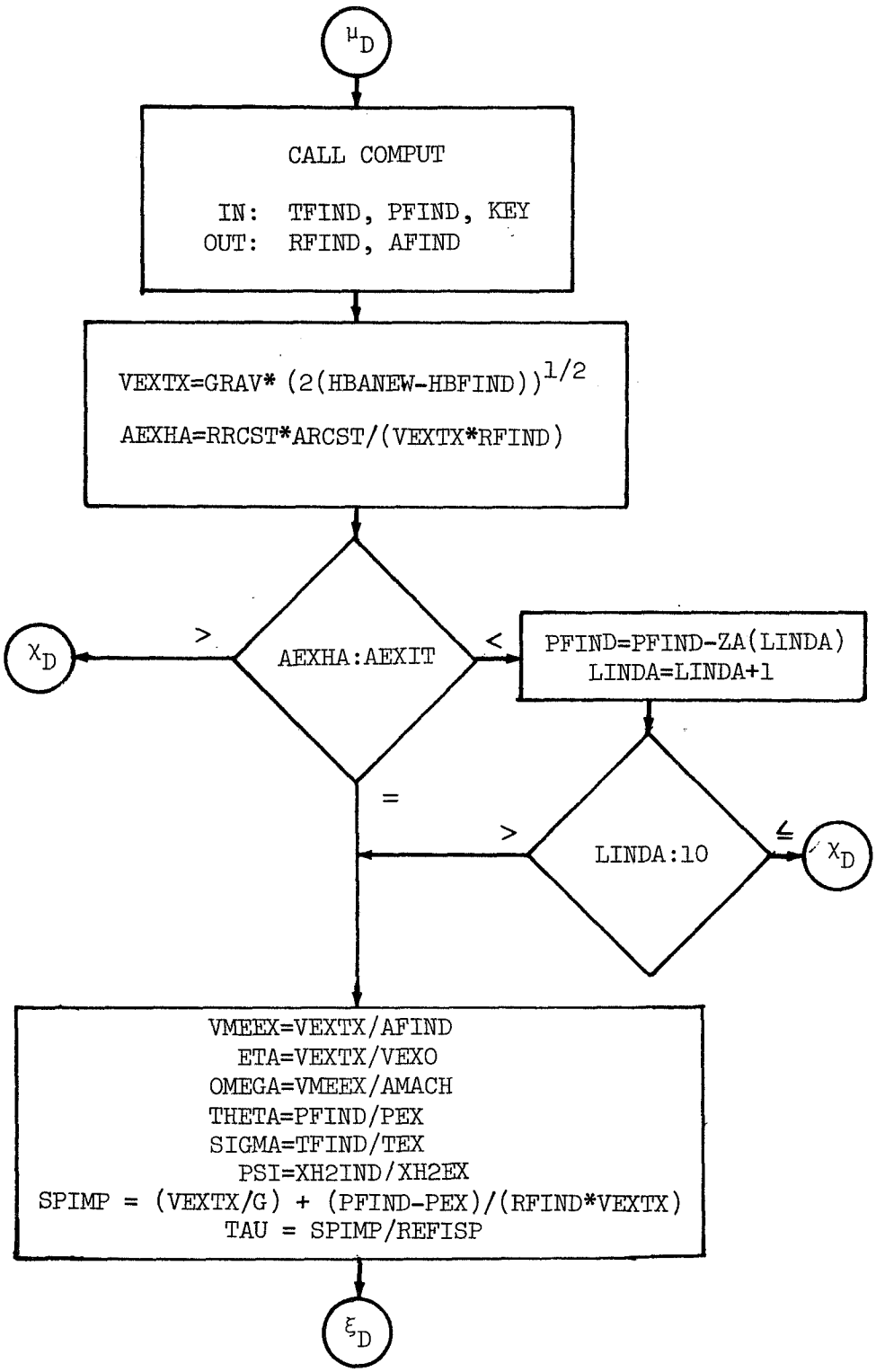

Figure 18.- Continued.

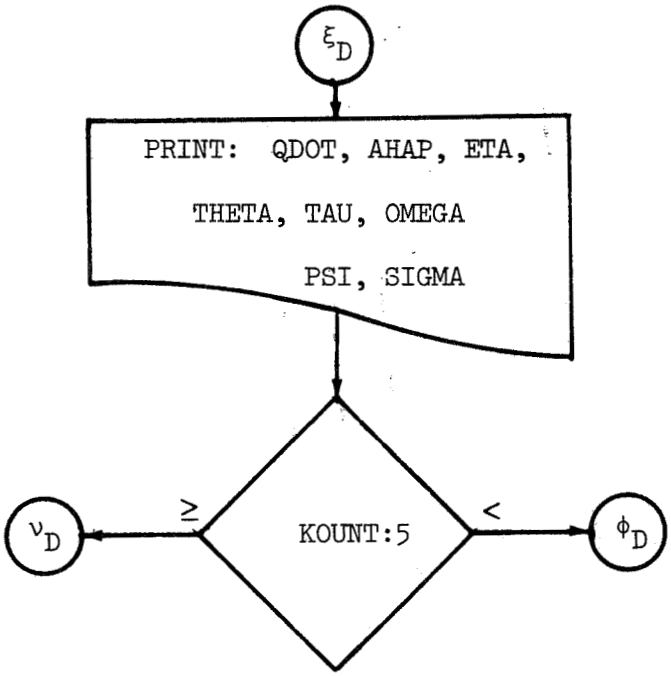

Figure 18.- Concluded.

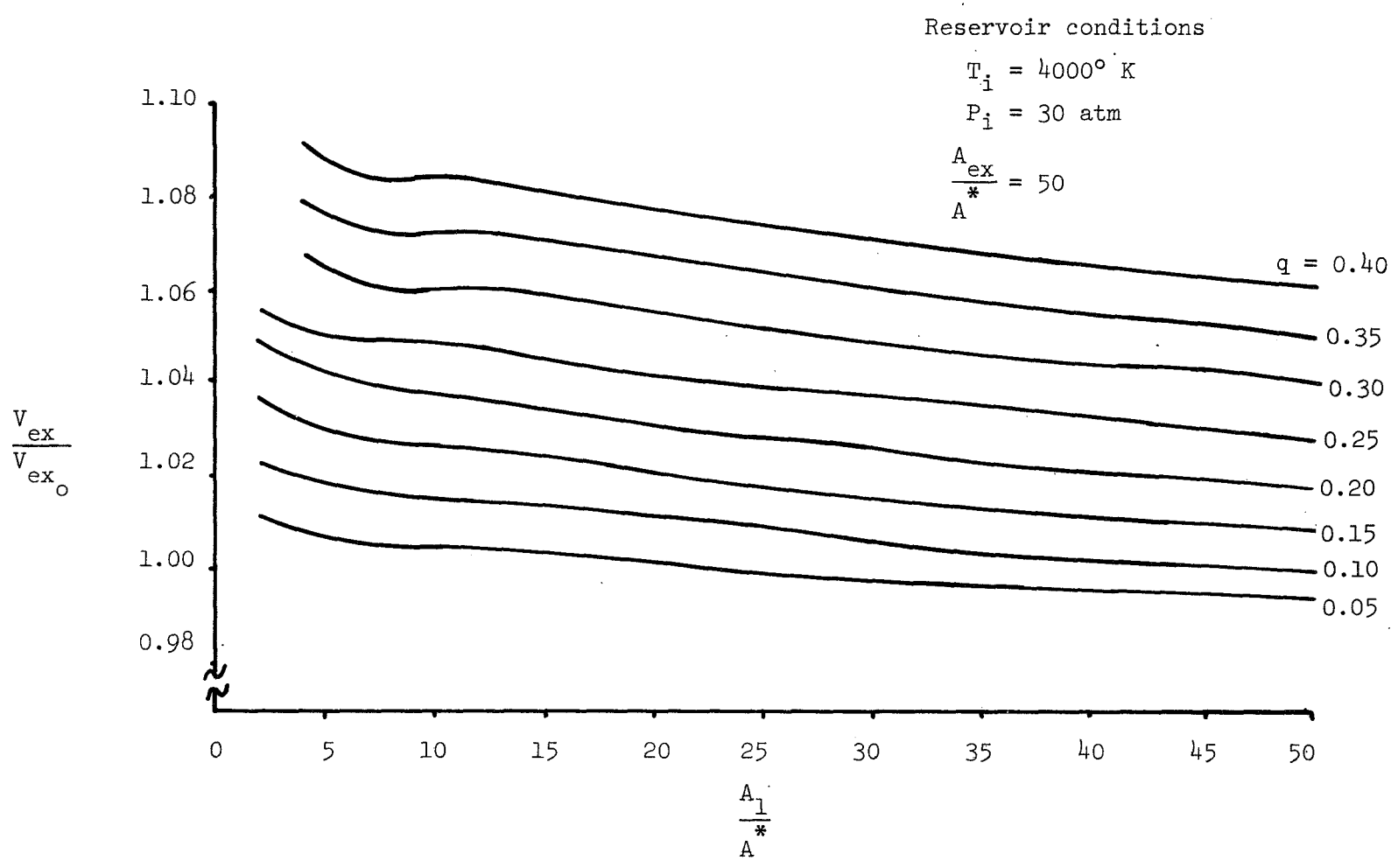

Figure 19.- Exit velocity ratio versus area ratio of heat addition for various values of the heat exchange parameter (reacting gas with heat addition).

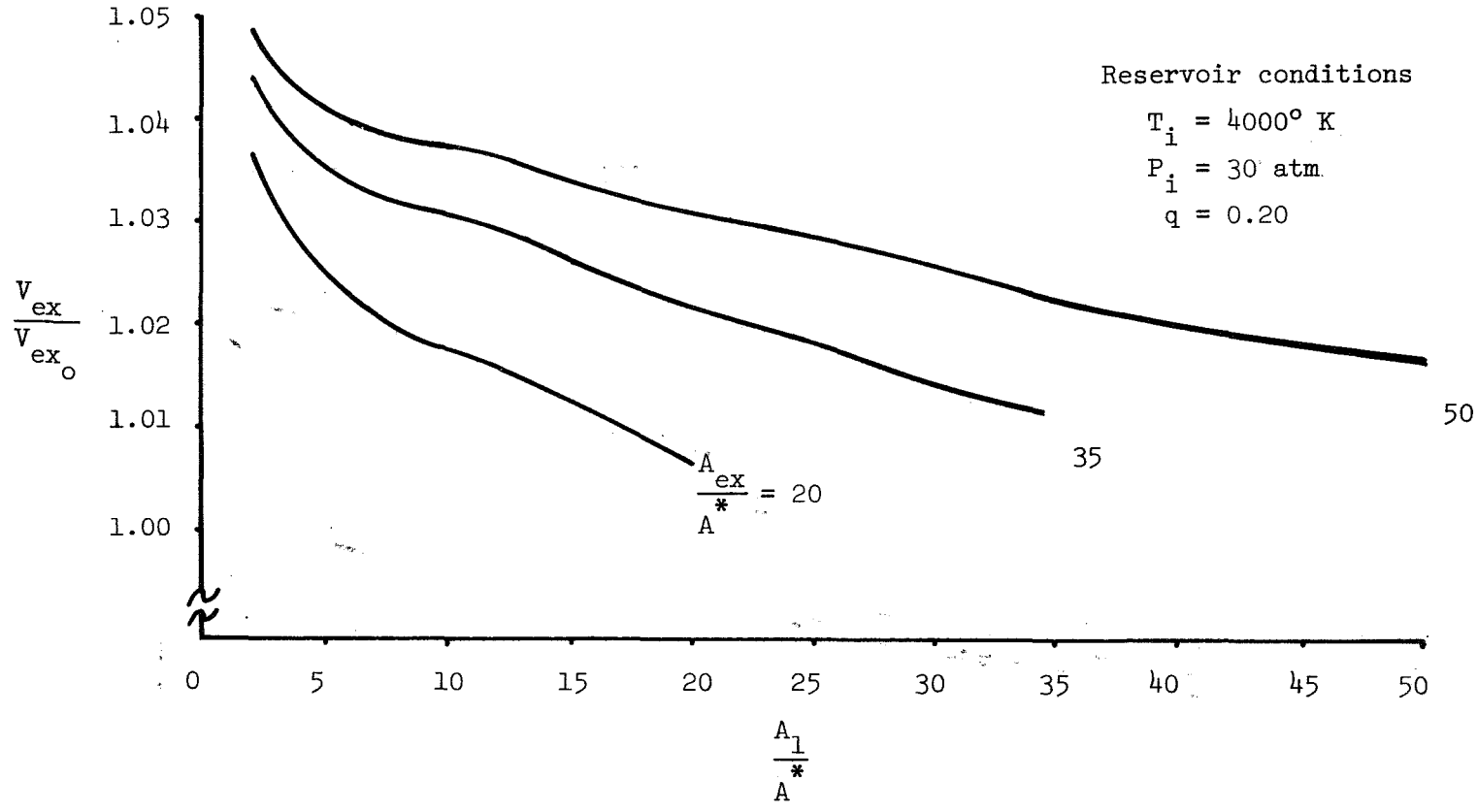

Figure 20.- Exit velocity ratio versus area ratio of heat addition for three values of the exit area ratio (reacting gas with heat addition).

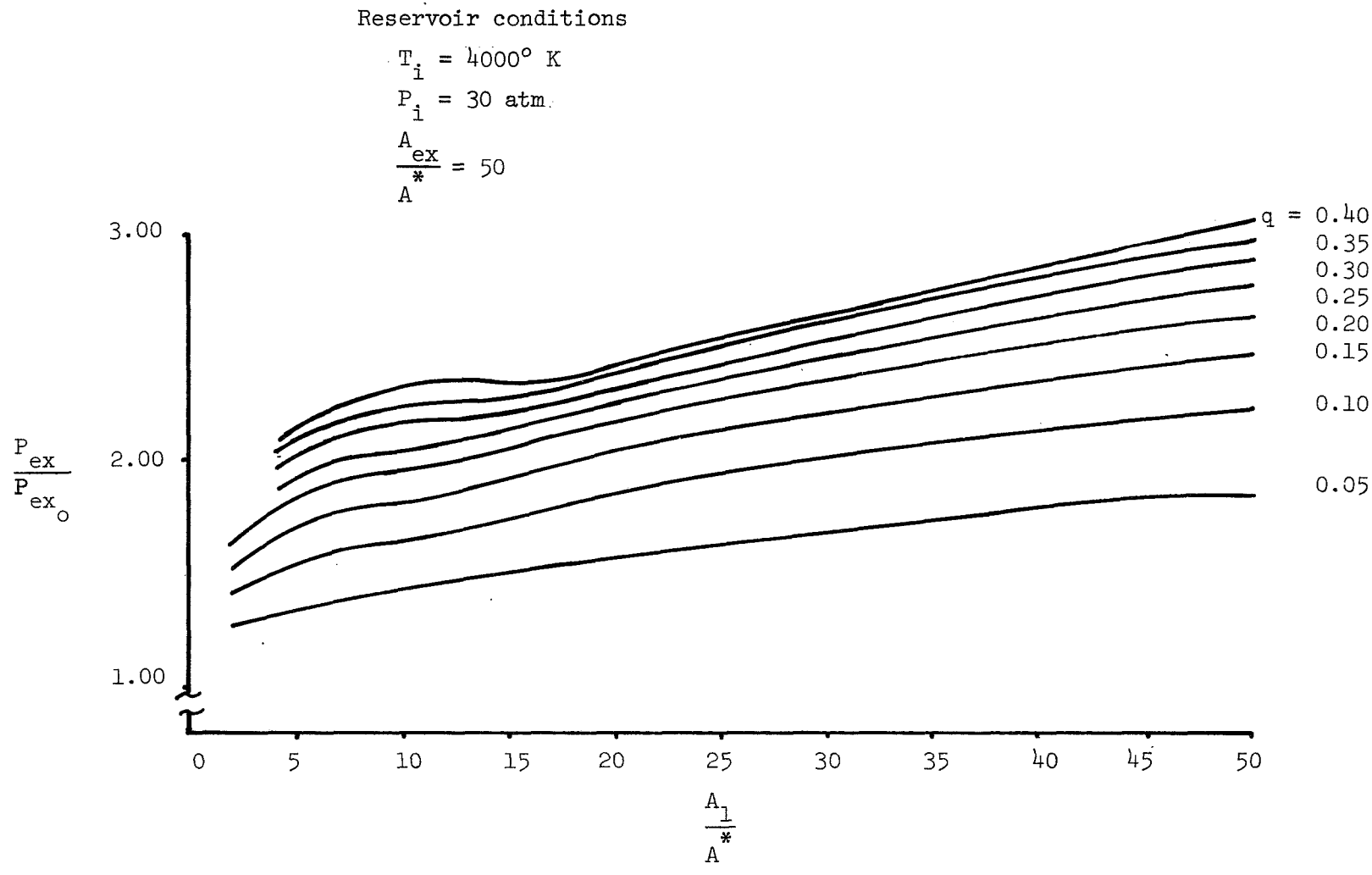

Figure 21.- Exit pressure ratio versus area ratio of heat addition for various values of the heat exchange parameter (reacting gas with heat addition).

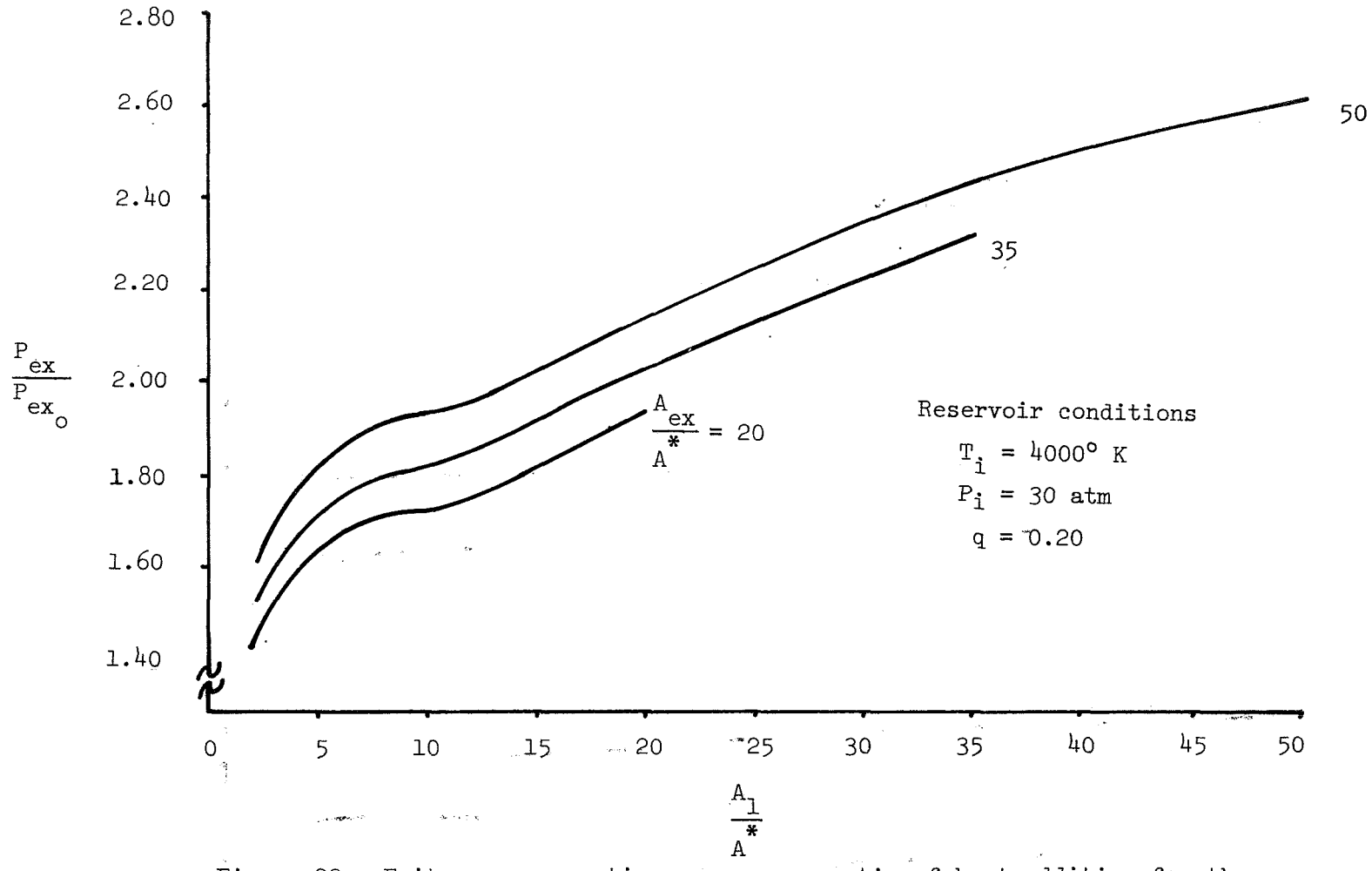

Figure 22.- Exit pressure ratio versus area ratio of heat addition for three values of the exit area ratio (reacting gas with heat addition).

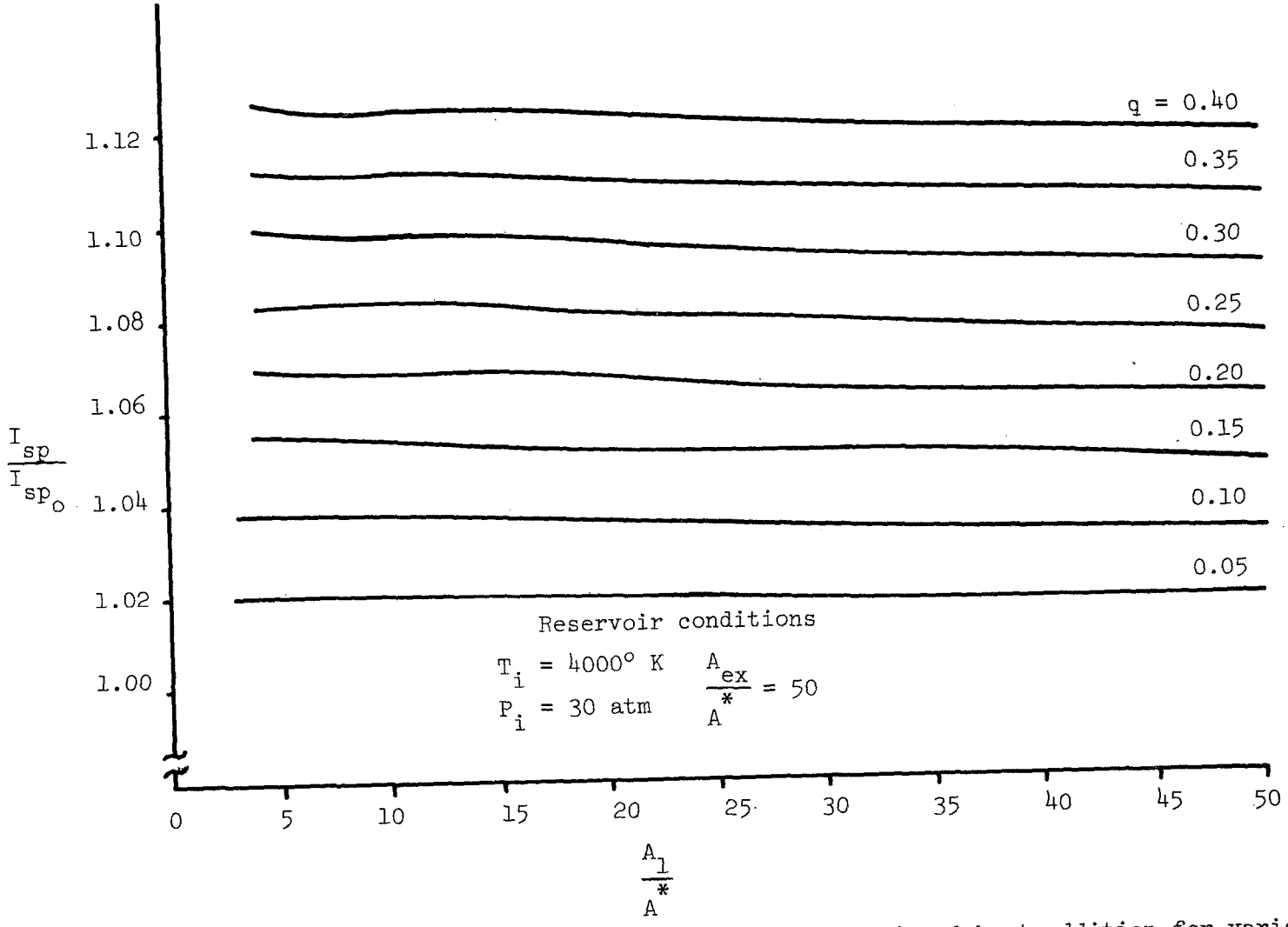

Figure 23.- Specific impulse ratio versus area ratio of heat addition for various values of the heat exchange parameter (reacting gas with heat addition).

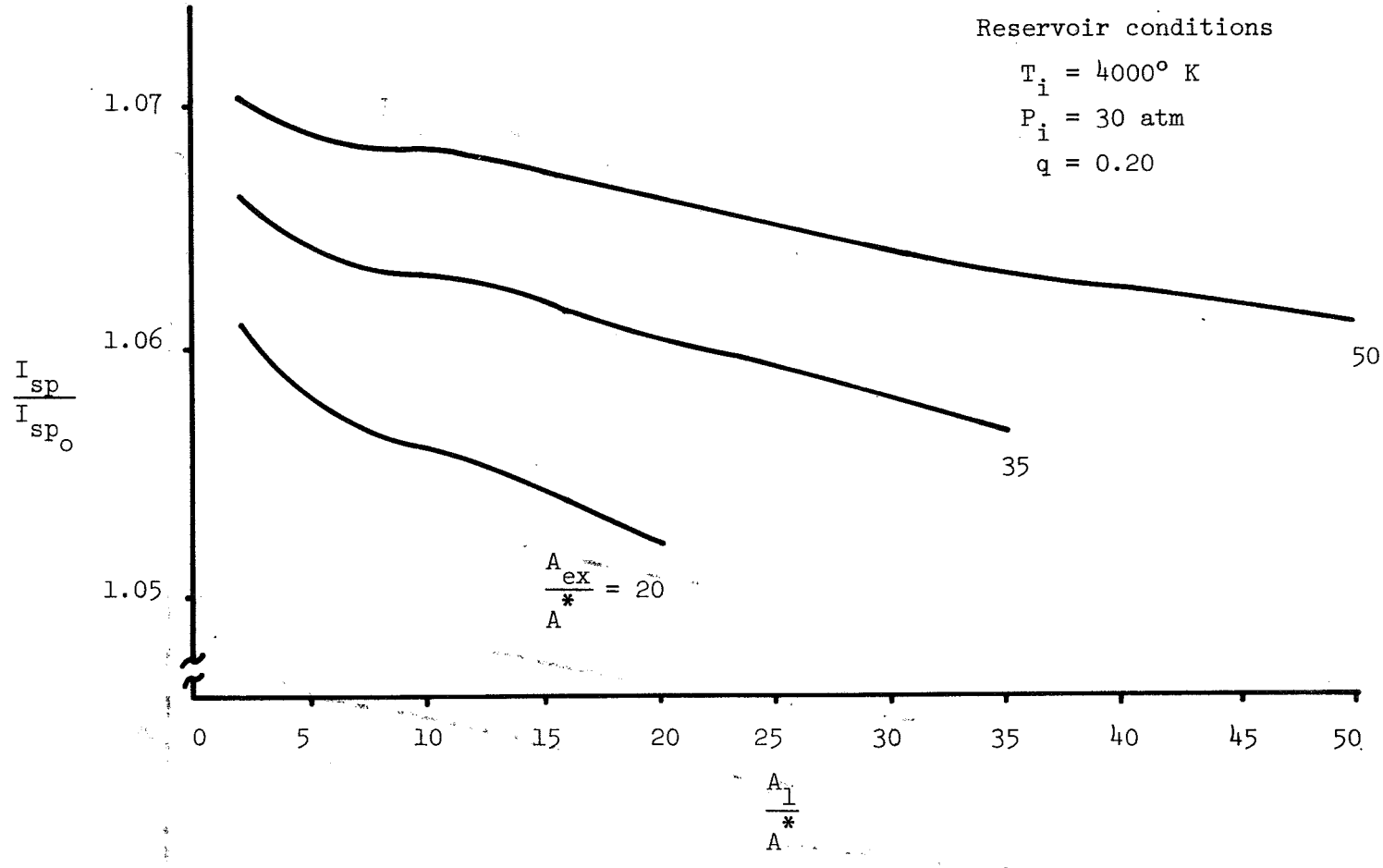

Figure 24.- Specific impulse ratio versus area ratio of heat addition for three values of the exit area ratio (reacting gas with heat addition).

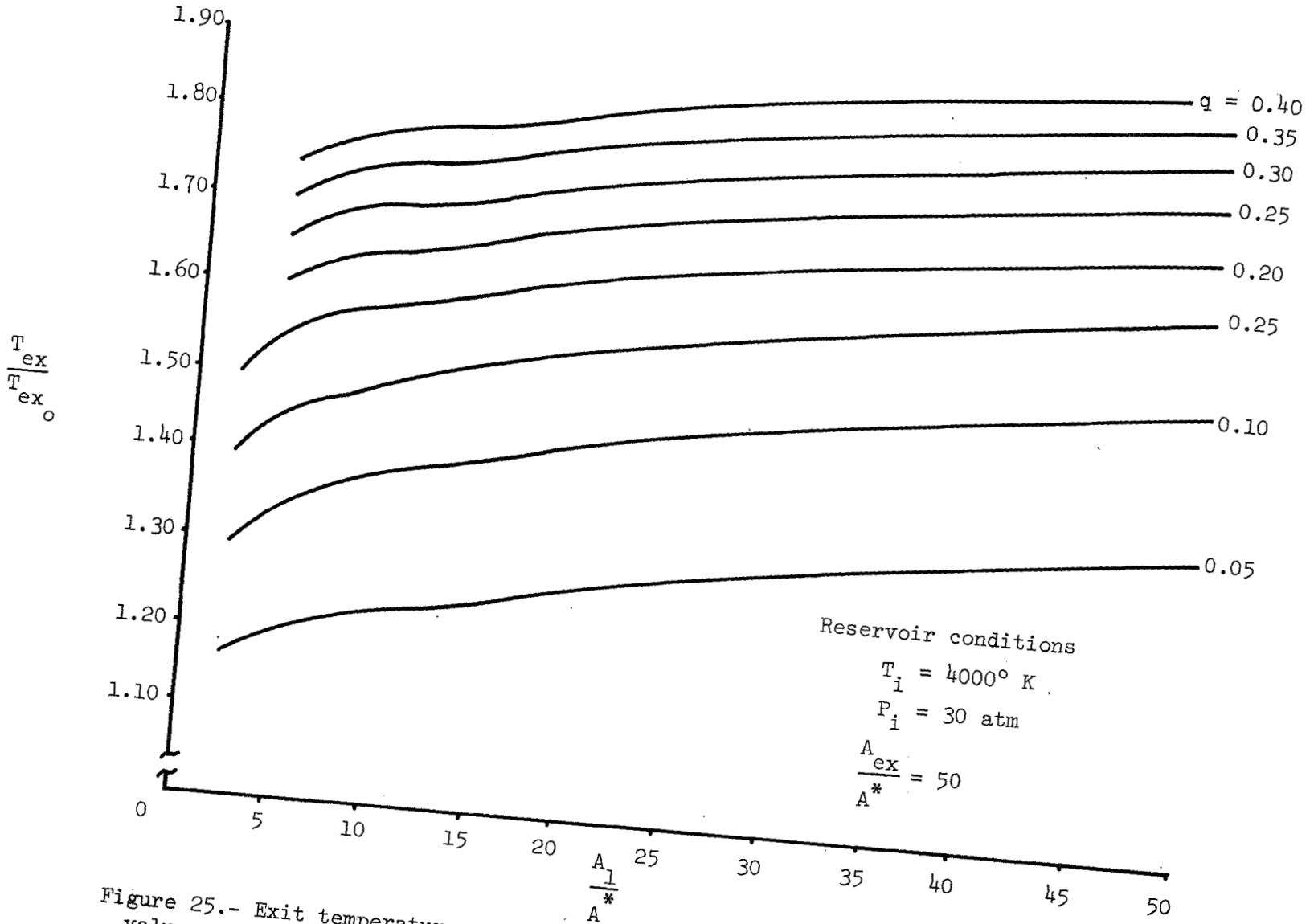

Figure 25.- Exit temperature ratio versus area ratio of heat addition for various values of the heat exchange parameter (reacting gas with heat addition).

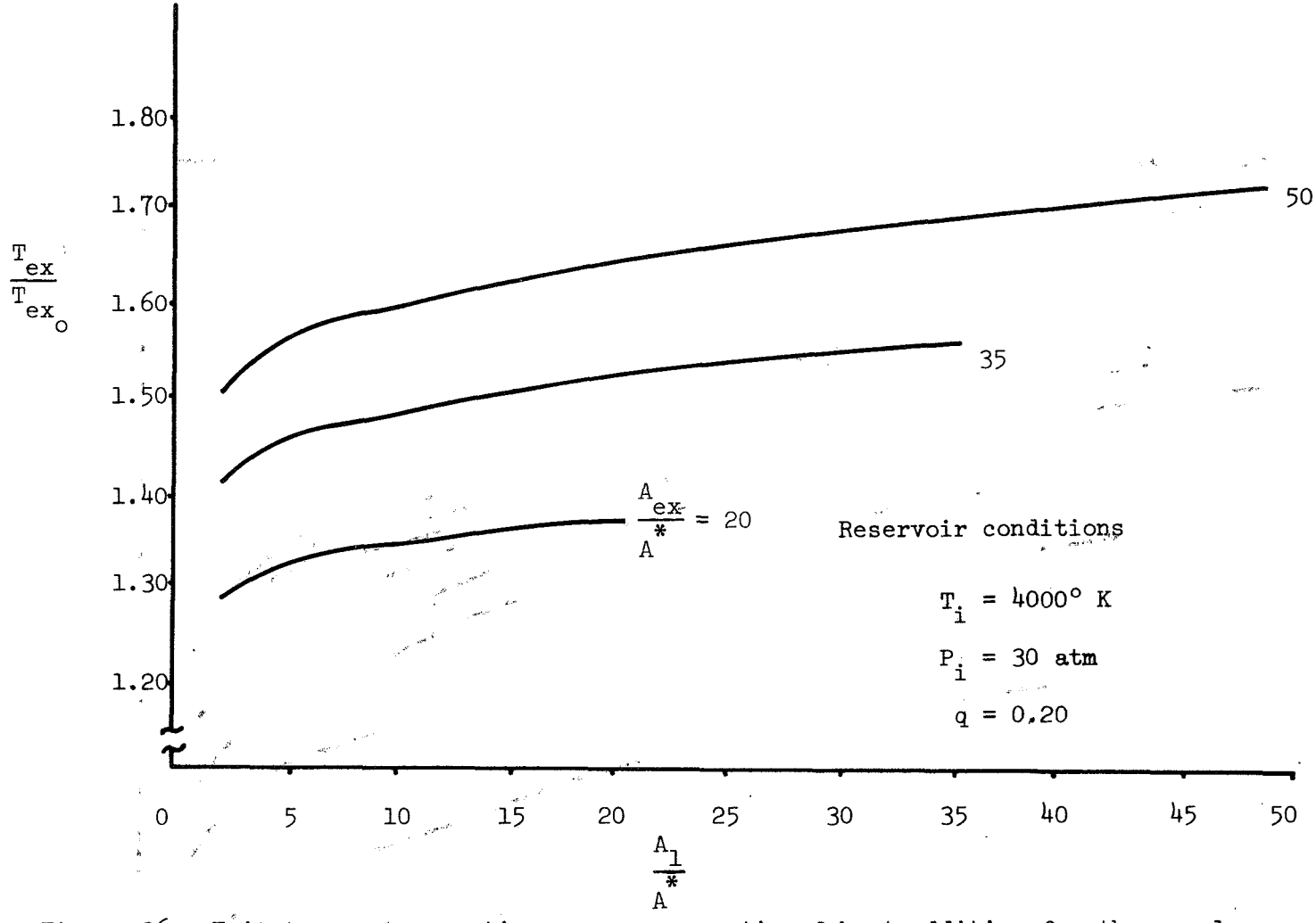

Figure 26.- Exit temperature ratio versus area ratio of heat addition for three values of the exit area ratio (reacting gas with heat addition).

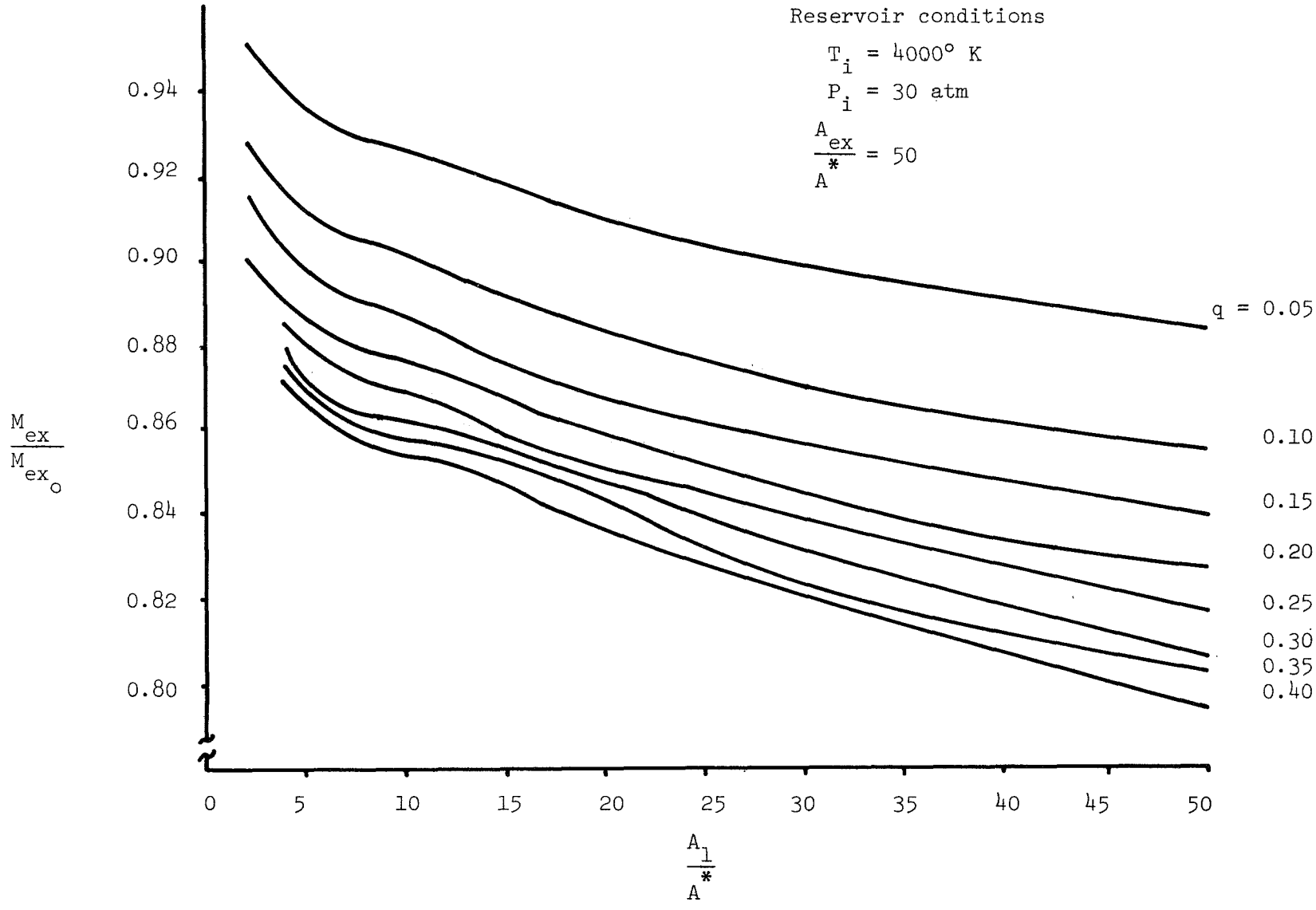

Figure 27.- Exit Mach number ratio versus area ratio of heat addition for various values of the heat exchange parameter (reacting gas with heat addition).

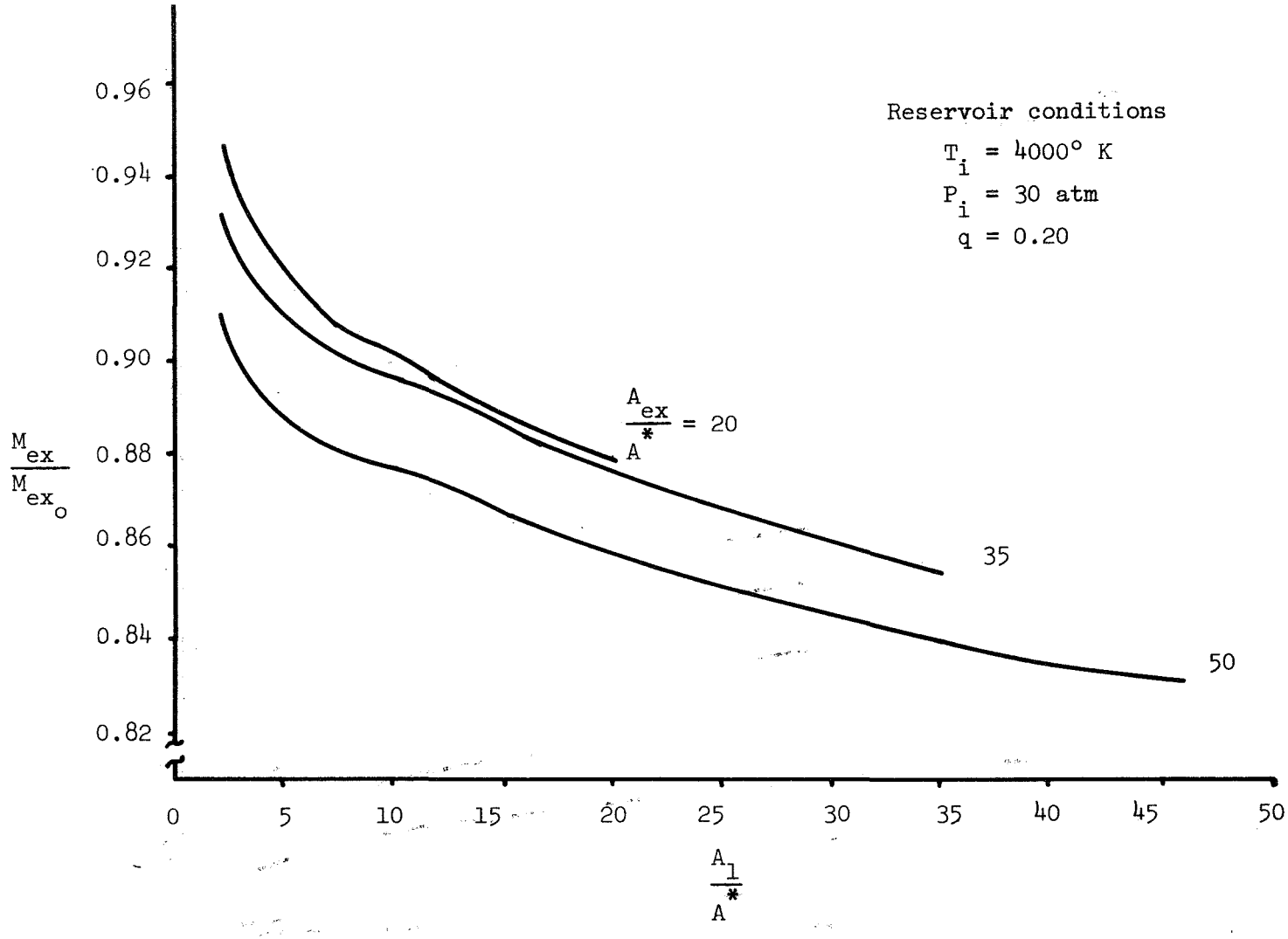

Figure 28.- Exit Mach number ratio versus area ratio of heat addition for three values of the exit area ratio (reacting gas with heat addition).

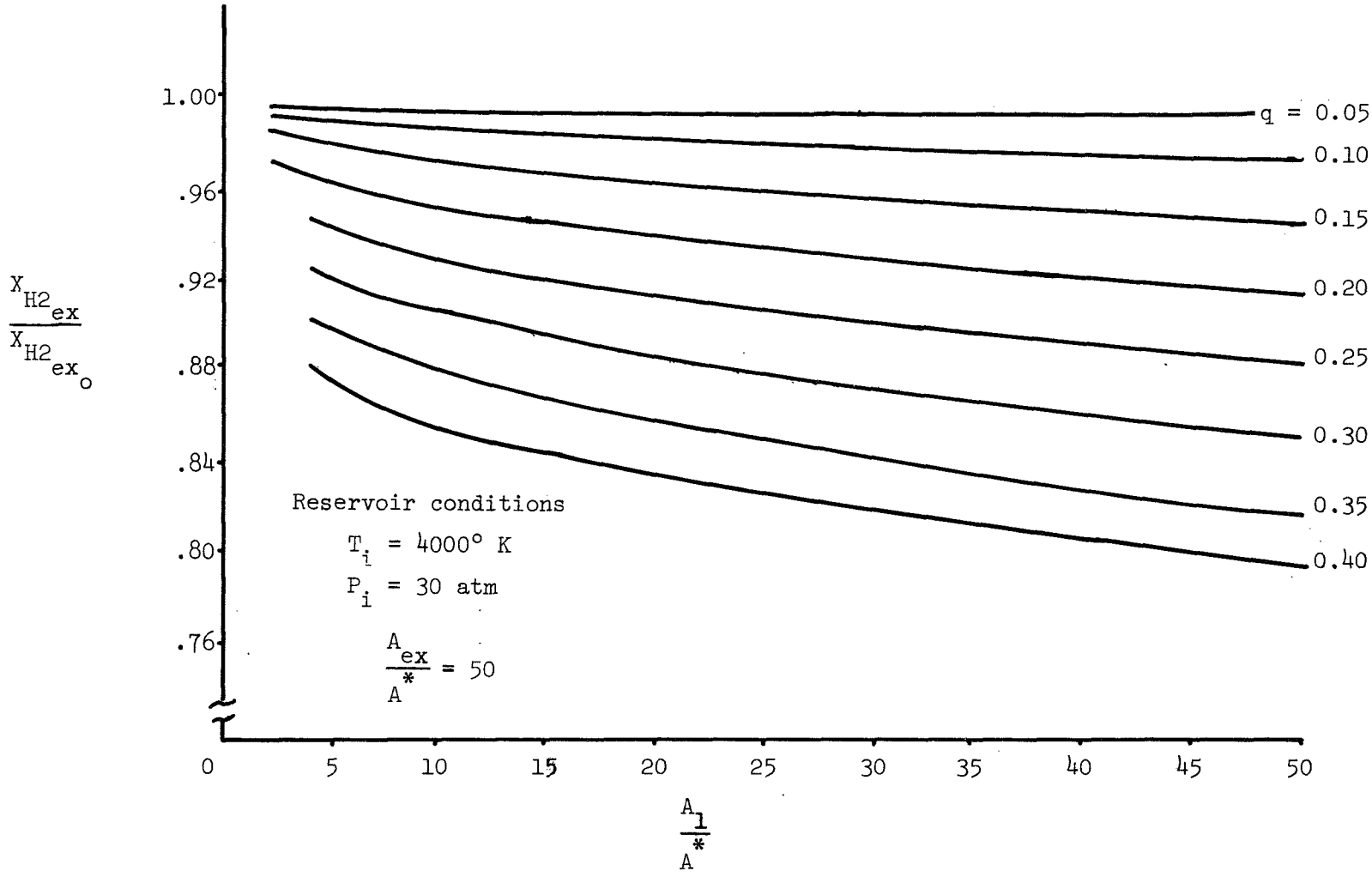

Figure 29.- Exit molecular hydrogen mole fraction ratio versus area ratio of heat addition for various values of the heat exchange parameter (reacting gas with heat addition).

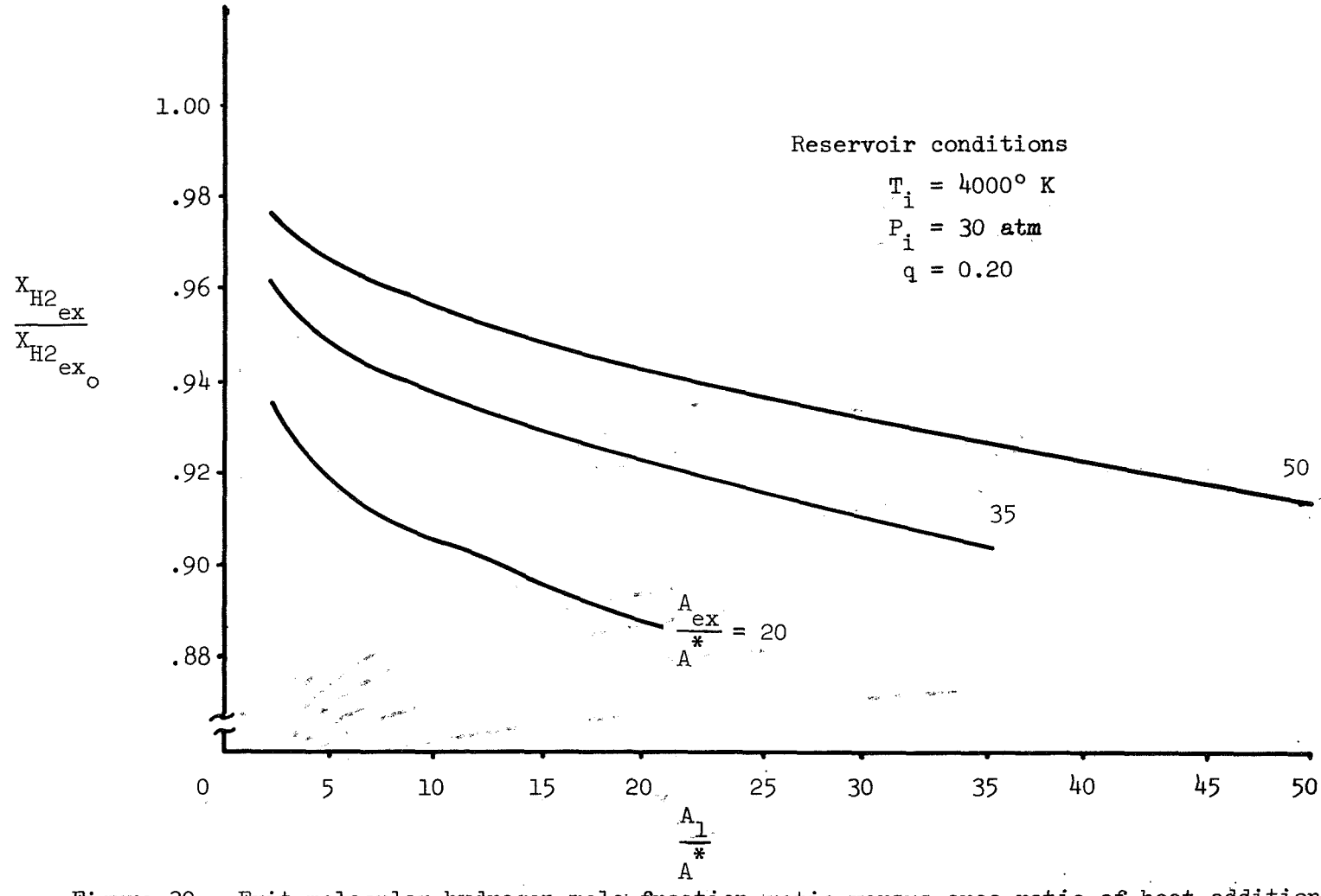

Figure 30.- Exit molecular hydrogen mole fraction ratio versus area ratio of heat addition for the three values of the exit area ratio (reacting gas with heat addition).

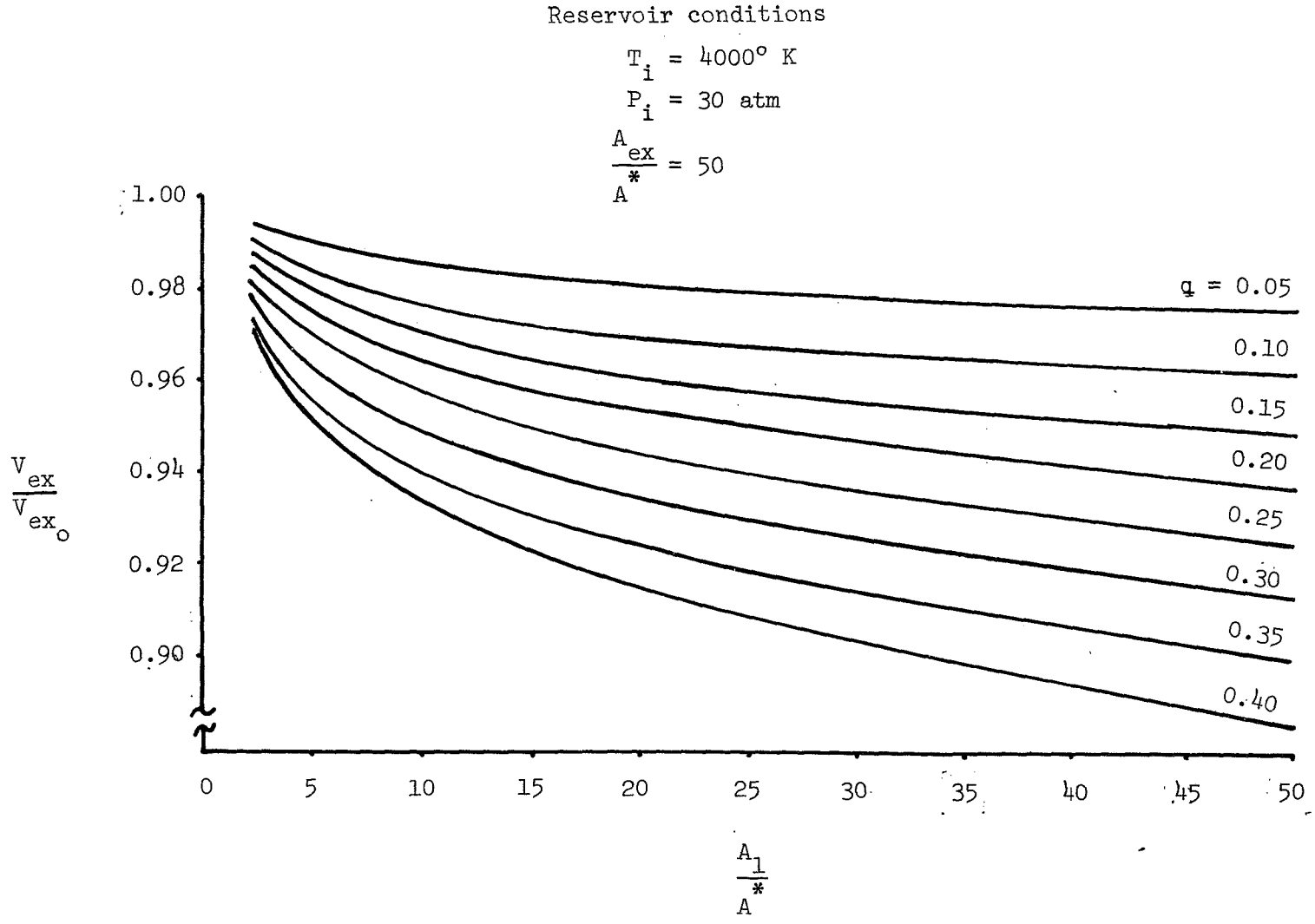

Figure 31.- Exit velocity ratio versus area ratio of heat addition for various values of heat exchange parameter (reacting gas with heat transfer).

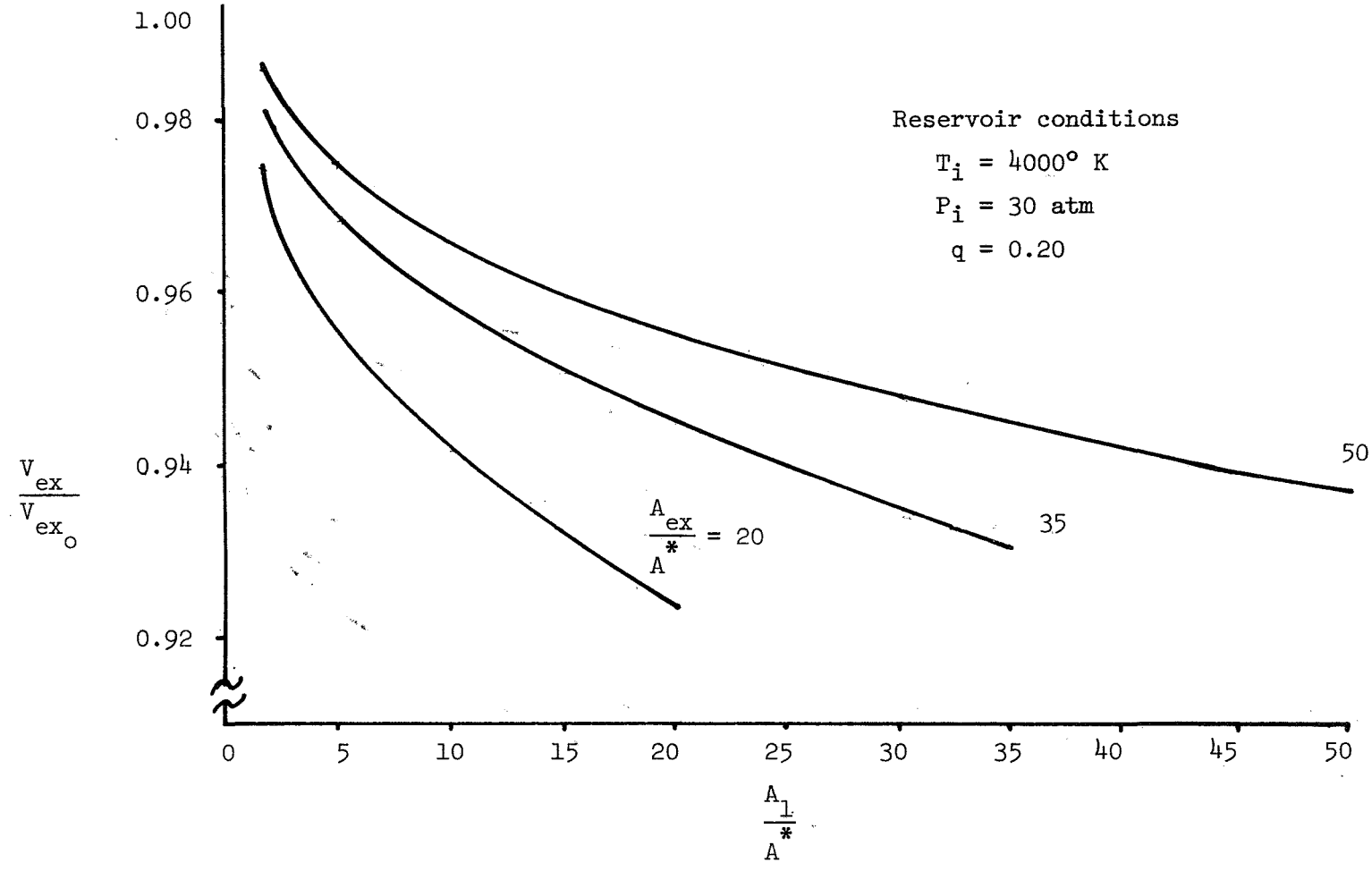

Figure 32.- Exit velocity ratio versus area ratio of heat addition for three values of exit area ratio (reacting gas with heat transfer).

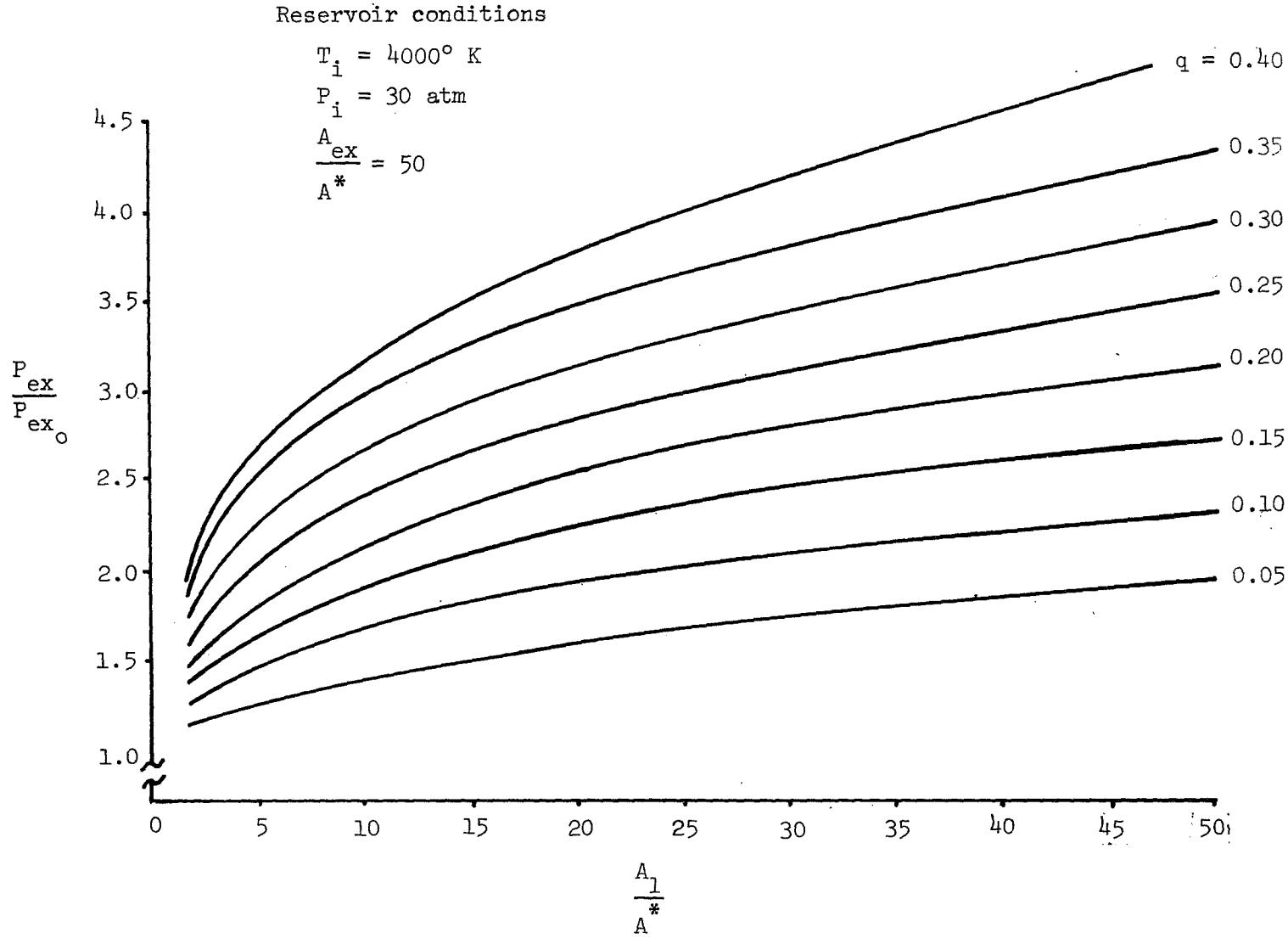

Figure 33.- Exit pressure ratio versus area ratio of heat addition for various values of heat exchange parameter (reacting gas with heat transfer).

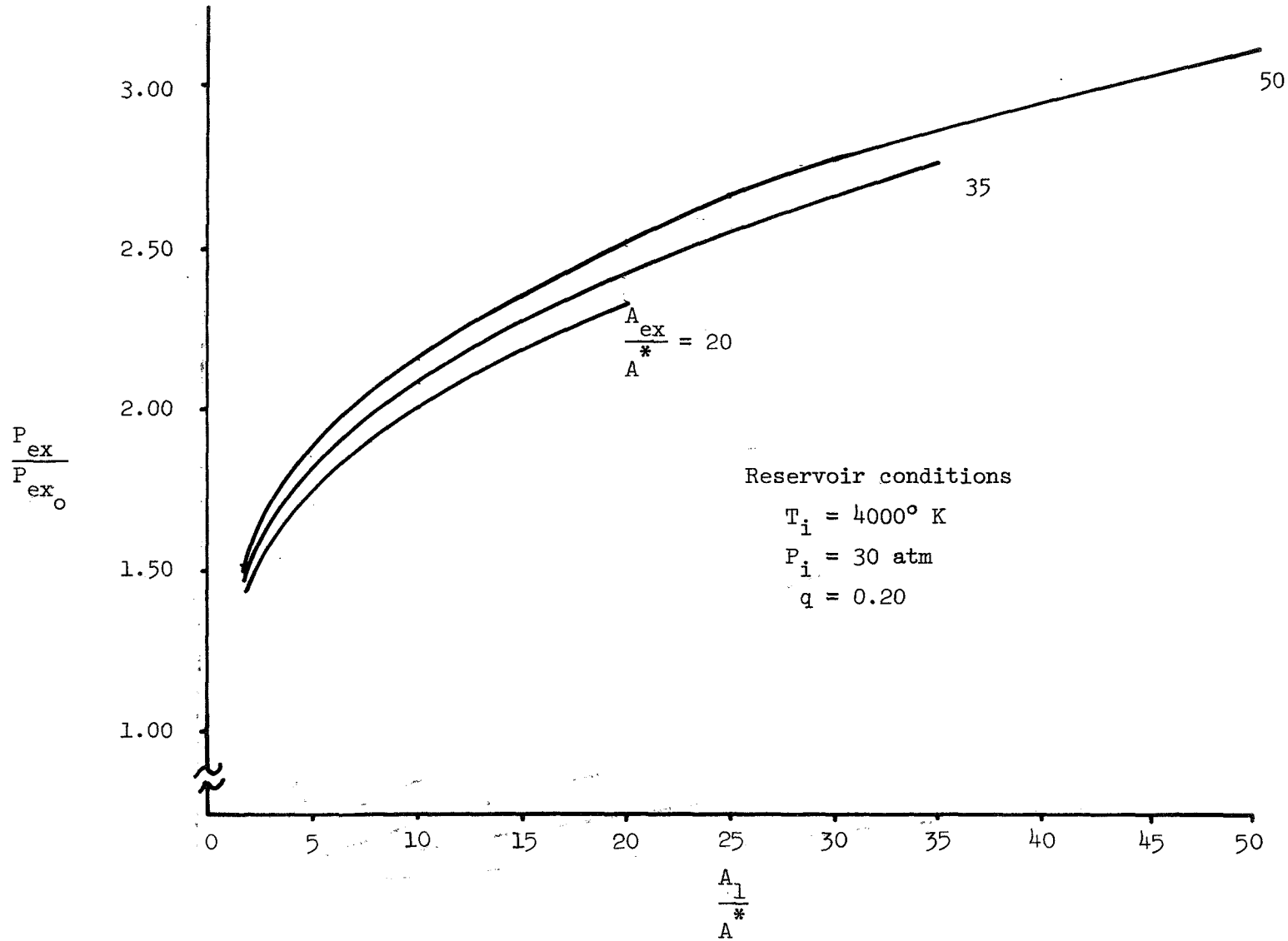

Figure 34.- Exit pressure ratio versus area ratio of heat addition for three values of the exit area ratio (reacting gas with heat transfer).

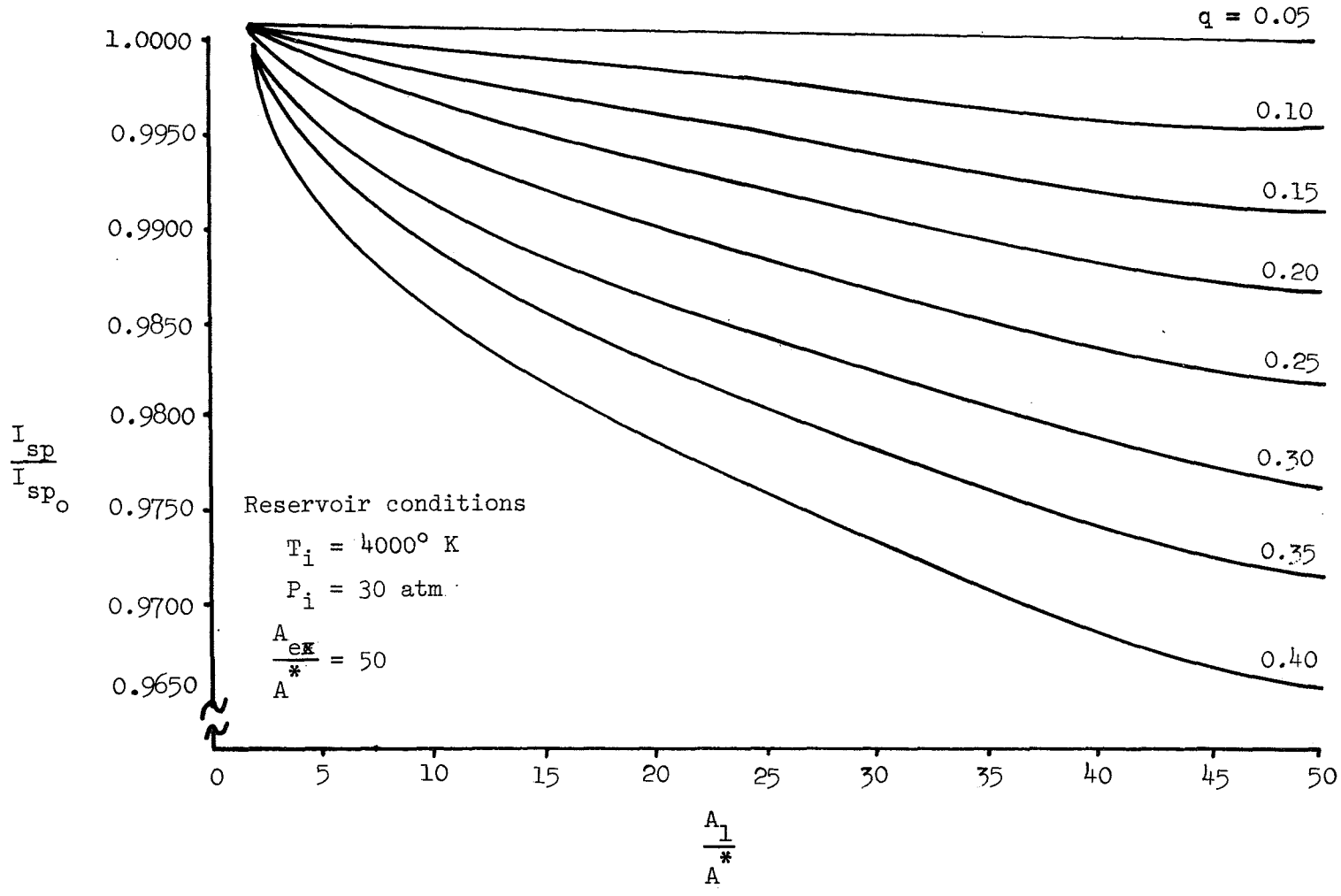

Figure 35.- Specific impulse ratio versus area ratio of heat addition for various values of heat exchange parameter (reacting gas with heat transfer).

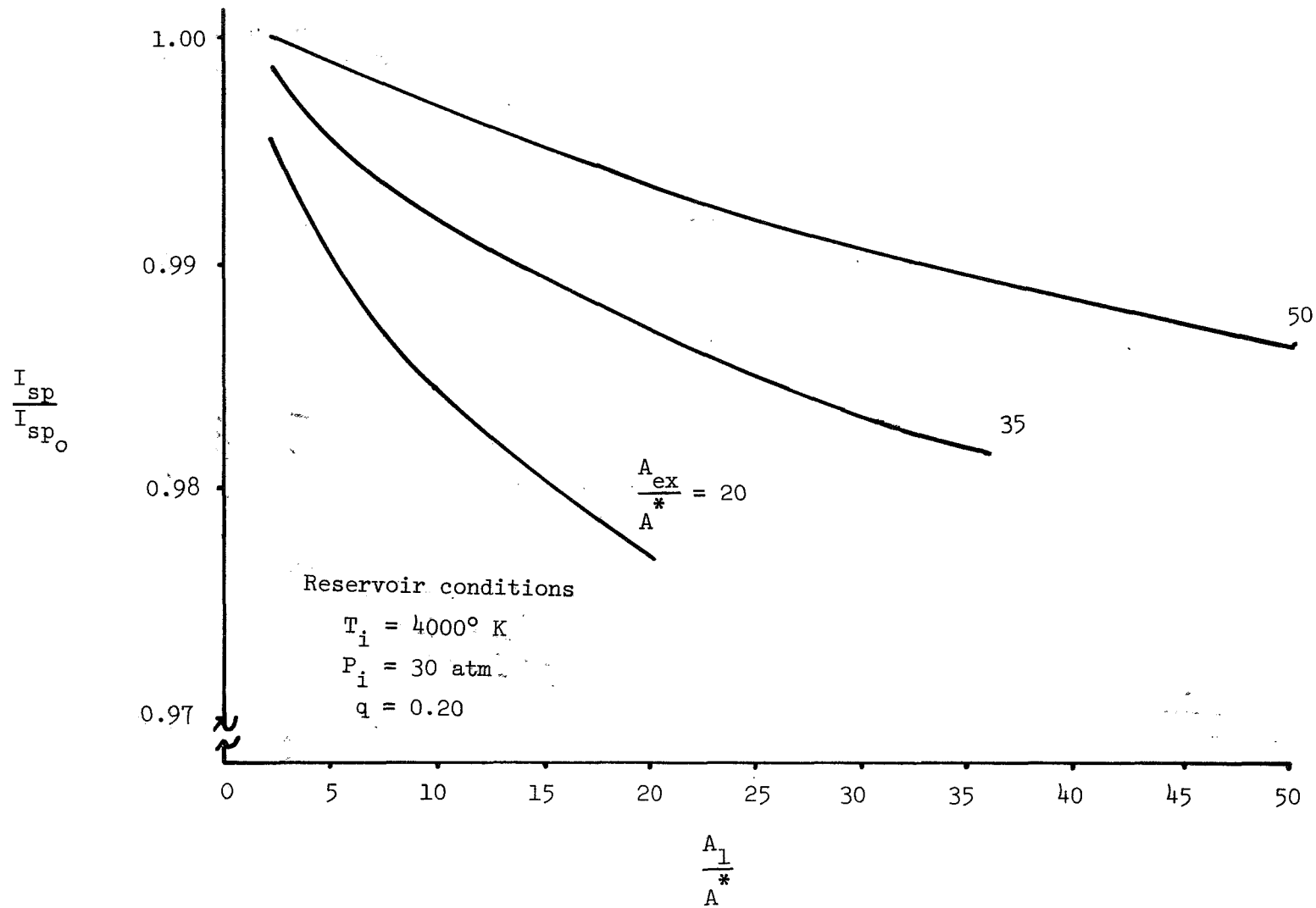

Figure 36.- Specific impulse ratio versus area ratio of heat addition for three values of the exit area ratio (reacting gas with heat transfer).

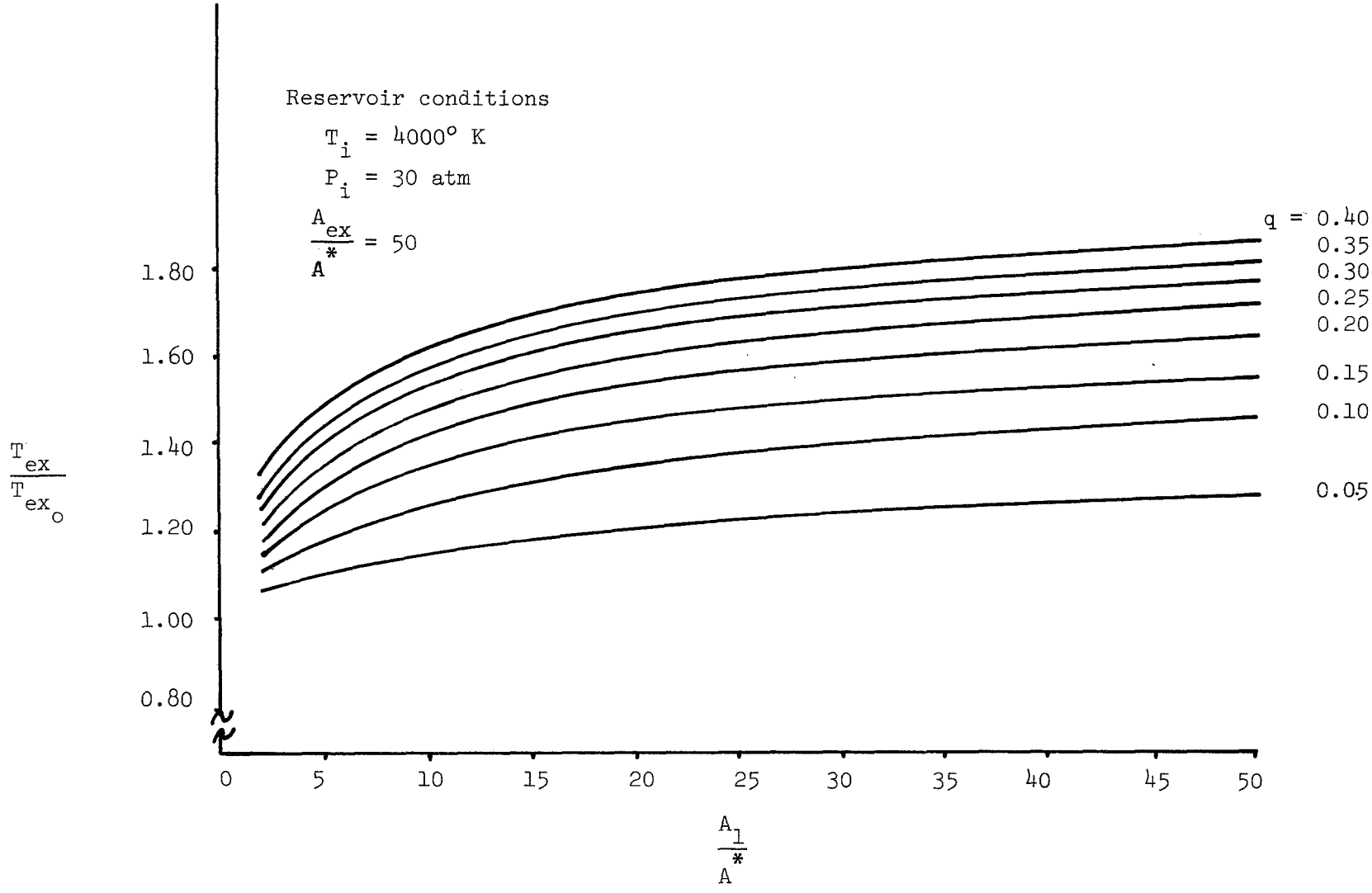

Figure 37.- Exit temperature ratio versus area ratio of heat addition for various values of heat exchange parameter (reacting gas with heat transfer).

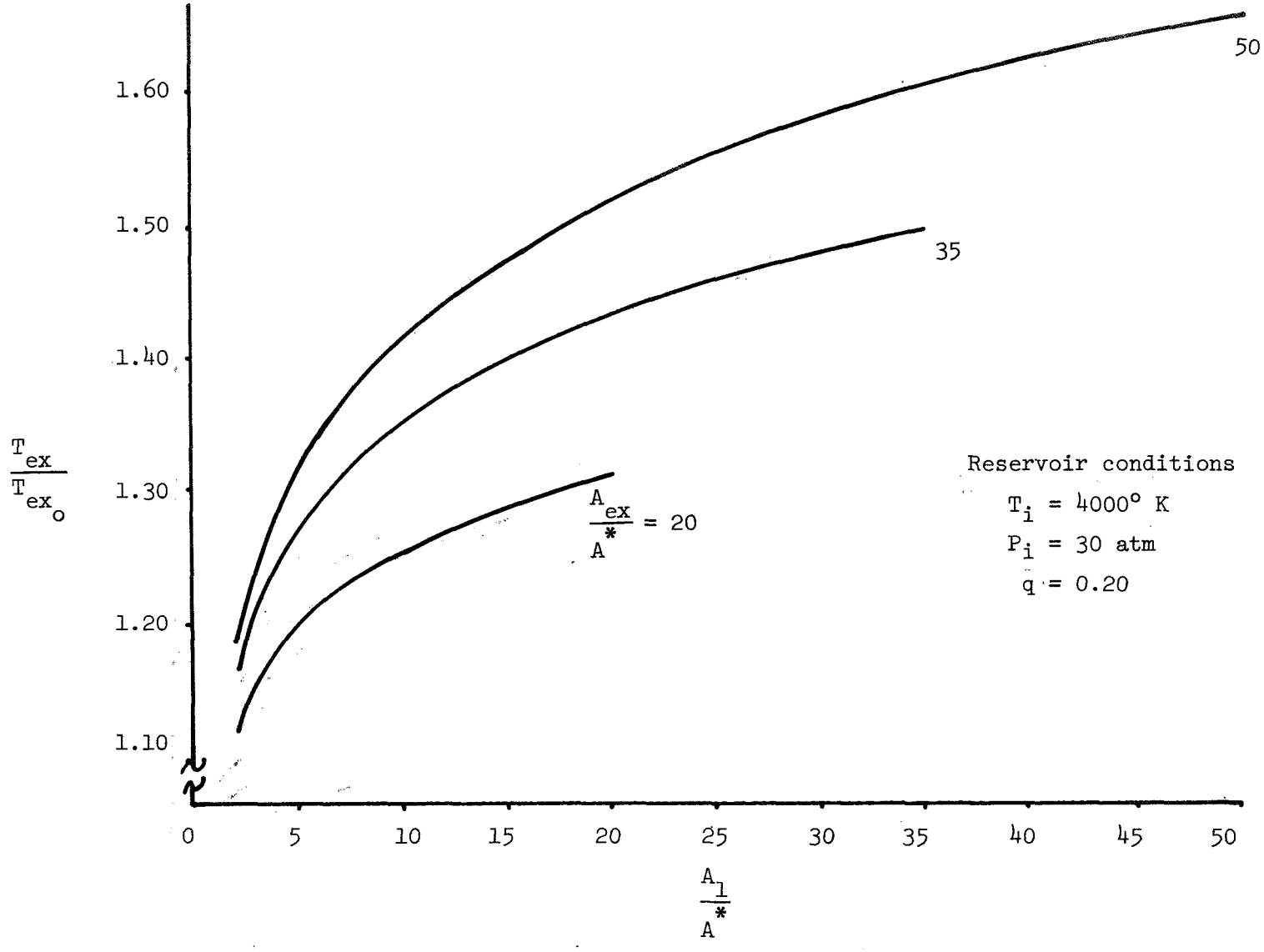

Figure 38.- Exit temperature ratio versus area ratio of heat addition for three values of the exit area ratio (reacting gas with heat transfer).

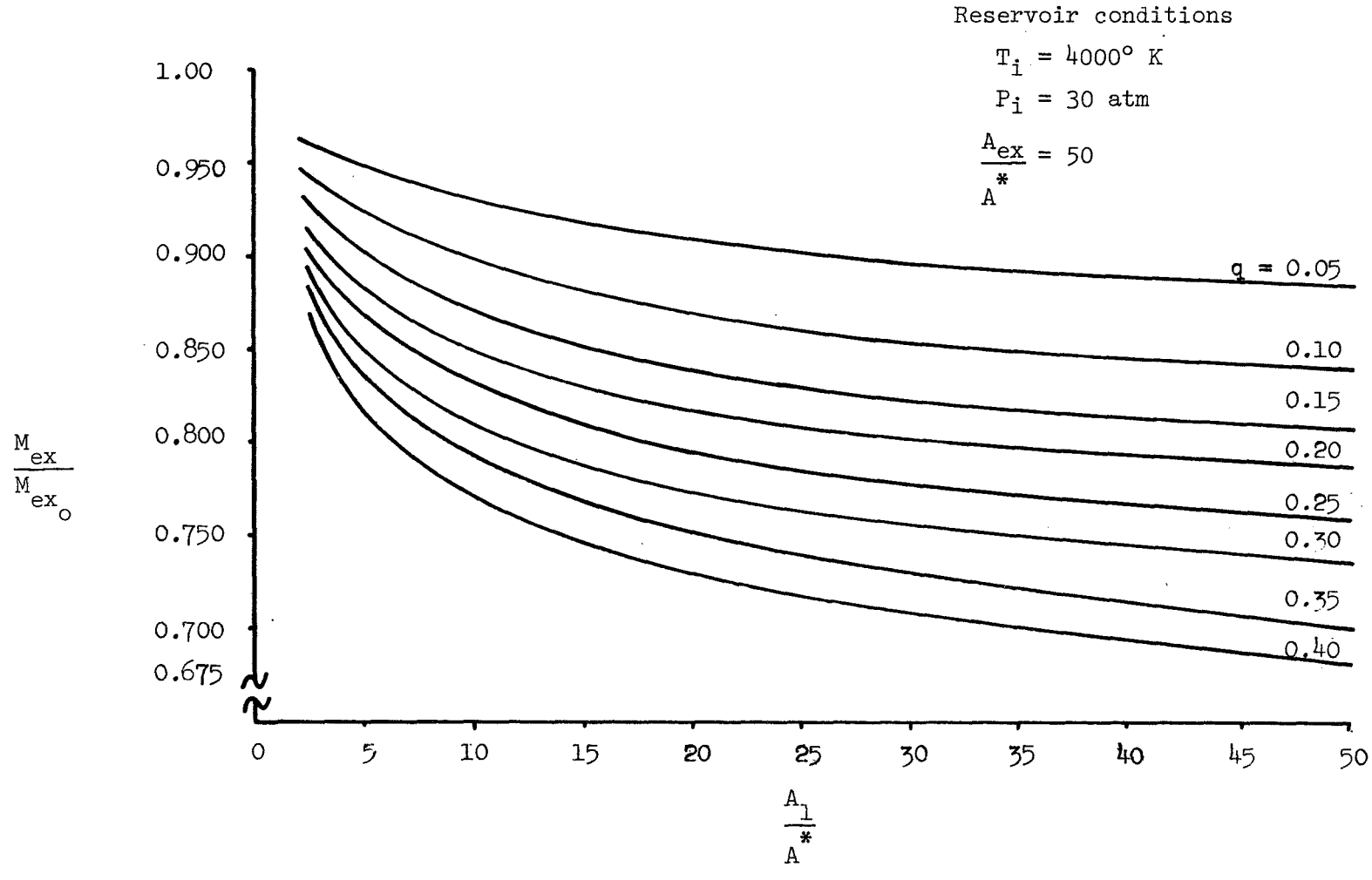

Figure 39.- Exit Mach number ratio versus area ratio of heat addition for various values of heat exchange parameter (reacting gas with heat transfer).

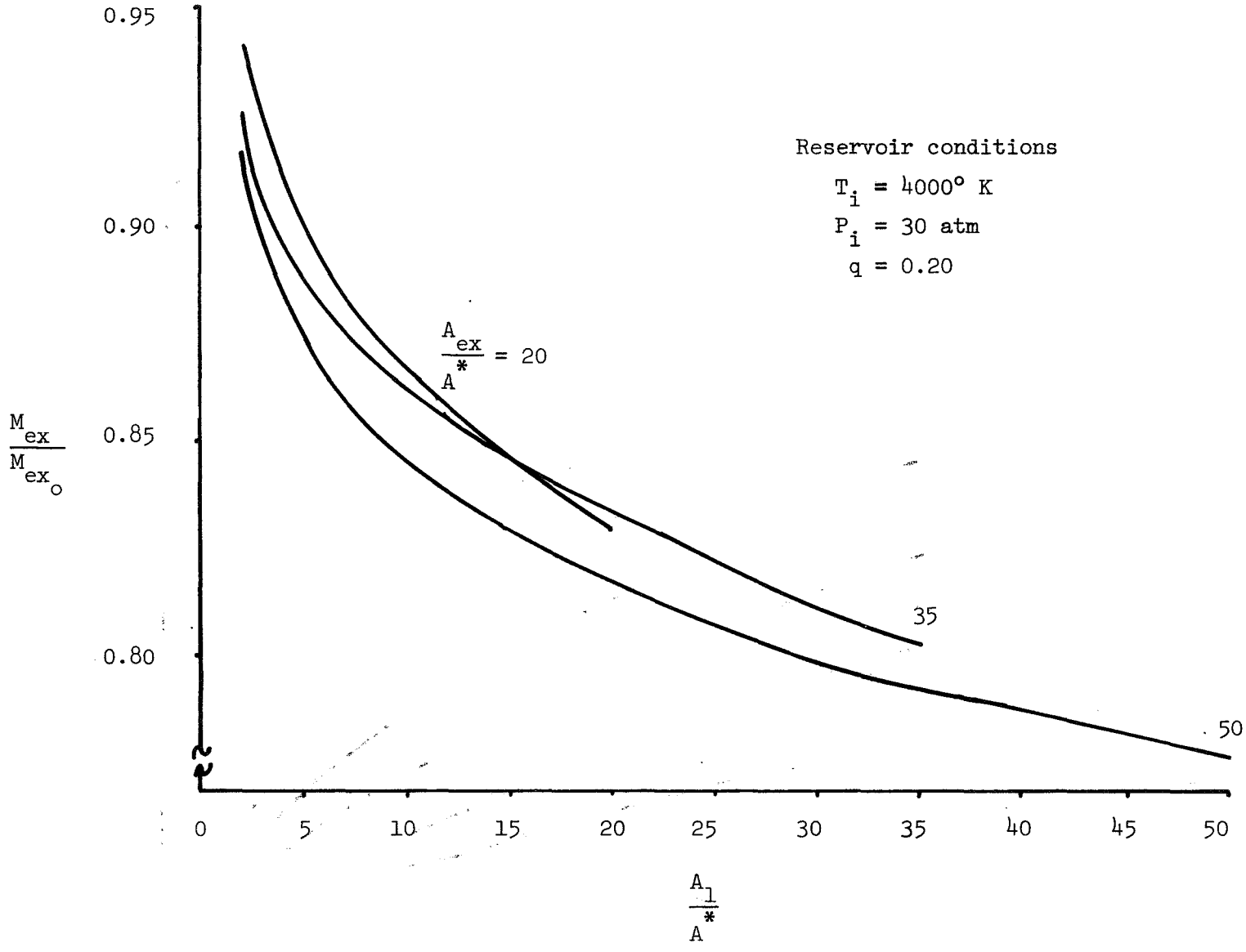

Figure 40.- Exit Mach number ratio versus area ratio of heat addition for three values of the exit area ratio (reacting gas with heat transfer).

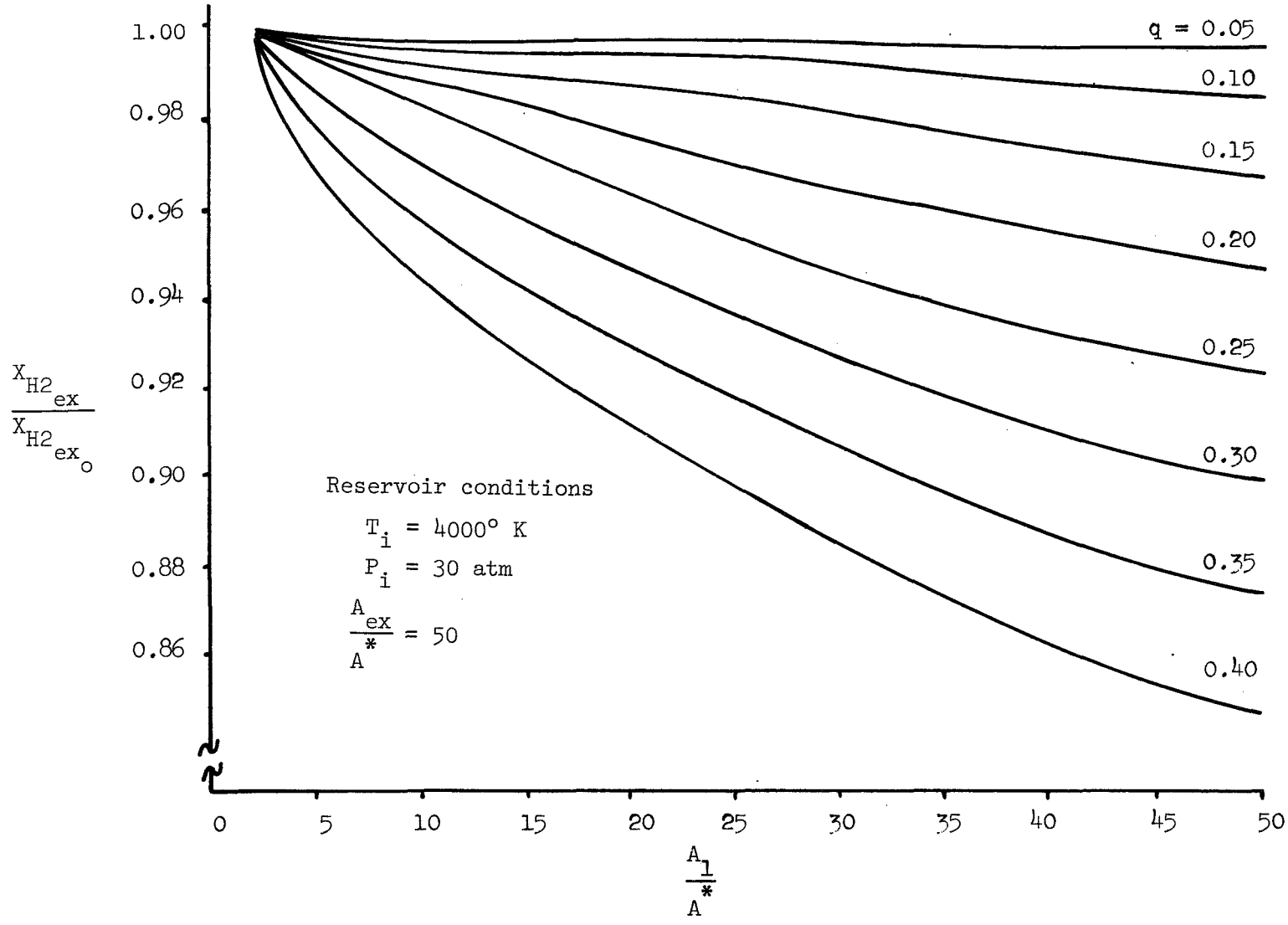

Figure 41.- Exit molecular hydrogen mole fraction ratio versus area ratio of heat addition for various values of heat exchange parameter (reacting gas with heat transfer).

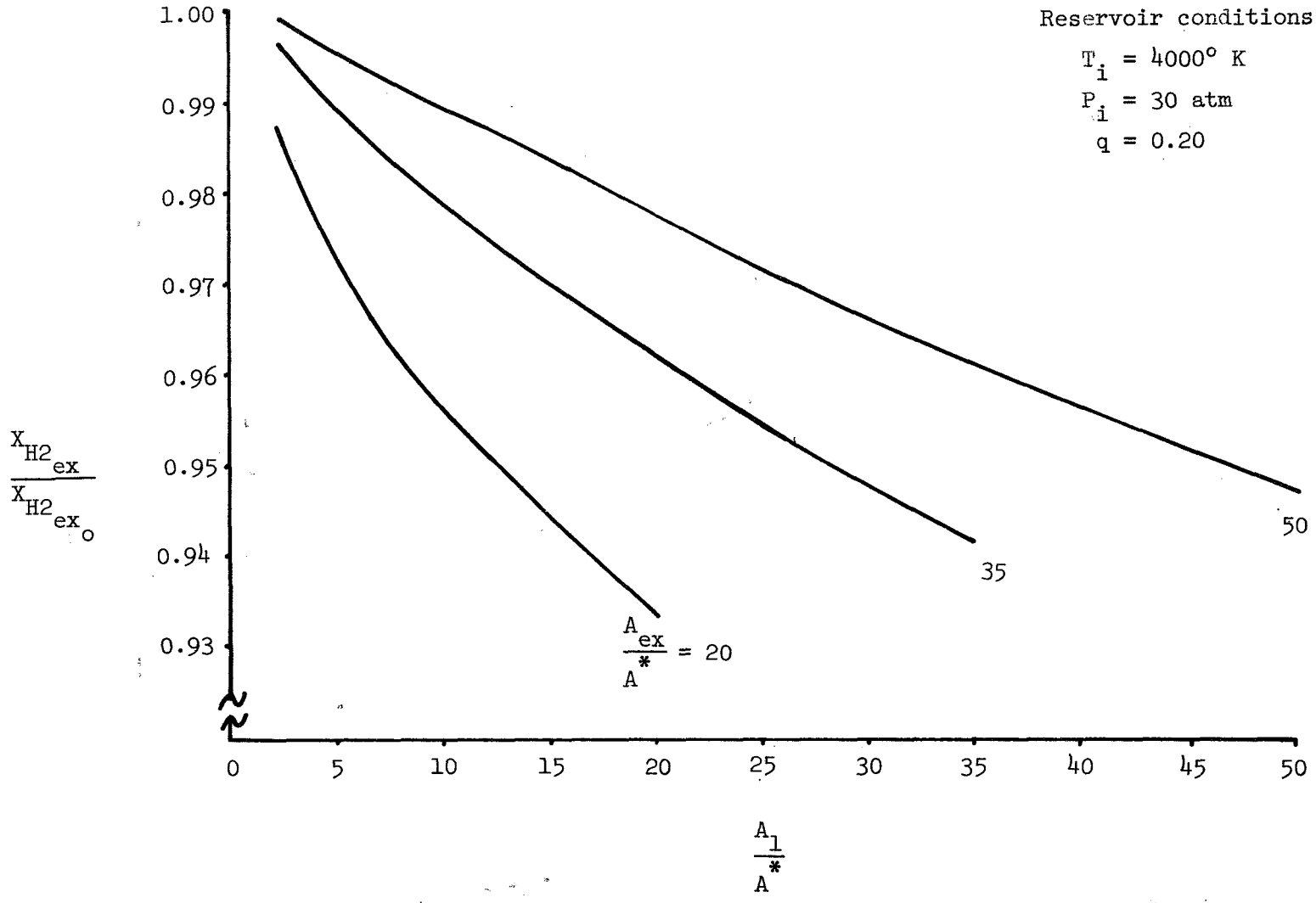

Figure 42.- Exit molecular hydrogen mole fraction ratio versus area ratio of heat addition for three values of the exit area ratio (reacting gas with heat transfer).

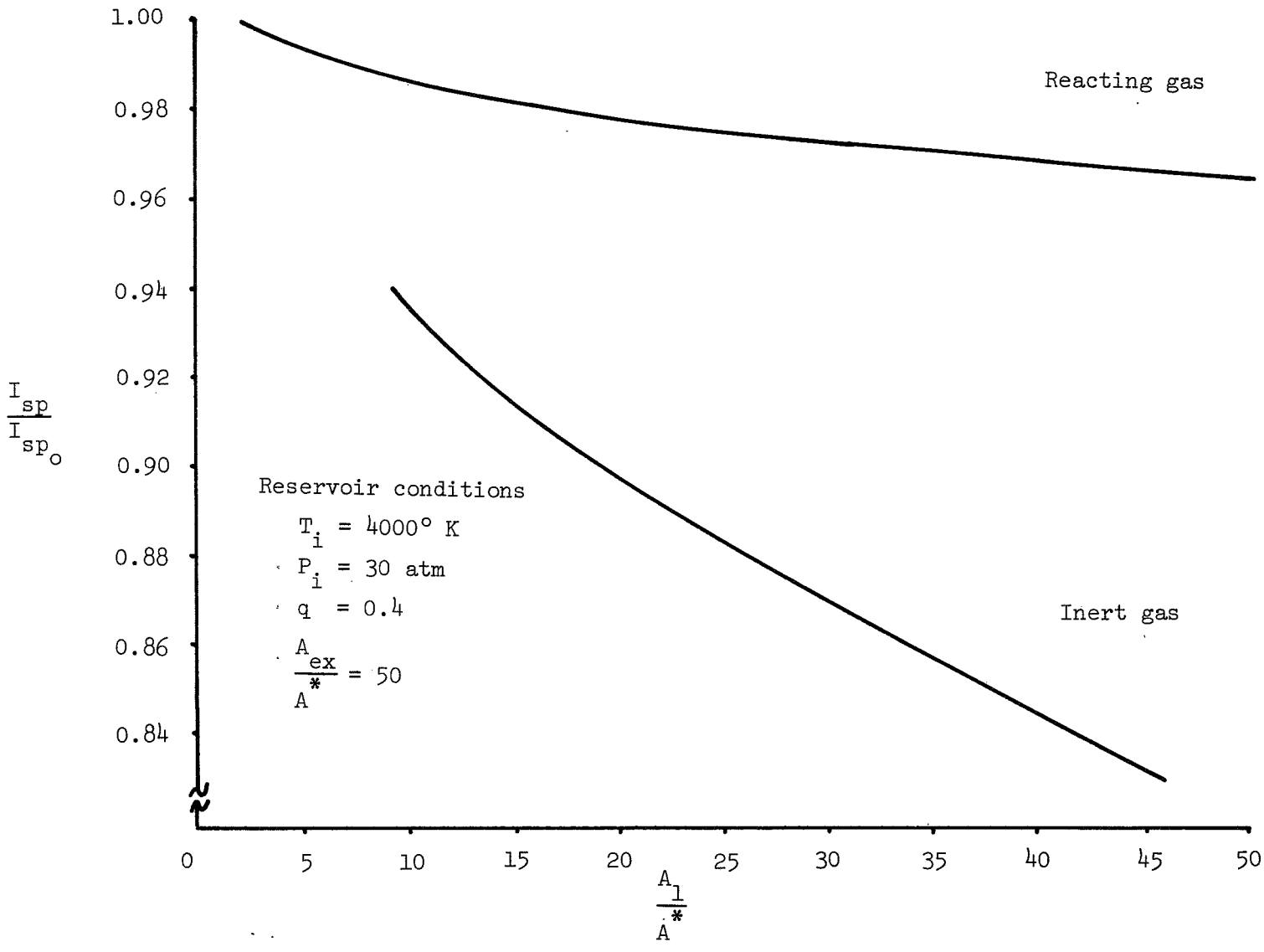

Figure 43.- Comparison of specific impulse ratio versus area ratio of heat addition for the inert gas and reacting gas heat transfer cases.

VITA

Raymond LeRoy Nieder was born in [redacted], on [redacted], to Ellen Kaufman Nieder and Leonard Raymond Nieder of Butler, Missouri. After graduating from Butler High School in 1962, he entered the University of Kansas at Lawrence, Kansas where in 1966 he received the degree of Bachelor of Science in Aerospace Engineering. During the summer of 1966, he was employed by Lear Jet Corporation, Wichita, Kansas. In September of that year he entered the Graduate School of the University of Texas. Since September 1967 he has been employed as a structural dynamics engineer by the National Aeronautics and Space Administration at the Manned Spacecraft Center, Houston, Texas. He was married to Miss Frances Joanne Hicks of Stuttgart, Arkansas on September 1, 1968.

Permanent address: 14 Redbud Lane
Stuttgart, Arkansas 72160

This thesis was typed by: Colleen Hall, ITT/FEC

NASA — MSC